Fluid Antenna Systems: Redefining Reconfigurable Wireless Communications

Wee Kiat New, *Member, IEEE*, Kai-Kit Wong, *Fellow, IEEE*, Chao Wang, *Senior Member, IEEE*, Chan-Byoung Chae, *Fellow, IEEE*, Ross Murch, *Fellow, IEEE*, Hamid Jafarkhani, *Fellow, IEEE*, and Yang Hao, *Fellow, IEEE*

***Abstract*—Sixth-generation (6G) networks are rapidly becoming a focal point of global technological innovation, driven by the need to support hyper-reliable, low-latency, and intelligent connectivity for applications such as immersive extended reality, autonomous systems, and ubiquitous sensing. While 6G promises transformative advancements in wireless communication, achieving its ambitious goals poses significant fundamental challenges. One natural direction is to scale multiple-input multiple-output (MIMO) technology to unprecedented levels; however, doing so introduces substantial hardware complexity and power consumption. To overcome these limitations, recent research has explored antenna reconfigurability as a novel degree of freedom (DoF) at the physical (PHY) layer. Among these efforts, the fluid antenna system (FAS) has emerged as a compelling concept, offering reconfigurability in both spatial positioning and physical structure. This idea has inspired related innovations, including movable antennas, flexible-position MIMO, reconfigurable MIMO architectures, and adaptive antenna arrays, collectively referred to as next-generation reconfigurable antenna (NGRA) systems. While prior work has primarily focused on spatial flexibility, this article introduces a generalized model of FAS that incorporates both structural and morphological fluidity, enabling the vision of "*shapeless and formless*" antennas in future wireless systems. We analyze FAS's potential to enhance key performance metrics such as coverage, energy efficiency, reliability, and spectral capacity. In addition, we outline implementation challenges and explore synergies with key 6G enablers, including reconfigurable intelligent surfaces (RIS), non-terrestrial networks (NTN), integrated sensing and communication (ISAC), and artificial intelligence (AI). This survey provides a comprehensive overview of NGRA systems and identifies promising directions for future research in reconfigurable wireless technologies.**

***Index Terms*—6G, artificial intelligence, deep learning, flexible antenna array, fluid antenna system (FAS), integrated sensing and communications (ISAC), internet-of-things (IoT), machine learning, movable antenna system, next-generation multiple access, next-generation reconfigurable antenna system, non-orthogonal multiple access (NOMA), non-terrestrial networks, rate-splitting multiple access (RSMA), and unmanned aerial vehicle (UAV).**

The work of K. K. Wong was in part supported by the Engineering and Physical Sciences Research Council (EPSRC) under grant EP/W026813/1.

The work of C. Wang was in part supported by the National Natural Science Foundation of China under Grant 62371357, the Funds for International Cooperation and Exchange of the National Natural Science Foundation of China under Grant 12411530120, and the International Postdoctoral Exchange Fellowship Program under Grant PC2021060.

The work of C.-B. Chae was in part supported by the Institute for Information and Communication Technology Planning and Evaluation (IITP)/NRF grant funded by the Ministry of Science and ICT (MSIT), South Korea, under Grant RS-2024-00428780 and 2022R1A5A1027646.

The work of R. Murch was in part supported by the Hong Kong Research Grants Council Area of Excellence Grant AoE/E-601/22-R.

The work of H. Jafarkhani was in part supported by the NSF Award CNS-2229467.

The work of Y. Hao was funded by the EPSRC grants (EP/R035393/1 and EP/X02542X/1). Y. Hao would like to thank the Institution of Engineering and Technology (IET) for the award of an A. F. Harvey Engineering Research Prize and the Royal Academy of Engineering for the Research Chair Award.

W. K. New and K. K. Wong are with the Department of Electronic and Electrical Engineering, University College London, London WC1E 7JE, United Kingdom. K. K. Wong is also affiliated with Yonsei Frontier Laboratory, Yonsei University, Seoul, 03722 Republic of Korea.

C. Wang is with the Integrated Service Networks Lab, Xidian University, Xi'an 710071 China.

C.-B. Chae is with the School of Integrated Technology, Yonsei University, Seoul, 03722 Republic of Korea.

R. Murch is with the Department of Electronic and Computer Engineering and Institute for Advanced Study (IAS), Hong Kong University of Science and Technology, Clear Water Bay, Hong Kong SAR, China.

H. Jafarkhani is with the Department of Electrical Engineering and Computer Science, University of California, Irvine, CA, USA.

Y. Hao is with the School of Electronic Engineering and Computer Science, Queen Mary, University of London, London, United Kingdom.

Corresponding author: Kai-Kit Wong (e-mail: kai-kit.wong@ucl.ac.uk).

I. Introduction

WIRELESS communication technologies are advancing at an unprecedented pace, transforming lives in profound ways, from voice-only services to rich multimedia [1], from physical presence to fully virtual immersion [2], and from raw data transmission to semantic-level communication [3]. As we move toward sixth-generation (6G) networks, a new frontier emerges—one that transcends traditional communication services to incorporate advanced sensing and intelligence, fundamentally reshaping how we live and connect [4]. The vision for 6G seeks to seamlessly integrate the digital and physical worlds, enabling novel interactions amongst people, devices, and the environment [5]. In alignment with this vision, the International Telecommunication Union's Telecommunication Standardization Sector (ITU-T) has reached a consensus on the key usage scenarios that will define 6G, including [6]

(i) Immersive communications,
(ii) Hyper-reliable low-latency communications (HRLLC),
(iii) Massive communications,
(iv) Artificial intelligence (AI) and communications,
(v) Ubiquitous connectivity, and
(vi) Integrated sensing and communications (ISAC).

6G is expected to meet ambitious demands, including data rates of up to 100 Gbps, peak speeds reaching 1 Tbps, sub-millisecond latency, ultra-high reliability at 99.9999%, a connection density of 10^7 devices per km^2, cm-level positioning accuracy, seamless connectivity across terrestrial, maritime, aerial, and space environments, as well as local data processing within a secure framework [7], [8], [9], [10]. While the precise technical enablers and driving forces remain uncertain [11], it is clear that achieving these ambitious goals will require a convergence of multiple technologies. Consequently, researchers and engineers are exploring a range of cutting-edge technologies such as reconfigurable intelligent surface (RIS) [12], [13], [14], next generation multiple access (NGMA) [15], non-terrestrial networks (NTN) [16], ISAC [17], AI [18], and more, to realize the ambitious vision of 6G networks.

At the physical layer, several approaches have been investigated. These include the use of mid-band [19] and terahertz (THz) frequencies [20], along with extremely-large multiple-input multiple-output (XL-MIMO) [21], which can sometimes be referred to as holographic multiple-input multiple-output (MIMO) [22], continuous aperture MIMO (CP-MIMO) [23], or continuous aperture arrays [24], with subtle differences in their definitions. Mid-band frequencies strike a good balance between providing bandwidth gains and maintaining manageable coverage challenges, making them attractive for a broad range of wireless applications [25]. Furthermore, THz frequencies are advantageous for their ability to deliver bandwidth gains of several orders of magnitude, accommodating massive device connectivity, accurate sensing, and ultra-high data rates [26]. Meanwhile, XL-MIMO is a natural evolution in MIMO technology, where scaling the number of antennas significantly boosts capacity by fully exploiting spatial resources [27].

On the other hand, reconfigurable antennas have long been anticipated as a supporting technology for wireless communications. One of the earliest designs is the electromechanically scanned trough waveguide antenna introduced in 1960 [28], which provides pattern reconfigurability. Additionally, in the late 1970s, utilizing phased arrays for beam reconfiguration in satellite communications was remotely regarded as a reconfigurable antenna [29], [30]. However, according to [31], antenna reconfigurability refers to the ability to alter a radiator's fundamental operating characteristics through electrical, mechanical, optical, material or other means. New reconfigurable antenna designs can be found in [32], [33], [34].

Different switching techniques, including PIN-diode, field-effect transistor (FET), and micro-electro-mechanical systems (MEMS) switches have been used in designing reconfigurable antennas [35], [36], [37]. Reconfigurable antennas can modify their physical structures through these switches to change their characterizations, for example polarization, radiation and frequency properties. They have also been employed in reconfigurable antenna arrays consisting of reconfigurable antenna elements [38]. These architectures, for example, allow different element separations in reconfigurable antenna arrays [39]. Dynamically reconfiguring the structural geometry of array elements constructs multi-functional reconfigurable antennas that can adapt their radiation patterns to varying channel conditions. The possibility of a favorable radiation pattern for a given physical channel condition can be used in an adaptive MIMO system to select different antenna designs, by reconfiguring the multi-functional reconfigurable antenna, under different channel conditions [40].

The growth of reconfigurable antenna research was subsequently driven by the need in cognitive radio applications [41], [42], [43]. In cognitive radios, a mobile device needs to have the ability to reconfigure its operating frequency to take advantage of spectrum holes. To this end, many frequency and pattern reconfigurable antennas have been designed, e.g., [44], [45], [46], [47], [48], [49], [50], [51]. Despite this, the impact of reconfigurable antennas appears to be limited to providing the basic function of a radio transceiver that is required by the next-generation wireless communications technologies.

This is about to change with the advent of next-generation reconfigurable antennas (NGRAs). A key lesson learned from MIMO systems is that the position of an antenna can significantly impact communication performance at any given time, as multiple channel paths combine differently at different locations, a classical phenomenon known as *spatial diversity*. The potential of spatial diversity to increase capacity was first recognized in the 1990s by Paulraj [52], before MIMO began to revolutionize wireless communications through the seminal work of Foschini *et al.* [53], [54]. Space-time coding for diversity gain [55], [56], [57] and spatial multiplexing [58] subsequently became foundational technologies. Furthermore, the combination of spatial and multiuser diversity led to the development of multiuser MIMO systems [59], [60], [61], [62], [63], [64], which have evolved into the massive MIMO architectures widely deployed today [65], [66].

Recognizing the reconfigurable antennas can increase spatial diversity [67], the notion of reconfigurable antenna can be expanded to include antenna position reconfigurability in NGRA. Leading the innovations is the umbrella concept of fluid antenna system (FAS) which is a groundbreaking paradigm of *shape-flexible and position-flexible* antenna technologies [68], [69], [70]. The concept was inspired by Bruce Lee's philosophy on combat [71], [72].

Bruce Lee once famously said [73]:

> *"Empty your mind, be formless. Shapeless, like water. If you put water into a cup, it becomes the cup. You put water into a bottle and it becomes the bottle. You put it in a teapot, it becomes the teapot. Now, water can flow or it can crash. Be water, my friend."*

Applying this philosophy to communications, Wong *et al.* in 2020 envisaged that antennas could be formless and shapeless like water or fluid, adaptable to different situations [71], [72]. More precisely, FAS refers to any software-controllable fluidic, conductive, or dielectric structure that can dynamically modify its shape and position to reconfigure key parameters such as gain, polarization, radiation pattern, operating frequency, and other characteristics. Under this definition, FAS is not limited to a specific implementation but encompasses a wide range of reconfigurable antennas, including liquid-based antennas [74], [75], [76], [77], movable antennas [78], [79], metamaterial-based antennas [80], [81], reconfigurable radio-frequency (RF) pixels [82], [83], and flexible antenna arrays [84], [85], [86], etc. Most recently in [87], a theoretical interpretation for FAS from the electromagnetic perspective was provided.

With this in mind, Wong *et al.* investigated the information-theoretic performance of a position-flexible FAS channel [88], [89]. The main concept of FAS is to fully exploit the spatial diversity using shape/position flexibility within a given space, fully utilizing the allowable space for performance enhancement. FAS has subsequently inspired several related research endeavors, including movable antenna systems [90], flexible-position MIMO systems [91], reconfigurable antenna MIMO systems [92], flexible antenna arrays [93], and several others. Beyond these developments, there are dynamic metasurface antennas (DMA) [94], [95], [96] or more precisely leaky-wave antennas (LWA)[1] [97], [98] that have been explored to reduce cost and power consumption for XL-MIMO systems. In fact, those approaches could also be interpreted as FAS.

A. *Related Works and Main Contributions*

Unlike traditional antenna systems (TAS) with fixed configurations, NGRA systems like FAS can reconfigure the antenna platform, the position, the polarization, and the dimensions or size of the radiating structures, etc. These capabilities provide unprecedented flexibility and adaptability that are unthinkable before and pivotal for the next-generation wireless networks. Thus far, several review articles have touched upon various aspects of FAS and related topics. For instance, there is a recent three-part series briefly introducing FAS from an information-theoretic perspective [99], highlighting research opportunities [100], and discussing a paradigm involving distributed artificial scattering surfaces (DASS) for massive access [101]. Also, [68] investigated the synergy between MIMO, RIS, and FAS, and [70] emphasized the relevance of FAS in 6G networks while [72] identified six promising research topics. There are also survey articles that focused on RF design and implementation of liquid-based antenna designs [74], [75], [76], [77], fluid antenna multiple access (FAMA) [231], and FAS-related networking perspectives [249]. In [90], the opportunities and challenges of mechanically movable antennas were examined. Further exploration of related technologies can also be found in [91], which discusses the fundamentals, challenges, and future research directions for flexible-position MIMO antenna systems. Last but not least, a comprehensive tutorial covering communication theory, optimization, and the hardware aspects of FAS is provided in [69]. The summary of different review and survey papers related to FAS is presented in Table I.

In contrast to existing works, this paper provides a novel unified perspective and an in-depth overview of FAS/NGRA systems that encompass a variety of key antenna reconfigurations. More uniquely, it envisions a next-generation wireless communication paradigm that treats antenna reconfigurability as a new resource dimension, inspiring innovative features, communication strategies, and signal processing techniques, rather than constraining system design within the limits of state-of-the-art antenna technologies. The main contributions of this paper are summarized as follows:

- To begin with, we present a new system model, termed multi-dimensional FAS,[2] which builds upon the concept of formless and shapeless antennas for future wireless communications, as originally introduced in [71]. In this system, the antenna platform, the positions of radiating elements, their polarization, and their dimensions/size can all be reconfigured, offering ultimate flexibility in the physical layer for future wireless networks.
- We highlight the advantages of multi-dimensional FAS by demonstrating that its various types of antenna reconfiguration can provide significant flexibility or substantial performance gains for wireless communication systems compared to TAS with fixed configurations.
- To fully unlock the potential of multi-dimensional FAS, we identify the key research areas for further advancement and discuss potential techniques, including developing optimization techniques tailored to its various capabilities, designing efficient strategies for acquiring full channel state information (CSI), exploring applications and scenarios in which the antenna reconfiguration can deliver the most impact, inventing novel uncoordinated communication strategies, and investigating innovative designs and materials for hardware development.
- Finally, we discuss how FAS and other NGRA systems can be integrated with cutting-edge technologies such as RIS, NGMA, NTN, ISAC, and AI to advance future wireless communications. Specifically, we review recent advancements, present concrete case studies showcasing their combined benefits, and highlight the new opportunities and challenges introduced by NGRA systems.

B. *Organization*

As illustrated in Fig. 1, this paper is organized as follows. Section II introduces multi-dimensional FAS, discusses its advantages, and outlines key research directions. It is worth noting that several mathematical fomulations are presented to provide readers with a rigorous theoretical foundation for this novel technology. Then Section III explores the integration of FAS and other NGRA systems with other cutting edge technologies, covering recent advancements, case studies, and detailed discussions of new opportunities and challenges. Finally, Section IV presents the conclusions. The abbreviations of this paper are listed in Table II.

II. Multi-Dimensional FAS: An NGRA System for Future Wireless Communications

In this section, we introduce the multi-dimensional FAS model, a new NGRA system model that establishes the concept of formless and shapeless antennas, as originally introduced in [71] for future wireless communications. As illustrated in Fig. 2, the platform of the antenna is highly flexible, capable of dynamically altering its shape in a given three-dimensional (3D) space. The radiating elements, usually active, including their number, size, positions, and orientations, can be adjusted dynamically. As a result, by modifying the position and shape of the antennas, this system can reconfigure the polarization, operating frequency, radiation pattern, and other performance metrics [72], [87]. This remarkable flexibility can provide new

[1] Some of the FAS prototypes are also designed based on LWA, e.g., [81].

[2] Technically, multi-dimensional FAS is the same as the original concept of FAS. However, as existing system models typically consider one (mostly position reconfiguration) or only a few antenna reconfigurations, we specifically refer to this NGRA model as multi-dimensional FAS to differentiate it from existing FAS models, highlighting its infinite reconfiguration dimensions.

degrees of freedom (DoF) to greatly enhance system performance across various applications, such as cellular networks, wireless fidelity (Wi-Fi), Internet of Things (IoT), Internet of Everything (IoE), wearable devices, and many others.

Taking into account various antenna reconfiguration capabilities, we present a new system model, which is a modified version of the one proposed in [102]. Specifically, the channel frequency response between the transmit and receive multi-dimensional FAS for the k-th subcarrier can be modeled as

$$\boldsymbol{H}_k = \sum_{l=1}^{L} \underbrace{\boldsymbol{P}_{\mathrm{r}}^H(\boldsymbol{\psi}_{\mathrm{r}})\bar{\boldsymbol{J}}_{l,\mathrm{r}}^H}_{\text{rx-polarization}} \Bigg(\Bigg(\underbrace{\beta_{l,k}}_{\text{ch. gain}} \underbrace{\boldsymbol{a}_{\mathrm{r}}\left(\boldsymbol{q}_{\mathrm{r}}, \boldsymbol{\theta}_{\mathrm{r}}^l\right) \boldsymbol{a}_{\mathrm{t}}^H\left(\boldsymbol{q}_{\mathrm{t}}, \boldsymbol{\theta}_{\mathrm{t}}^l\right)}_{\substack{\text{position of}\\ \text{radiating elements}}} \odot \underbrace{\boldsymbol{g}_{k,\mathrm{r}}\left(\boldsymbol{\theta}_{\mathrm{r}}^l, \boldsymbol{l}_{\mathrm{r}}\right) \boldsymbol{g}_{k,\mathrm{t}}^H\left(\boldsymbol{\theta}_{\mathrm{t}}^l, \boldsymbol{l}_{\mathrm{t}}\right)}_{\substack{\text{sizes of}\\ \text{radiating elements}}} \Bigg) \otimes \underbrace{\boldsymbol{V}\boldsymbol{D}_{l,k}}_{\text{depol.}} \Bigg) \underbrace{\bar{\boldsymbol{J}}_{l,\mathrm{t}}\boldsymbol{P}_{\mathrm{t}}(\boldsymbol{\psi}_{\mathrm{t}})}_{\text{tx-polarization}}, \tag{1}$$

where

$$\bar{\boldsymbol{J}}_{l,s} = \mathrm{blkdiag}\left(\boldsymbol{J}_1, \ldots, \boldsymbol{J}_{M_s}\right) \in \mathbb{C}^{2M_s \times 2M_s}, \tag{2}$$

$$\boldsymbol{P}_s(\boldsymbol{\psi}_s) = \mathrm{blkdiag}\left(\boldsymbol{p}\left(\psi_s^1\right), \ldots, \boldsymbol{p}\left(\psi_s^{M_s}\right)\right) \in \mathbb{R}^{2M_s \times M_s}, \tag{3}$$

$$\boldsymbol{g}_{k,s}(\boldsymbol{\theta}_s, \boldsymbol{l}_s) = [g_k(\boldsymbol{\theta}_s, \boldsymbol{l}_1) \ \cdots \ g_k(\boldsymbol{\theta}_s, \boldsymbol{l}_{M_s})]^T \in \mathbb{C}^{M_s \times 1}, \tag{4}$$

$$\boldsymbol{a}_s(\boldsymbol{q}_s, \boldsymbol{\theta}_s) = [a(\boldsymbol{q}_1, \boldsymbol{\theta}_s) \ \cdots \ a(\boldsymbol{q}_{M_s}, \boldsymbol{\theta}_s)]^T \in \mathbb{C}^{M_s \times 1}, \tag{5}$$

$$\boldsymbol{J}_m = \begin{bmatrix} G_{c,m} & G_{x,m} \\ G_{x,m} & -G_{c,m} \end{bmatrix} \in \mathbb{C}^{2\times 2}. \tag{6}$$

In (1), L denotes the total number of propagation paths, $\beta_{l,k}$ is the l-th path complex channel gain (including effects such as path loss, shadowing, and etc.), $\boldsymbol{V}$ accounts for the orientation difference between the transmitter and receiver, $\boldsymbol{D}_{l,k}$ accounts for the depolarization effect due to multipath fading, and $\bar{\boldsymbol{J}}_{l,s}$ accounts for the co-polarized and cross-polarized gain of the radiating elements, where $G_{c,m}$ and $G_{x,m}$ are the co-polarized and cross-polarized of the m-th active radiating element.

Furthermore, $\boldsymbol{P}_s(\boldsymbol{\psi}_s)$ in (3) represents the overall polarization reconfiguration of the radiating elements, $\boldsymbol{g}_s(\boldsymbol{l}_s, f_k)$ in (4) represents the gain of the radiating elements for specific size reconfiguration, and $\boldsymbol{a}_s(\boldsymbol{q}_s, \boldsymbol{\theta}_s)$ in (5) represents the positions of the radiating elements, which must lie within the 3D flexible platform, $\mathcal{Q}_s$, for $s \in \{\mathrm{r}, \mathrm{t}\}$. Also, M_s for $s \in \{\mathrm{r}, \mathrm{t}\}$ is the number of active radiating elements. Note that the transmitter and receiver can have a maximum of $M_{\mathrm{t}}^{\max}$ and $M_{\mathrm{r}}^{\max}$ active radiating elements, respectively. Consequently, the number of active elements must satisfy $M_{\mathrm{t}} \leq M_{\mathrm{t}}^{\max}$ and $M_{\mathrm{r}} \leq M_{\mathrm{r}}^{\max}$.

It is worth noting that in some scenarios, it may be advantageous to have $M_{\mathrm{t}} < M_{\mathrm{t}}^{\max}$ and $M_{\mathrm{r}} < M_{\mathrm{r}}^{\max}$, such as when energy efficiency is prioritized in the system. Next, we will adopt the channel model in (1) to explore the reconfiguration of the platform, position, polarization, and radiation size in greater detail, showcasing the superiority of multi-dimensional FAS over TAS with fixed configurations. It is also important to note that most of existing NGRA system models are typically a special case of (1). Furthermore, specific fading distributions and spatial correlation models may be a special case of (1).

A. Platform Reconfiguration

In general, $\mathcal{Q}_s$ represents the antenna platform or region in a 3D space where the radiating elements can be activated. This antenna platform can take various flexible shapes, such as a straight line, a wiggle line, a flat plane, a folded plane, a deflected plane, a cube, or other configurations, depending on the antenna materials and design. In this section, we focus on a flat two-dimensional (2D) plane within a 3D space and consider several linear and nonlinear transformations to make the antenna platform flexible, as considered in [93]. Let us define a flat 2D plane within a 3D space as

$$\mathcal{Q}_s^{\mathrm{2D}} = \left\{ \boldsymbol{q} \,\middle|\, -\frac{X\lambda}{2} \leq q_x \leq \frac{X\lambda}{2}, -\frac{Y\lambda}{2} \leq q_y \leq \frac{Y\lambda}{2} \right\}, \tag{7}$$

where $\boldsymbol{q} = [q_x \ q_y \ q_z]^T$ for some arbitrary q_z, while $X\lambda$, and $Y\lambda$ define the dimensions of the plane along the x- and y-axes, respectively. Fundamentally, we can rotate $\mathcal{Q}_s^{\mathrm{2D}}$ about the z-axis using the following rotation matrix

$$Q_{\mathrm{rot}}(\phi_{\mathrm{rot}}) = \begin{bmatrix} \cos(\phi_{\mathrm{rot}}) & -\sin(\phi_{\mathrm{rot}}) & 0 \\ \sin(\phi_{\mathrm{rot}}) & \cos(\phi_{\mathrm{rot}}) & 0 \\ 0 & 0 & 1 \end{bmatrix}. \tag{8}$$

Applying this transformation yields the rotated 2D plane

$$\mathcal{Q}_{s,\mathrm{rot}}^{\mathrm{2D}} = \left\{ \boldsymbol{q}_{\mathrm{rot}} \,\middle|\, \boldsymbol{q}_{\mathrm{rot}} = Q_{\mathrm{rot}}(\phi_{\mathrm{rot}})\,\boldsymbol{q}, \forall \boldsymbol{q} \in \mathcal{Q}_s^{\mathrm{2D}} \right\}, \tag{9}$$

which represents the 2D plane rotated by ϕ_{rot}.[3]

Also, we can fold $\mathcal{Q}_s^{\mathrm{2D}}$ along the y-axis using the matrix[4]

$$Q_{\mathrm{fold}}(\phi_{\mathrm{fold}}) = \begin{bmatrix} \cos(\phi_{\mathrm{fold}}) & 0 & 0 \\ 0 & 1 & 0 \\ \sin(\phi_{\mathrm{fold}}) & 0 & 1 \end{bmatrix}. \tag{10}$$

To effectively apply this transformation, we divide $\mathcal{Q}_s^{\mathrm{2D}}$ into two halves as

$$\mathcal{Q}_{s+}^{\mathrm{2D}} = \left\{ \begin{bmatrix} q_x \\ q_y \\ 0 \end{bmatrix} \,\middle|\, 0 \leq q_x \leq \frac{X\lambda}{2}, -\frac{Y\lambda}{2} \leq q_y \leq \frac{Y\lambda}{2} \right\}, \tag{11}$$

and

$$\mathcal{Q}_{s-}^{\mathrm{2D}} = \left\{ \begin{bmatrix} q_x \\ q_y \\ 0 \end{bmatrix} \,\middle|\, -\frac{X\lambda}{2} \leq q_x \leq 0, -\frac{Y\lambda}{2} \leq q_y \leq \frac{Y\lambda}{2} \right\}. \tag{12}$$

Then we can fold the plane by an angle toward the negative z-direction as

$$\mathcal{Q}_s^{\mathrm{2D,fold}} = \left\{ \boldsymbol{q}_{\mathrm{fold}} \,\middle|\, \boldsymbol{q}_{\mathrm{fold}} = Q_{\mathrm{fold}}(\pm\phi_{\mathrm{fold}})\,\boldsymbol{q}, \forall \boldsymbol{q} \in \mathcal{Q}_{s\pm}^{\mathrm{2D}} \right\}. \tag{13}$$

[3]If each location in $\mathcal{Q}_s^{\mathrm{2D}}$ has a vector directed normal to the plane, then the direction of this vector will remain normal to the rotated plane. However, if the polarization in $\mathcal{Q}_s^{\mathrm{2D}}$ is initially vertical, it will be rotated by an angle ϕ_{rot} along with the plane.

[4]Note that with slight modifications, $\mathcal{Q}_s^{\mathrm{2D}}$ can be folded along any arbitrary direction in the 3D space.

TABLE I
SUMMARY OF REVIEW AND SURVEY PAPERS RELATED TO FAS AND NGRA SYSTEMS.

Reference	Focus / Topic	Key Contributions or Highlights
[99]	Information-theoretic perspective of FAS	Introduces fundamental concepts of FAS and examines its performance limits from an information-theoretic viewpoint.
[100]	Research opportunities in FAS	Highlights open problems and potential research directions for future FAS developments.
[101]	DASS for massive access	Discusses the DASS paradigm as a generalization of FAS for supporting large-scale device connectivity.
[68]	Synergy between MIMO, RIS, and FAS	Investigates how MIMO, RIS, and FAS can jointly enhance communication performance and adaptability.
[70]	Role of FAS in 6G networks	Emphasizes the potential of FAS as a key enabling technology for 6G communication systems.
[72]	FAS research roadmap	Identifies six early research directions, including channel modeling, optimization, and implementation aspects.
[74], [75], [76], [77]	RF design and implementation of liquid-based antennas	Surveys the design principles, fabrication techniques, and performance characteristics of liquid-metal and fluidic antennas.
[231]	FAMA	Reviews the principles, benefits, and challenges of FAMA as an emerging multiple-access technique based on FAS.
[249]	Networking perspectives of FAS	Provides a high-level overview of FAS from a networking viewpoint.
[90]	Mechanically movable antenna system	Examines the opportunities and challenges associated with mechanically reconfigurable or movable antennas.
[91]	Flexible-position MIMO antenna systems	Discusses fundamentals, challenges, and future research trends in flexible-position MIMO, closely related to FAS concepts.
[69]	Comprehensive FAS tutorial	Provides an extensive overview of FAS covering communication theory, optimization frameworks, and hardware implementation.
This paper	Multi-dimensional FAS and integration of FAS with other NGRA systems and cutting-edge technologies	Presents a multi-dimensional FAS as a unified framework that encompasses reconfiguration across multiple domains, including the antenna platform, element positions, polarization states, and physical dimensions.

In addition, it is possible to bend the 2D plane around a cylinder with radius $R_{\rm def}$, deflecting it away from the original plane. The deflected region can be expressed as

$$\mathcal{Q}_s^{\rm 2D,def}\left(R_{\rm def}\right)=\left\{\boldsymbol{q}_{\rm def}\left|\boldsymbol{q}_{\rm def}=f\left(R_{\rm def},\boldsymbol{q}\right),\forall \boldsymbol{q}\in\mathcal{Q}_s^{\rm 2D}\right.\right\}, \tag{14}$$

where $R_{\rm def}\geq\pm\frac{X\lambda}{\pi}$ for practical purposes, and

$$f\left(R,\boldsymbol{q}\right)=\begin{bmatrix} R\sin\left(\frac{q_x}{R}\right)\\ q_y\\ R\cos\left(\frac{q_x}{R}\right)-R\end{bmatrix}. \tag{15}$$

It is noteworthy that as $R_{\rm def}\to\infty$, we have $\mathcal{Q}_s^{\rm 2D,def}\to\mathcal{Q}_s^{\rm 2D}$, restoring the flat 2D plane.[5]

In Fig. 3, we illustrate an example of a flexible antenna platform leveraged in multi-dimensional FAS. Compared to a rigid antenna platform in TAS, such as the flat 2D plane, reconfigurable platform provides diverse types of coverage, potentially enhancing system efficiency and versatility across a broad range of scenarios. Furthermore, they are essential for future wireless communications because they allow antennas to adapt to irregular or curved surfaces, making them ideal for applications such as wearable devices [75], integration with non-planar structures [103], or near-field communications [84]. On the other hand, the ability to tailor antenna shapes for specific applications creates new opportunities to enhance performance such as coverage while reducing costs. Clearly, the model here is mainly geometric, assuming that all points on the platform radiate outward from it towards the direction of normal. But in reality, a point of radiation comes from a carefully designed structure that takes up some space depending on the frequency and other radiation parameters.

[5]If each location in $\mathcal{Q}_s^{\rm 2D}$ has a vector directed normal to the plane, then after folding or bending, the direction of this vector will be rotated by $\pm\theta_{\rm flip}$ or $\frac{q_x}{R}$ in the azimuth angle, respectively. However, if the antenna polarization in $\mathcal{Q}_s^{\rm 2D}$ is initially vertical, then the polarization in $\mathcal{Q}_s^{\rm 2D,fold}$ or $\mathcal{Q}_s^{\rm 2D,def}$ will remain vertical after folding or bending.

B. Position Reconfiguration

With recent advancements in antenna technologies, position reconfiguration has become one of the most widely considered aspects of antenna reconfiguration [79]. Specifically, the positions of the active radiating elements can be adjusted within a predefined 3D space, denoted as $\mathcal{Q}_s$, as discussed earlier. Let us define the wave vector as

$$\boldsymbol{k}\left(\boldsymbol{\theta}\right)=\frac{2\pi}{\lambda}\begin{bmatrix}\cos\left(\theta_{\rm ele}\right)\sin\left(\theta_{\rm azi}\right)\\ \sin\left(\theta_{\rm ele}\right)\\ \cos\left(\theta_{\rm ele}\right)\cos\left(\theta_{\rm azi}\right)\end{bmatrix}, \tag{16}$$

where $\boldsymbol{\theta}=\left[\theta_{\rm azi},\theta_{\rm ele}\right]^T$, with $\theta_{\rm azi}$ and $\theta_{\rm ele}$ representing the azimuth and elevation angles, respectively.[6] The position of the m-th radiating element is given by

$$\boldsymbol{q}_s^m=\left[q_x^{m,s}\ q_y^{m,s}\ q_z^{m,s}\right]^T, \tag{17}$$

where $\boldsymbol{q}_s^m\in\mathcal{Q}_s$, and $\mathcal{Q}_s$ represents the position-reconfigurable region in a 3D space. Accordingly, the response vector can then be expressed as [104]

$$\boldsymbol{a}_s\left(\boldsymbol{Q}_s,\boldsymbol{\theta}\right)=\left[e^{j\boldsymbol{k}(\boldsymbol{\theta})^T\boldsymbol{q}_s^1}\ \ \dots\ \ e^{j\boldsymbol{k}(\boldsymbol{\theta})^T\boldsymbol{q}_s^{M_s}}\right]^T. \tag{18}$$

Intuitively, if two of the coordinates (e.g., $q_y^{m,s},q_z^{m,s},\forall n$) are fixed, the position can only be adjusted along a straight one-dimensional (1D) line. Similarly, if one of the coordinates (e.g., $q_z^{m,s},\forall n$) is fixed, the position can only be reconfigured

[6]Note that the distribution of $\boldsymbol{\theta}$ should account for the flexible shape of the antenna platform.

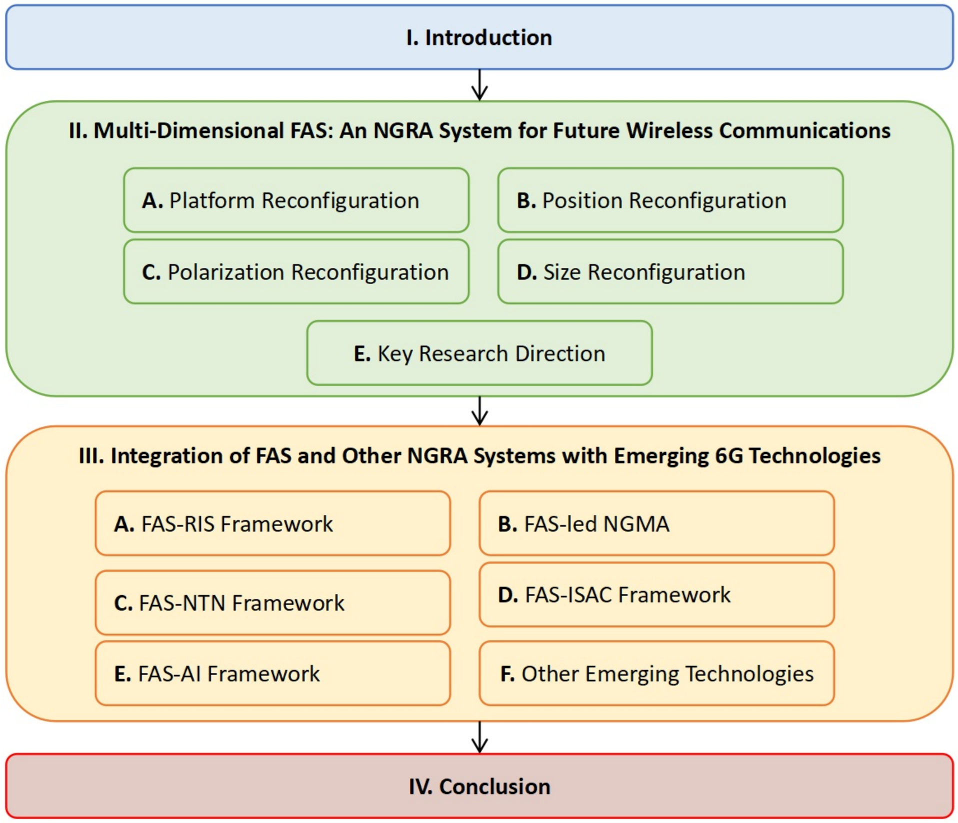

Fig. 1. Organization of the paper.

within a flat 2D plane. Fig. 4 shows an example where the antenna platform is a flat 2D plane, the m-th active radiating element is located at $\boldsymbol{q}_s^m$ with an impinging plane wave characterized by elevation angle θ_{azi} and azimuth angle θ_{ele}.

In practice, position reconfiguration is often discrete because any mechanism is likely digitally controlled. Hence, it is reasonable to discretize $\mathcal{Q}_s$ into a finite set of possible positions. These positions are also referred to as ports in the literature of FAS. Consider a special case where the antenna platform is a 2D plane, (i.e., $\mathcal{Q}_s = \mathcal{Q}_s^{\text{2D}}$), with $q_z = 0$. If the x- and y-axes of $\mathcal{Q}_s^{\text{2D}}$ are discretized into $2N_x+1$ and $2N_y+1$ ports, respectively, the (n_x, n_y)-th position can be expressed as[7]

$$\boldsymbol{q}_s^{n_x,n_y} = \left[n_x \frac{X\lambda}{2N_x} \quad n_y \frac{Y\lambda}{2N_y} \quad 0 \right]^T, \tag{19}$$

where

$$n_x \in \mathbb{Z}, -N_x \leq n_x \leq N_x, \tag{20}$$
$$n_y \in \mathbb{Z}, -N_y \leq n_y \leq N_y. \tag{21}$$

The overall response vector in $\mathcal{Q}_s^{\text{2D}}$ can be rewritten as

$$\dot{\boldsymbol{a}}_s(\boldsymbol{\theta}) = \begin{bmatrix} e^{-j\pi X \cos(\theta_{\text{ele}})\sin(\theta_{\text{azi}})} \\ \vdots \\ e^{j\pi X \cos(\theta_{\text{ele}})\sin(\theta_{\text{azi}})} \end{bmatrix} \otimes \begin{bmatrix} e^{-j\pi Y \sin(\theta_{\text{ele}})} \\ \vdots \\ e^{j\pi Y \sin(\theta_{\text{ele}})} \end{bmatrix}. \tag{22}$$

[7]Similarly, we can apply several linear and nonlinear transformations on the coordinates to consider a flexible antenna platform.

If the m-th active radiating element is located at the (n_x, n_y)-th position, the m-th entry of the response vector becomes

$$a_s^m(\boldsymbol{\theta}) = e^{j\pi\left[\frac{n_x X}{N_x}\cos(\theta_{\text{ele}})\sin(\theta_{\text{azi}}) + \frac{n_y Y}{N_y}\sin(\theta_{\text{ele}})\right]}, \tag{23}$$
$$= \left(\boldsymbol{b}_s^m\right)^T \dot{\boldsymbol{a}}_s(\boldsymbol{\theta}), \tag{24}$$

where $\boldsymbol{b}_s^m = \boldsymbol{e}_n$ is an all-zero vector except for a unity at the n-th position such that n is the 1D index corresponding to the 2D indices (n_x, n_y). For example, the relationship between the 1D index n and the 2D indices (n_x, n_y) is given by

$$n = (n_x + N_x)(2N_y + 1) + (n_y + N_y) + 1. \tag{25}$$

Using this discretization approach, it is sometime useful to introduce the following activation port matrix

$$\boldsymbol{B}_s = \left[\boldsymbol{b}_s^1 \ \cdots \ \boldsymbol{b}_s^{M_s}\right], \tag{26}$$

where $\boldsymbol{b}_s^m \neq \boldsymbol{b}_s^{m'}, \forall m \neq m'$, so that the active ports do not overlap or collide. This leads to

$$\boldsymbol{a}_s(\boldsymbol{\theta}) = \boldsymbol{B}_s^T \dot{\boldsymbol{a}}_s(\boldsymbol{\theta}). \tag{27}$$

Beyond the application of active port matrices or vectors, other methods are also viable to ensure this constraint. When N_x and N_y are arbitrarily large, the discrete positions effectively approximate the continuous position reconfiguration.

By reconfiguring the position of the active radiating elements, a multi-dimensional FAS can achieve extreme energy efficiency [105] or diversity gain [106], [107], [108], [109], [110], [111]. Fig. 5 illustrates the average transmit power to

TABLE II
ABBREVIATIONS

Abbrev.	Definition	Abbrev.	Definition
1D	One-Dimensional	LDMA	Location Division Multiple Access
2D	Two-Dimensional	LWA	Leaky-Wave Antennas
3D	Three-Dimensional	LEO	Low-earth orbit
6G	Sixth Generation	Li-Fi	Light Fidelity
AI	Artificial Intelligence	LoS	Line-of-Sight
AirComp	Air Computation	LSTM	Long Short-Term Memory
AWGN	Additive White Gaussian Noise	MEO	Medium-earth orbit
BS	Base Station	MEMS	Micro-Electro-Mechanical Systems
CP-MIMO	Continuous-Aperture MIMO	MIMO	Multiple-Input Multiple-Output
CSI	Channel State Information	MLP	Multi-Layer Perceptron
CUMA	Compact Ultra Massive Antenna Array	MSE	Mean Squared Error
DASS	Distributed Artificial Scattering Surfaces	NGMA	Next-Generation Multiple Access
DL	Deep Learning	NGRA	Next Generation Reconfigurable Antenna System
DMA	Dynamic Metasurface Antennas	NLoS	Non-Line-of-Sight
DoF	Degree of Freedom	NOMA	Non-Orthogonal Multiple Access
DRL	deep RL	NTN	Non-Terrestrial Networks
ETSI	European Telecommunications Standards Institute	OFDM	Orthogonal Frequency Division Multiplexing
FAS	Fluid Antenna System	OMA	Orthogonal Multiple Access
FAMA	Fluid Antenna Multiple Access	OTA-FL	Over-the-Air Federated Learning
FDMA	Frequency-Division Multiple Access	PHY	Physical
FET	Field Effect Transistor	RSMA	Rate-Splitting Multiple Access
FPA	Fixed-Position Antenna	RIS	Reconfigurable Intelligent Surface
GEO	Geostationary earth orbit	RL	Reinforcement Learning
HAP-UAV	High-altitude platform UAV	SDMA	Space Division Multiple Access
HRLCC	Hyper-Reliable Low-Latency Communications	SINR	Signal-to-Interference-plus-Noise Ratio
IoE	Internet-of-Everything	SNR	Signal-to-Noise Ratio
IoT	Internet-of-Things	TAS	Traditional Antenna Systems
ISAC	Integrated Sensing And Communications	TDMA	Time-Division Multiple Access
ISCC	Integrated Sensing, Communication, and Computing	UAV	Unmanned Aerial Vehicle
ISG	Industry Specification Group	Wi-Fi	Wireless Fidelity
ITU-T	International Telecommunication Union's Telecommunication	XL-MIMO	Extremely-Large MIMO
LAP-UAV	Low-altitude platform UAV	XL-STARS	Large-Scale Transmission and Reflection Surfaces

achieve the same rate for multi-dimensional FAS and TAS with fixed-position antennas (FPAs) (or fixed-position TAS). In this result, we consider that the position can only be adjusted along a straight 1D line and assume that the polarization of the transmitter and receiver is perfectly aligned, while the gain of the radiating elements for specific size reconfiguration is normalized to one. As shown, with position reconfiguration alone, the average transmit power of the multi-dimensional FAS is significantly lower than that of the fixed-position TAS, highlighting the benefits of position reconfiguration.

C. Polarization Reconfiguration

Generally, the orientation of the active radiating elements—specifically, their yaw, pitch, and roll—can be reconfigured depending on the chosen implementation method. This reconfiguration typically affects the polarization. More concretely, polarization is the orientation of oscillations in electromagnetic waves as it travels through space [112]. Antennas are typically designed for a specific polarization, known as co-polarization, but the radiation may also occur in an orthogonal polarization, referred to as cross-polarization [113]. When the transmitter and receiver polarizations are properly aligned, the received signal strength can be maximized, whereas misalignment can lead to signal degradation [114]. There are several types of polarization such as linear polarization, circular polarization, and elliptical polarization. In this section, for simplicity, we focus on linear polarization with a single feed.

For brevity, our discussion focuses on reconfiguring the roll of the active radiating elements, while assuming that the pitch and yaw of the transmit and receive elements are aligned to face each other, i.e., $\boldsymbol{V} = \boldsymbol{I}$. Unlike rotation of the entire platform, this reconfiguration allows for adjusting only the active radiating elements rather than the entire region. When the active radiating elements are rotated by an angle ψ_s^m, the linear polarization would also be rotated by ψ_s^m. Let us denote this polarization angle vector as

$$\boldsymbol{p}\left(\psi_s^m\right) = \left[\cos\left(\psi_s^m\right) \;\; \sin\left(\psi_s^m\right)\right]^T. \tag{28}$$

Moreover, let us denote the co-polarized and cross-polarized gain of the m-th active radiating element at s side as $G_{s,m}^{\mathrm{c}}$ and $G_{s,m}^{\mathrm{x}}$, respectively. According to [115], $G_{s,m}^{\mathrm{c}}$ and $G_{s,m}^{\mathrm{x}}$ can be modeled as $G_{s,m}^{\mathrm{c}} = \sqrt{\frac{1}{1+\chi_{\mathrm{ant}}}}$ and $G_{s,m}^{\mathrm{x}} = \sqrt{\frac{\chi_{\mathrm{ant}}}{1+\chi_{\mathrm{ant}}}}$, while more thorough calculations are also available [116]. The horizontal and vertical polarization gain of the m-th active radiating element can be expressed as [115]

$$\boldsymbol{r}_{\mathrm{pol}}^m = \boldsymbol{p}\left(\psi_s^m\right)^T \begin{bmatrix} G_{s,m}^{\mathrm{c}} & G_{s,m}^{\mathrm{x}} \\ G_{s,m}^{\mathrm{x}} & -G_{s,m}^{\mathrm{c}} \end{bmatrix}. \tag{29}$$

The depolarization effect can be modeled as [117]

$$\boldsymbol{D}_{l,k} = \begin{bmatrix} \delta_{HH} & \delta_{HV} \\ \delta_{VH} & \delta_{VV} \end{bmatrix}, \tag{30}$$

where δ_{AB} represents the correlation between polarization 'A' at the receiver side and polarization 'B' at the transmitter side,

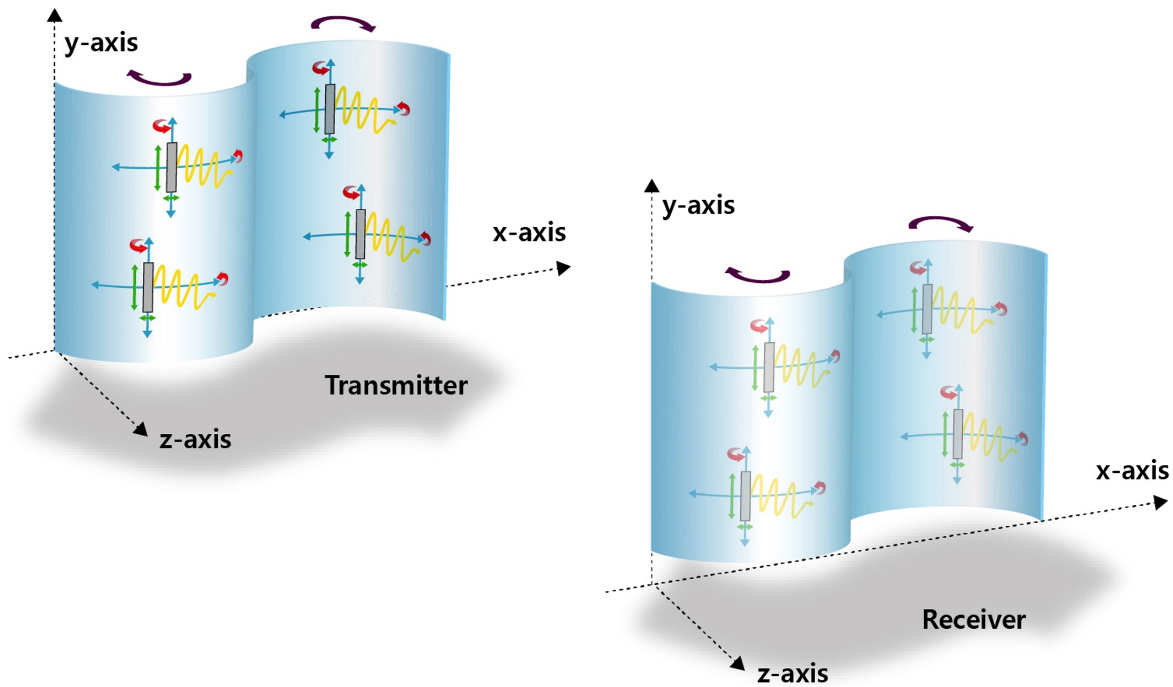

Fig. 2. Multi-dimensional FAS: Formless and shapeless antennas.

and both 'A' and 'B' can be either H standing for horizontal or V for vertical polarization. For $HV \rightarrow HV$, we have

$$\mathrm{vec}\left(\boldsymbol{D}\right)=\begin{bmatrix} 1 & \sqrt{\mu\chi}\vartheta^* & \sqrt{\chi}\sigma^* & \sqrt{\mu}\delta_1^* \\ \sqrt{\mu\chi}\vartheta & \mu\chi & \sqrt{\mu}\chi\delta_2^* & \sqrt{\chi}\mu\sigma^* \\ \sqrt{\chi}\sigma & \sqrt{\mu}\chi\delta_2 & \chi & \sqrt{\mu\chi}\vartheta^* \\ \sqrt{\mu}\delta_1 & \sqrt{\chi}\mu\sigma & \sqrt{\mu\chi}\vartheta & \mu \end{bmatrix}\boldsymbol{z}, \tag{31}$$

where μ and χ are the co- and cross-polarization ratios, σ and ϑ are the correlation coefficients between VV and HV, HH and HV, VV and VH or HH and VH, δ_1 is the correlation between the VV and the HH components, and δ_2 denotes the correlation between the VH and the HV components, and $\boldsymbol{z}$ is a circularly symmetric complex exponential vector with unit amplitude and uniformly distributed phase between 0 to 2π.

To highlight the advantages of polarization reconfiguration, Fig. 6 compares the outage probability of a multi-dimensional FAS with that of a TAS with fixed polarization (or fixed-polarization TAS) against the signal-to-noise ratio (SNR). For this analysis, it is assumed that $\mu = 0.7$, $\chi = 0.252$, $\sigma = 0.8$, $\vartheta = 0.8$, $\delta_1 = 0.9$, $\delta_2 = 0.9$, and $\chi_{\rm ant} = 0.2$. Furthermore, we assume that the gain of the radiating elements for specific size reconfigurations is normalized to one. As observed, with polarization reconfiguration alone, the outage probability decreases as the SNR increases, and the performance gap between the FAS and TAS widens with increasing SNR as well. This result clearly indicates that communication reliability can be further enhanced if the polarization is always aligned.

D. Size Reconfiguration

At extremely high frequency, the wavelengths become exceptionally small [118] and the bandwidth is significantly large [119]. In such systems, having the ability to reconfigure the size of radiating elements, such as their length, width, and depth, can be highly useful in optimizing the performance for specific azimuth and elevation angles, as well as subcarrier frequencies [97], [98], [120]. Generally, the gain of a radiating element for a given size depends on the antenna design and implementation. For brevity, this discussion will focus on LWA and assume that the depth is fixed. However, it is worth noting that the depth could also be reconfigured to enhance flexibility.

A LWA is an antenna type that uses a waveguide structure to generate radiation by progressively allowing electromagnetic waves to 'leak' out along a length of ℓ_l and width of ℓ_w, as illustrated in Fig. 7. An example of such antenna for FAS is given in [81]. Using a similar approach as in [121], the far-field radiation pattern at $\boldsymbol{\theta}$ and channel k can be derived as

$$g_k\left(\boldsymbol{\theta},\boldsymbol{\ell}\right)=\ell_l\,\mathrm{sinc}\left(\beta_k-\frac{2\pi}{\lambda}\sin\left(\theta_{\rm azi}\right)\cos\left(\theta_{\rm ele}\right)\frac{\ell_l}{2}\right) \times\ell_w\mathrm{sinc}\left(\frac{2\pi}{\lambda}\sin\left(\theta_{\rm ele}\right)\frac{\ell_w}{2}\right), \tag{32}$$

where $\beta_k=\sqrt{\left(\frac{2\pi}{\lambda}\right)^2-\left(\frac{\pi}{\ell_d}\right)^2}$, and ℓ_d denotes the depth of the LWA.[8] If the width of the LWA is small, the radiation pattern along the elevation angle is similar and the far-field radiation pattern can be simplified as [121]

$$g_k\left(\boldsymbol{\theta},\boldsymbol{\ell}\right)=\ell_l\,\mathrm{sinc}\left(\beta_k-\frac{2\pi}{\lambda}\sin\left(\theta_{\rm azi}\right)\frac{\ell_l}{2}\right). \tag{33}$$

[8] In this paper, $\mathrm{sinc}\left(x\right)\triangleq\frac{\sin(x)}{x}$. Therefore, ℓ_l and ℓ_w are introduced to conform to the definition.

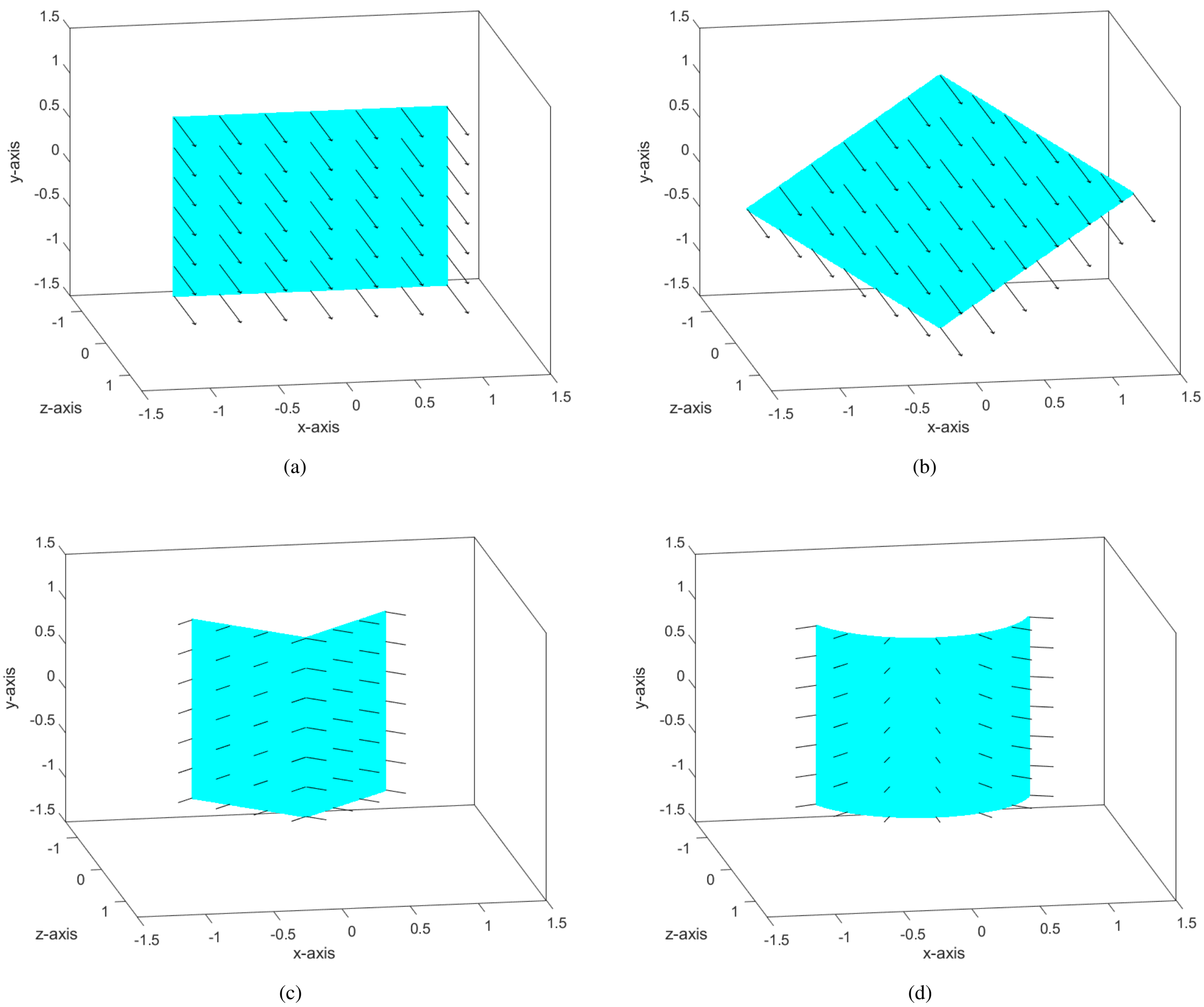

Fig. 3. Examples of a flexible antenna platform in multi-dimensional FAS–The cyan plane represents the antenna platform and the sparse arrow indicates the vector (e.g., coverage) normal to the plane: (a) a flat 2D plane; (b) a rotated 2D plane with $\phi_{\rm rot} = 45$; (c) a folded 2D plane with $\phi_{\rm fold} = -45$; and (d) a deflected 2D plane with $R_{\rm def} = \frac{X\lambda}{\pi} + 0.2$.

Fig. 8 illustrates the radiation gain across different lengths and azimuth angles when the carrier frequency is set to 28 GHz, ℓ_d is fixed at $\frac{\lambda}{2}$ and ℓ_l is varied from 0.01λ to λ. The result indicates that when the azimuth angle is 0°, maximizing the length leads to the highest gain. However, for azimuth angles exceeding $\pm 45^\circ$, there is clearly an optimal length that maximizes the radiation gain, which is neither the maximum nor the minimum length.

Fig. 9 presents the sum-rate of multi-dimensional FAS and TAS with a fixed radiation's length (or fixed-radiation TAS) across different number of users to highlight the benefits of radiation reconfiguration. In this simulation, users are randomly distributed across azimuth angles, with each user assigned a single subcarrier and there is only one dominant path due to the extreme-high frequency. In multi-dimensional FAS, each user can dynamically adjust the length of its radiating elements to optimize its rate while for the TAS case, each user has a single FPA with horizontal polarization. As expected, the sum-rate increases with the number of users in both schemes due to the greater utilization of subcarriers. However, the more interesting observation is that the performance gap between multi-dimensional FAS and fixed-radiation TAS widens as the number of users increases. This highlights the significant advantages of radiation reconfiguration in massive communication or multiuser communication scenarios.

E. Key Research Directions

Following the above explorations, multi-dimensional FAS clearly offers great advantages across various applications and scenarios due to its rich antenna reconfiguration capabilities. The above examples demonstrate that each type of antenna reconfiguration can lead to substantial performance enhancements, and clearly combining multiple reconfiguration capabilities has the potential to further elevate system performance. However, these improvements come with several challenges. Below we identify key research areas that require further exploration and suggest some potential approaches to fully unlock the potential of multi-dimensional FAS.

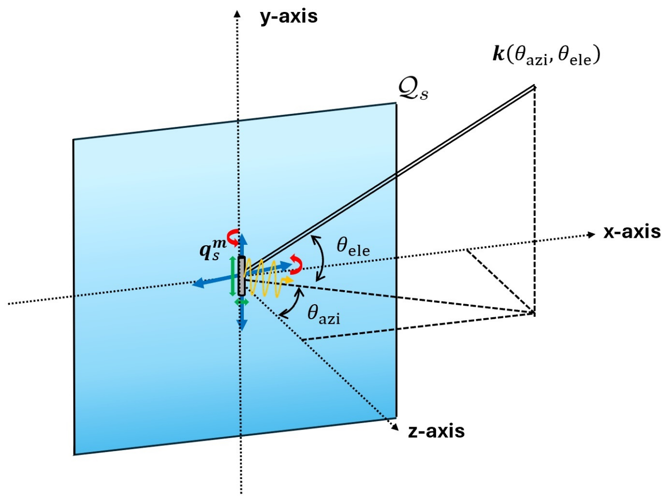

Fig. 4. A flat 2D plane with an impinging plane wave from elevation angle θ_{azi} and azimuth angle θ_{ele}.

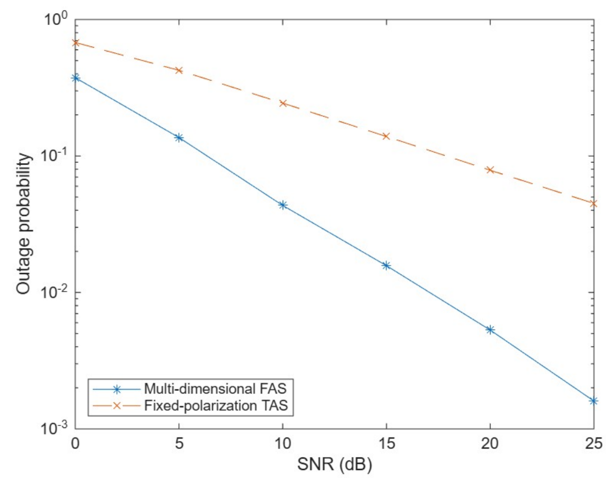

Fig. 6. Outage probability versus SNR.

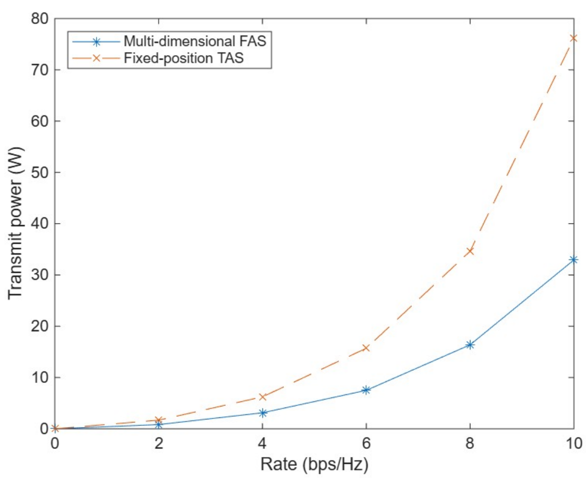

Fig. 5. Average transmit power against the achievable rate.

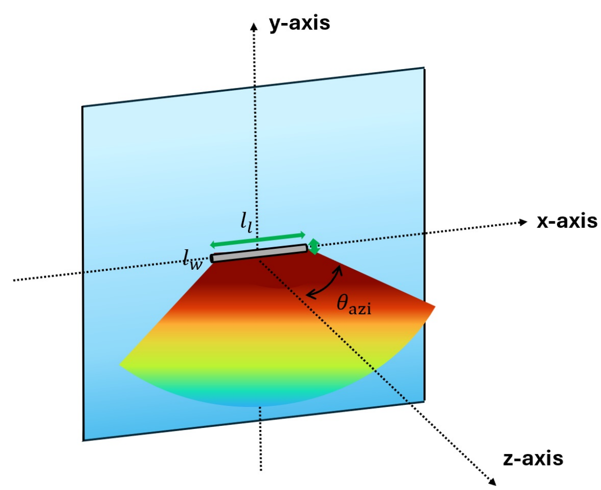

Fig. 7. Radiation with a length of ℓ_l and width of ℓ_w.

1) Optimization and complexity: One of the key challenges is the joint optimization of multiple antenna reconfiguration capabilities, which comes with prohibitive computational complexity. This highlights the importance of evaluating the trade-off between increased complexity and performance enhancement in multi-dimensional FAS. For example, optimizing the position reconfiguration within a discrete set of ports alone can render the optimization problem NP-hard. Further considering other types of reconfiguration—such as polarization, which may be discrete; shape, which potentially offers infinite possibilities; and length, which becomes more complex in multi-carrier systems—adds additional layers of complexity. With so many reconfiguration options, it is much more reasonable to seek for a local optimal solution than a global optimal solution. A more practical alternative is to optimize each reconfiguration using the block coordinate descent method, which optimizes a particular antenna reconfiguration while keeping the other antenna reconfigurations fixed. Within each antenna reconfiguration, convex relaxation, sequential optimization, and other mathematical techniques can be applied to further simplify the optimization problem. In this context, it is also important to investigate the overall algorithm's convergence.

2) Channel estimation and reconstruction: Obtaining full CSI in multi-dimensional FAS is also essential but it presents significant challenges. Unlike traditional TAS with fixed configurations, acquiring complete CSI becomes highly complex due to the various antenna reconfiguration options. To address this, it is important to leverage implicit properties such as channel sparsity, as well as temporal, frequency, and spatial correlations, along with other side information, to reduce the overhead associated with channel estimation. This approach may necessitate the integration of physics-inspired machine learning, antenna and electromagnetic theory, and advanced signal processing techniques. In the context of machine learning and signal processing, both supervised and unsupervised methods can play a pivotal role in identifying non-linear

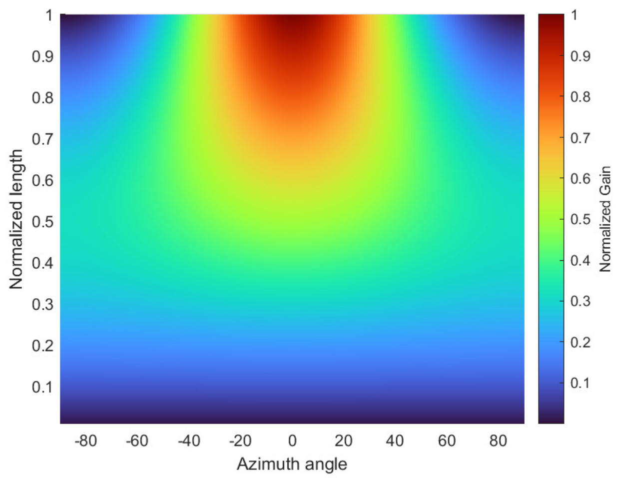

Fig. 8. Normalized radiation gain across varying length and azimuth angles.

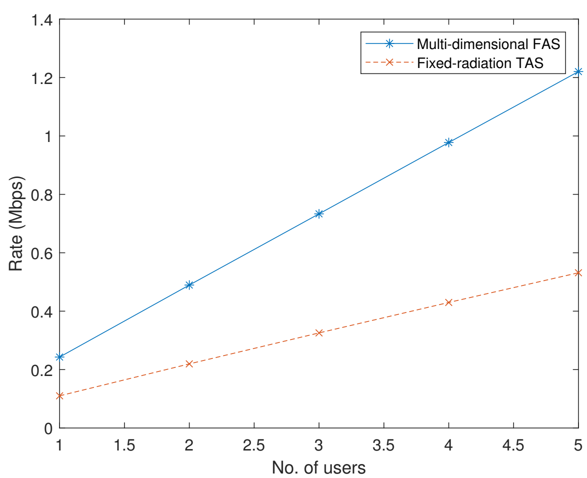

Fig. 9. Sum-rate versus number of users.

characteristics that are not readily discernible through human intuition. In the realm of antenna and electromagnetic theory, existing knowledge of reconfiguration mechanisms, polarization effects, and propagation phenomena can provide valuable insights to the channel estimation and reconstruction process. Compared to conventional approaches, these strategies could significantly reduce the number of channel estimations required. In fact, only a few channel estimation steps should be performed, while the remaining channel parameters should be reconstructed using the identified implicit properties through methods such as interpolation or extrapolation, offering a more efficient solution to the full CSI acquisition problem.

3) Applications and scenarios: It is vital to investigate how specific antenna reconfiguration strategies play a more critical role in certain scenarios and applications. More precisely, not all antenna reconfigurations deliver substantial gain regardless of the channel conditions. Thus, certain antenna reconfiguration can be excluded in specific scenarios to lessen channel estimation for more efficient data transmission. For example, if the number of multipath components is limited, the position of the antennas could remain fixed, as altering their location would not provide significant spatial diversity. If depolarization effects are negligible, polarization reconfiguration can be omitted since orientation misalignment would have minimal impact. Likewise, if the time period for acquiring full CSI is limited, we can either exploit uncoordinated communication strategies or fix the antenna configurations for more robust performance. Compared to TAS, these scenarios still provide valuable insights into the advantages of multi-dimensional FAS. Thus, by selectively leveraging only the most impactful reconfiguration, multi-dimensional FAS can strike a balance between complexity and performance, tailoring its adaptability to the demands of the communication environment.

4) NGMA: Obtaining full CSI can be challenging and often incurs high overhead. Intriguingly, multi-dimensional FAS can advance uncoordinated communication strategies with superior interference immunity. For instance, position reconfiguration can naturally mitigate interference by exploiting fading effects, a principle utilized in FAMA [122], [123], [124], [125], [126], which will be elaborated in subsequent sections. Inspired by this, other forms of antenna reconfiguration may also simplify interference managament problems. For instance, they could enable techniques like blind interference alignment or inspire novel interference cancellation methods. Hence, investigating antenna reconfiguration to mitigate interference presents an exciting and promising research direction.

5) Hardware development: In general, developing a practical multi-dimensional FAS is challenging; however, achieving all the aforesaid antenna reconfigurations simultaneously is not impossible. To date, various antenna technologies such as liquid metal, mechanical movable antennas, RF-pixel reconfiguration, metasurfaces, conformal metamaterials, and DMA or LWA, have gained significant attention, with several FAS prototypes already developed using these technologies, e.g., [76], [77], [81], [82]. Inevitably, each of these technologies has its own advantages and limitations. For instance, liquid-metal and movable antennas may suffer from high latency and increased energy consumption during reconfiguration. RF-pixel and metasurface antennas can be affected by complex mutual coupling, while conformal metamaterials, DMAs, and LWAs may be subject to physical limitations or additional antenna constraints. Therefore, we encourage researchers and engineers to explore a broader range of antenna technologies to enable position-flexible and shape-flexible antenna structures, rather than restricting their efforts to a limited set of existing designs. It is important to recognize that FAS is not confined to a specific implementation but may encompass a wide range of reconfigurable antenna technologies.

6) Commercialization and Standardization: From an industrial perspective, the value of multi-dimensional FAS lies not only in its performance gains and unique features but also in its ability to overcome practical deployment challenges. Its benefits must outweigh drawbacks such as signaling overhead, larger spatial requirements, and robustness issues across diverse scenarios. Therefore, future work should also address issues such as the cost-effectiveness of scalable fabrication and integration, the challenges of embedding FAS into compact devices or BSs, and the trade-off between reconfiguration flexibility and the added complexity of signal processing, calibration, and control. Interoperability and standardization readiness are equally critical as FAS must coexist with TAS for backward compatibility, while new signaling, feedback, and protocol elements must be developed for inclusion in IEEE 802.11 and the 3rd Generation Partnership Project (3GPP).

Also, it is essential to examine specific use cases in which different reconfiguration dimensions offer the greatest benefits. For instance, polarization reconfiguration may be particularly advantageous in RIS and unmanned aerial vehicle (UAV) applications, while shape reconfiguration can enhance adaptability in IoT or wearable devices. Furthermore, position and size reconfiguration may prove more effective for NGMA, radar, and ISAC systems. In addition, AI can play a pivotal role in enabling multi-dimensional reconfiguration and in assessing the suitability of different use cases through experiments and data-driven analysis. Addressing these considerations will clarify the industrial relevance of multi-dimensional FAS and support its evolution from a conceptual innovation to practical deployment in next-generation wireless systems.

In summary, the multi-dimensional reconfiguration capabilities of FAS provide a powerful means to enhancing performance in wireless communication systems. By leveraging key reconfigurations and employing strategies tailored to specific scenarios, FAS can effectively adapt to dynamic environments and address critical challenges in future wireless networks. In the next section, we will delve into its applications, and explore how FAS can revolutionize wireless communication systems when integrated with other emerging 6G technologies.

III. Integration of FAS and Other NGRA Systems with Emerging 6G Technologies

To meet the ambitious goals of 6G networks, the integration of multiple advanced technologies is essential. Understanding how FAS and other NGRA systems can be combined with emerging technologies is crucial for the development of 6G networks. In this section, we will explore how FAS and other NGRA systems can be integrated with some of the cutting-edge technologies such as RIS, NGMA, NTN, ISAC, and AI to further improve the performance of wireless networks. While FAS is primarily used as an example in our discussion, it is important to emphasize that the same principles can be applied to other NGRA systems without any loss of generality.

A. FAS-RIS Framework

1) Introduction: One technology that is anticipated to play a key role in 6G is RIS [127], [128]. RIS is a transformative technology consisting of large arrays of controllable metasurface elements that can manipulate the reflection, refraction, and scattering of electromagnetic waves, hence with the ability to engineer the propagation environments. It has the potential to restore coverage, achieve high spectral and energy efficiency in wireless networks, making it a promising solution [129], [130], [131]. By optimally adjusting the phase shifts of these elements, RIS can direct and focus radio wave signals toward desired locations, thereby providing DoF that does not exist before for a wide range of wireless applications. The technology has matured quickly over the past few years [132] and the European Telecommunications Standards Institute (ETSI) already launched an Industry Specification Group (ISG) for the formal standardization of RISs in 6G in 2021 [133].

In general, there are three main types of RIS architectures: passive, active, and hybrid, as explained below.

- **Passive RIS**: This architecture composed of only passive elements that can control the phase shifts of its elements to reflect and scatter incident electromagnetic waves. The key advantages of passive RIS include high array gain, low cost, low power consumption, and negligible noise [127], [128], [132]. However, passive RIS is typically effective only when the RIS link is sufficiently strong or when the direct link between the transmitter and receiver is too weak to communicate [134], [135], [136].
- **Active RIS**: To address this limitation, [137] has proposed an active RIS. Unlike passive RIS, an active RIS composes of elements with amplifiers that not only control the phase but can also amplify the reflected signals, making them suitable for scenarios with severe double path loss effect at the expense of higher cost [138].
- **Hybrid RIS**: Hybrid RIS combines both passive and active elements, enabling passive phase shifting and selective signal amplification [139]. This architecture provides a balance between power consumption and performance, while also addressing issues related to estimation of the cascaded channel matrices [140].

While FAS and RIS are two independent technologies, there are many exciting opportunities for synergy. For example, RIS provides reconfigurable structures in the environment while the antenna reconfiguration enabled at the base station (BS) and/or users expands the signal dimensionality within the allowable space at the terminals for greater DoF. The FAS concept can also be introduced into designing more powerful RISs when the reflecting elements can be flexible. Nonetheless, challenges in synergizing RIS and FAS include channel estimation, signal processing optimization, coordination between terminals, and co-existence amongst different RIS operators. Here, we offer insights into how some of the challenges RIS face might be addressed through FAS, and discuss what opportunities ahead when we contemplate the synergy between RIS and FAS.

2) Recent advancements: While RIS is asserting itself as a core enabling technology for 6G, there are concerns regarding its scalability. In particular, despite many advances in channel estimation for RIS, e.g., [141], [142], [143], it is not clear if the performance gain will ever justify the added complexity. There is also doubt how RISs from cross-operators coexist and avoid messing up with one another's optimized reflection. To overcome this, FAS can be really useful. One of the earliest works to discuss the integration of RIS, FAS and MIMO was [68] in which RISs are repurposed as DASSs. The main idea is that even if the phase shifts of RIS are randomly chosen, it is actually still performing beamforming but the beamforming is just not yet optimized towards the desired user. Nonetheless, with FAS at the user, the antenna reconfiguration can enable the 'random' beamforming to become effective. That is to say, the FAS can be reconfigured to access the position where the

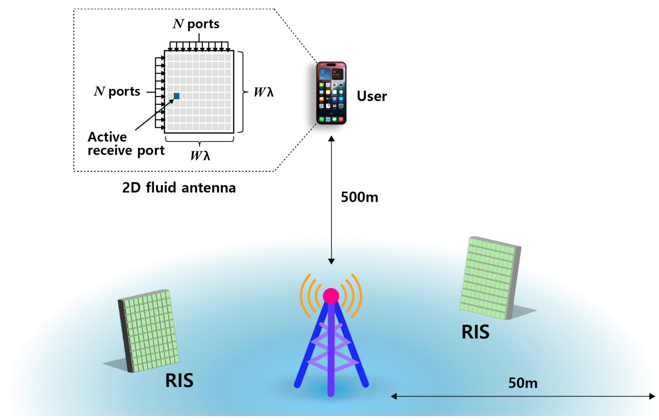

Fig. 10. A FAS-RIS communication scenario with RIS as DASS.

random beamforming from RIS happens to make the multipath add constructively at the user, so the beamforming is no longer 'random'. This approach significantly reduces optimization complexity, facilitates coexistence, and enhances the scalability of RIS. Another interpretation is that RIS as DASS provides the rich scattering conditions for FAS or FAMA to thrive, as explained in [101]. The unique advantage is that unlike conventional RIS schemes where CSI is mandatory at both the BS and RIS, FAMA eliminates the need for channel estimation and complex optimization processes. In [101], it was reported that FAMA with 20 randomized RIS units can support up to 64 users without BS precoding nor RIS optimization. This approach not only addresses the complexity issues at both the RIS and BS, but also facilitates massive connectivity.

Evidently, if RIS can afford CSI estimation and the complexity for intelligent reflect-beamforming, this will combine more effectively with FAS at the users. This was first studied in [144] using a Gaussian copula approach assuming the absence of a direct link and that the phase shifts of RIS are optimized perfectly. Later [145] proposed a comprehensive framework to jointly consider transmission design for both CSI-based and CSI-free schemes. Two approximations for the corresponding outage probabilities of the systems were introduced, and their system throughputs were maximized. The results have shown that the RIS-assisted FAS can significantly outperform the TAS counterpart (i.e., when the number of ports $N = 1$), validating the effectiveness of the strategies. Similar observations made for different setups can be found in [146], [147], [148].

Beyond passive RIS, active RIS can also be integrated with FAS. In [149], the authors explored whether FAS or active RIS plays a more important role in wireless communications. They proposed an algorithm to optimize the transmit beamforming vector, the reflection coefficients, and fluid antenna positions to maximize the user's rate. Their findings illustrated that FAS is more beneficial in simpler scenarios with fewer reflecting elements or transmission paths, whereas active RIS becomes more significant in more complex environments with numerous reflecting elements or transmission paths. It is possible to reduce the complexity for optimzing RIS-aided FAS by using only statistical CSI. In [150], the authors adopted the grating-lobe effect to obtain closed-form solutions for beamforming by exploiting only statistical CSI. In [151], a Newton Raphson based optimizer was proposed for the FAS-RIS framework.

There is also the promising direction to utilize FAS at the BS for index modulation that can work well with RIS to enhance the system spectral efficiency [152]. Besides, integrating FAS with RIS can improve physical layer security. For example, [153] is one of the first studies to investigate the integration of FAS with RIS for secrecy communications. In [153], the authors derived analytical expressions for secrecy metrics, and it was shown that FAS outperforms TAS in terms of secrecy performance, as the diversity gain provided by FAS, along with the enhanced signal directionality from RIS, results in a more secure transmission. Similar results have also been reported in [154] even when the eavesdropper is equipped with FAS.

On the other hand, the integration of FAS and RIS can be done within the RIS. This is the fluid RIS (FRIS) concept that was proposed in [155] and [156]. The idea is to design RIS with position-flexible elements, a.k.a. 'fluid' elements, that can enhance the performance of RIS without necessarily increasing the number of elements. In scenarios with discrete RIS phase shifters, the study highlights the importance of finding the optimal pattern for these phase shifters, focusing upon the phase distribution of the cascaded transmitter-RIS-receiver channels. By reconfiguring the positions of the RIS fluid elements, the system can achieve optimal alignment and eliminate phase offsets, bringing performance close to that of RIS with continuous phase shifters. More recently, fluid-based RIS designs with pattern reconfigurability have been introduced. Instead of relying on fixed element responses, these architectures allow the radiation patterns to adjust in real time according to the propagation environment, thereby tailoring the interaction with incoming signals. Achieving this flexibility requires more complex element designs, often leveraging advanced hardware such as pixel-level reconfiguration to realize dynamic control of the radiation patterns [248].

Apart from these, there is also the notion of making RIS a dynamic propagation medium [157]. Surface wave communication is a more controlled communication strategy that makes radio waves glide along and stays with a reconfigurable surface as the propagation goes, causing much less or no interference in the air, and having greater energy efficiency. In [68], the potential for such paradigm in 6G was discussed, illustrating the great benefits of using RIS as a reconfigurable waveguide to mitigate the effects of path loss and blockage. The path loss and surface impedance models have recently been presented in [158], [159]. Note that in a broad sense, the idea of using RIS as a reconfigurable surface-wave platform is well within the definition of FAS as it reconfigures its characteristics for better meeting the communication needs.

3) Case study for FAS-RIS: In this subsection, we examine a scenario where multiple RISs function as DASS. Specifically, the received signal of the u-th user can be modeled as

$$y_u = \boldsymbol{b}_u^T \underbrace{\left(\sum_{\forall s} \sqrt{\beta_{s,u}} \boldsymbol{H}_{s,u} \boldsymbol{\Theta} \boldsymbol{h}_{a,s} \sqrt{\beta_{a,s}} + \boldsymbol{h}_{a,u} \sqrt{\beta_{a,u}} \right)}_{\boldsymbol{h}_{\mathrm{RIS}}} x + \eta, \tag{34}$$

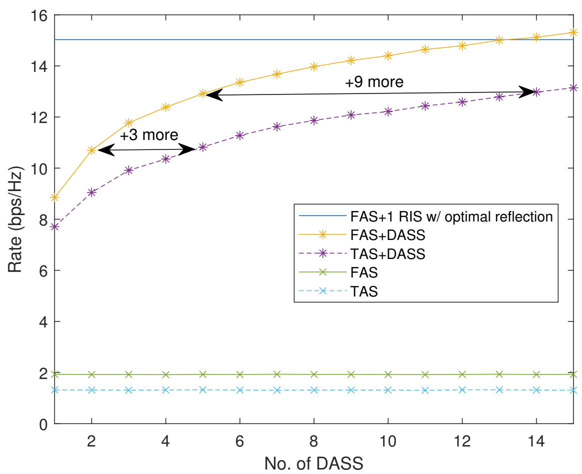

Fig. 11. Rate performance against the number of DASSs.

where $\boldsymbol{h}_{a,u}$, $\boldsymbol{h}_{a,s}$, and $\boldsymbol{H}_{s,u}$ represent the respective channels from the BS-to-user, BS-to-RIS, and RIS-to-user, while $\boldsymbol{\Theta} = \mathrm{diag}\left(e^{-j\theta_1}, \dots, e^{-j\theta_M}\right)$ denote the RIS reflection coefficients. Also, $\beta_{a,u}, \beta_{a,s}$, and $\beta_{s,u}$ are the pathloss from the BS-to-user, BS-to-RIS, and RIS-to-user, respectively, while $\boldsymbol{b}_u$ is the activation port vector, x is the information signal with $\mathbb{E}\{|x|^2\} = P$, and η is the additive white Gaussian noise (AWGN) with noise power spectral density of N_0. For ease of expositions, let us denote $\boldsymbol{h}_{\mathrm{RIS}} = \left[\begin{array}{ccc} h^1_{\mathrm{RIS}} & \cdots & h^N_{\mathrm{RIS}} \end{array}\right]^T = \sum_{\forall s}\sqrt{\beta_{s,u}}\boldsymbol{H}_{s,u}\boldsymbol{\Theta}\boldsymbol{h}_{a,s}\sqrt{\beta_{a,s}} + \boldsymbol{h}_{a,u}\sqrt{\beta_{a,u}}$.

To optimize performance, user u should activate the port with the highest gain, i.e., $\boldsymbol{b}^*_u = \boldsymbol{e}_{n^*}$ and the optimal port $n^* = \arg\max_n |h^n_{\mathrm{RIS}}|^2$. The rate of the u-th user is then[9]

$$R_u = \log\left(1 + \frac{P\left|\boldsymbol{b}^{*T}_u\boldsymbol{h}_{\mathrm{RIS}}\right|^2}{N_0}\right). \tag{35}$$

As shown in Fig. 10, the BS is positioned at the origin, and the user is located 500 meters away. Furthermore, S number of DASSs are randomly distributed over a semi-circular area with a radius of 50 meters to mitigate severe path loss. Each DASS is equipped with $M = 100$ reflecting elements, while the BS is equipped with a single FPA, and the user is equipped with a 2D fluid antenna. The 2D fluid antenna has a surface area of $(W\lambda)^2$, where $W = \frac{1}{2}$ and $N = 100$ ports. We assume a finite scattering model with a Rice factor of 7 for line-of-sight (LoS) path and 2 non-line-of-sight (NLoS) paths. The path loss exponent for the direct link is set to 4, while the exponent for the RIS link is 2.5. The transmit power P is 30 dBm and the noise level N_0 is -80 dBm. It is noted that as RISs are repurposed as DASS here, there is no complexity involved in channel estimation and optimization for RISs.

The rate performance results are provided in Fig. 11. As we can see, FAS provides only marginal rate gain over TAS in the absence of DASS, primarily due to limited spatial diversity in strong LoS channels. However, when RIS is tasked as DASS, FAS achieves a significantly higher rate gain than TAS as the number of DASSs increases. Remarkably, increasing the number of DASSs sufficiently can even surpass the performance of a single RIS with optimal reflection. Note that while deploying DASS requires more RIS, it does not require any coordination among the RIS, nor does it add complexity to the channel estimation process, which remains comparable to the case without RIS. For example, with a surface area of $(W\lambda)^2$, approximately $\lfloor 2W+2 \rfloor^2$ channel estimates are sufficient as $N \to \infty$ [160]. Therefore, if $W = \frac{1}{2}$, only 9 channel estimates are needed for FAS. In contrast, RIS with optimal reflection requires about $2M = 200$ times more channel estimates for the single RIS link, along with $M = 100$ optimal reflection coefficients. In addition, a FPA requires only 1 channel estimate but it delivers inferior performance as the number of DASSs increases. To compare their performance, for instance, to achieve 11 bps/Hz, TAS would require 3 more DASSs, and to reach 13 bps/Hz, it requires 9 more DASSs than FAS. Hence, FAS offers an efficient performance with significantly reduced channel estimation, coordination, and optimization complexity as the number of RISs increases.

4) New opportunities and challenges: Overall, there appear to be three common approaches for effectively integrating RIS with FAS. The first approach involves implementing FAS at the transmitter side, such as the BS, at the receiver, such as the users, or at both ends, while considering the presence of one or more RISs. To optimize network performance, both active and passive beamforming can be jointly configured, along with the selection of transmit and receive ports. Unlike TAS, FAS can dynamically adjust the positions of its radiating elements, thereby enhancing the array gain [161] and effectively utilizing both the RIS and direct transmission links. The RIS reflecting coefficients can be intelligently reconfigured to improve the desired signal or to mitigate interference [162]. Also, a fluid antenna user can reconfigure its port to ensure optimal signal reception [88], [144]. The key advantage of this approach is the ability to harness an M^2-gain, where M represents the number of reflecting elements. However, the major bottleneck lies in the channel estimation and optimization process. Specifically, the channel estimation overhead can be extremely high [163], and solving the optimization problem is highly challenging as the number of RISs or elements increases.

The second approach involves integrating FAS directly into the RIS structure itself. Given that RIS phase shifts are typically discrete in practical implementations, the introduction of reconfigurable position elements within RIS can eliminate phase distribution offsets, significantly improving system performance while reducing manufacturing complexity and cost [155], [156]. To maximize performance in this approach, it is essential to determine the optimal pattern for discrete phase shifts, considering the locations of the elements and phase distribution of the cascaded channels. Furthermore, reconfiguring the positions of the elements can also help to improve the resolutions of the discrete phase shifts, allowing them to more closely approximate continuous phase shifts. In addition, shape reconfiguration can also be considered for RIS. This approach can potentially be implemented using conformal metasurfaces, which allow shape reconfiguration without compromising their functionalities or designs [164]. This enables the optimization

[9] Unless otherwise stated, $\log(\cdot)$ denotes the base-2 logarithm.

of both the RIS and the spatial distribution of its elements, while adhering to the constraints imposed by the shape [165]. Intuitively, other antenna reconfigurations and technologies, such as polarization reconfiguration, size reconfiguration, and surface wave technology, could also be incorporated into RIS, although the overall benefits deserve proper investigation.

In the third approach, RIS can be utilized as DASS, where no CSI is needed for the cascaded channel, and no phase shift optimization is required [101], [166]. Evidently, this approach only provides an M-gain, which means that more RIS units are required to achieve performance gains. However, no coordination is required and the channel estimation can be performed as though the RIS were absent, which significantly simplifies implementation and reduces operational complexity, making it much easier to deploy in real-world and large-scale scenarios with multiple operators co-existing. Moreover, using RIS as DASS introduces spatial diversity, which complements the FAS implementation and further enhances network robustness. Therefore, this approach is particularly advantageous in future wireless networks where RIS are deployed at high densities, as it minimizes the overhead and computational burden associated with cascaded channel estimation, as well as the coordination and optimization of multiple RIS units.

B. FAS-led NGMA

1) Introduction: To enable extreme massive connectivity in 6G, effective interference management strategies are essential. Existing multiple access methods can be classified into orthogonal and non-orthogonal transmission strategies. Well-known orthogonal multiple access (OMA) strategies include:

- **Frequency-division multiple access (FDMA) [167]:** In FDMA, the frequency spectrum is divided into many non-overlapping frequency bands, with each user assigned to a specific band for communication. This prevents interference, as each user operates on a separate frequency.
- **Time-division multiple access (TDMA) [168]:** This scheme allows all users to share the entire bandwidth, but separate in time slots. Each user is allocated a specific time slot for data transmission or reception, ensuring synchronized communication without interference.

Non-orthogonal transmission strategies include:

- **Non-orthogonal multiple access (NOMA) [169]:** This approach permits several users to share the same time and frequency resources by superimposing their signals. One key technology in this scheme is successive interference cancellation (SIC), where receivers decode and subtract stronger signals from other users before decoding their own. NOMA enhances spectral efficiency by letting multiple users communicate simultaneously in the same resource block, supporting diverse user needs, such as high data rates and low-latency requirements.
- **Rate-splitting multiple access (RSMA) [170]:** RSMA splits each user's message into two parts: i) common message that can be decoded by multiple users and ii) a private message intended for a specific user. The common message is transmitted in such a way that it can be decoded and canceled by other users, while the private message is only decoded by the intended user. RSMA optimizes the allocation of information between the common and private messages, offering great flexibility.

It is worth stating that for NOMA and RSMA to function under the best conditions, power control and user clustering are important. Additionally, it is worth mentioning other multiple access methods, such as space division multiple access (SDMA) and location division multiple access (LMDA) [171], which adopt multiple antenna technologies to distribute users strategically in the spatial domain. The above list only includes some popular examples but is not meant to be complete.

Existing multiple access systems in previous and current generations are primarily based on OMA. But as 6G seeks to meet stringent requirements—such as ultra-low latency, high reliability, and massive connectivity—non-orthogonal transmission strategies are becoming increasingly appealing. The shift towards more advanced techniques, known as NGMA, will be crucial in achieving these goals [15]. To achieve this, FAS can not only enhance existing multiple access techniques but also enable new non-orthogonal strategies, such as FAMA or compact ultra massive antenna array (CUMA). We discuss how multiple access can be elevated through FAS below.

2) Recent advancements: The advent of FAS can not only give more spatial DoF in existing multiuser MIMO technologies [172] but also pave the way for innovative uncoordinated or non-coherent transmission methods.[10] Specifically, [122] is among the pioneering studies to propose a transmitter CSI-free multiple access scheme based on FAS, known as FAMA. The scheme in [122] is now regarded as fast FAMA [173], [174], [175], in which each FAS-equipped user optimizes its position on a symbol-by-symbol basis to maximize the instantaneous signal-to-interference-plus-noise ratio (SINR). Subsequently, a simpler scheme, referred to as slow FAMA [123], [176], [177], is proposed, where the user's antenna position is changed to obtain the highest average SINR whenever channel conditions fluctuate. Unlike fast FAMA, slow FAMA is more practical as it is much easier to identify the best position, a.k.a. port, and requires less frequent switching (only once during a coherence period). Evidently, slow FAMA has less DoF than the fast version which is expected to outperform slow FAMA if done correctly. Overall, the main principle of FAMA is to deal with interference as noise while allowing the receiver to access an opportunistic spatial moment for communication, ensuring that interference vanishes through deep fading.[11] In general, there are three main types of FAMA: fast FAMA [173], [174], [175], slow FAMA [123], [176], [177], coded FAMA [125], [126] and some combinations of them. There is also the variant of slow FAMA called CUMA [124], [166], [178] that chooses to activate a large number of ports for reception and then mixes the signals in the analogue domain for performance gain.

Several works have investigated the performance of FAMA. For example, [177] analytically derived the outage probability of FAMA via a two-stage approximation. Besides, [179] ex-

[10]For non-coherent transmission, we mean the method that does not need CSI at the transmitter side. The terms 'uncoordinated transmission' and 'non-coherent transmission' are used interchangeably in this paper.

[11]This strategy relies on interference coming from different source antennas, and can thus be viewed as an interference mitigation technique.

plored the integration of opportunistic scheduling with FAMA, a.k.a. opportunistic FAMA. Specifically, the authors derived the multiplexing gain of the opportunistic FAMA network, examined the required number of users in the pool to achieve a given multiplexing gain, investigated the required outage probability at each user for achieving a given network multiplexing gain, and analyzed the rate of increase of the multiplexing gain with respect to the number of users in the pool. Furthermore, [180] proposed utilizing decentralized reinforcement learning (RL) to autonomously select robust users and antenna ports to ensure efficient performance of opportunistic FAMA.

In this multi-agent RL framework, they also proposed a novel team-theoretic RL framework which includes a derivative network estimating the reward derivative with respect to the actions, efficiently guiding the multi-agent learning of each solution's policy networks. Regarding CUMA, it was revealed in [166] that randomized RISs can help scramble the channels to mimic rich scattering conditions to maximize the benefits of FAMA. The results in [178] further showed that if more RF chains are available at each user, then CUMA can deliver much greater performance. Note that CUMA at the users can greatly reduce the burden of acquiring CSI at the BS for spatial multiplexing. In [69, Section V-E], it was illustrated that the BS only needs to have the LoS channel information for precoding if CUMA is adopted at the users responsible for mitigating the inter-user interference. The results in that paper indicated that more than a thousand of users can be supported with very simple precoding requiring only statistical CSI and each user with a 2-RF chained FAS applying CUMA.

On the other hand, FAS can elevate other emerging multiple access techniques such as NOMA and RSMA. For example, [181] has explored the applications of FAS to enhance multiple access schemes like OMA and NOMA. The study reveals that FAS not only enhances the performance of these schemes but also discovers that OMA without CSI at the transmitter side in FAS (a non-coherent strategy) can outperform NOMA in TAS, highlighting new avenues for performance improvement. Also, it can be observed that FAS-NOMA achieves the best performance, followed by FAS-OMA, FAS-OMA without CSI, TAS-NOMA, and lastly TAS-OMA. Similar findings, albeit without non-coherent transmission strategies, are observed in the uplink [182]. An extension to the multi-antenna case has also been addressed in [183]. Most recently, RSMA has been integrated into FAS to further enhance the performance and it was shown that FAS-RSMA can outperform FAS-NOMA in certain scenarios [184], [185]. One explanation for the massive improvement in NOMA and RSMA by FAS is that it greatly improve the SINR for the first data stream (or the common message in the case of RSMA). From the implementation side, FAS can be pivotal to make NOMA and RSMA practical in the sense that heavy channel coding is no longer required to protect decoding before SIC is conducted. Note that a great deal of the rate gain of NOMA and RSMA might have lost if heavy error-correction coding needs to be applied.

The combination of FAS and NOMA has also found some niche applications. In [186], the authors analyzed the use of NOMA in FAS with a focus on short-packet communications, deriving the average block error rate and demonstrating that the diversity order for each user in FAS can scale with the number of preset locations (or ports). Moreover, the findings suggest that the performance gains achieved through FAS may even surpass those achieved with NOMA alone. Additionally, [187] investigated the outage probability of FAS alongside other state-of-the-art technologies such as cooperative NOMA, millimeter-wave, and full-duplex communications, while also accounting for hardware imperfections. Later, a similar advanced work was considered in [188]. Specifically, the authors explored a system for ISAC, where the users utilize FAS and NOMA, and considered integrated sensing with backscatter communication (ISABC), where a dual-functional BS not only communicates with two NOMA users equipped with FAS but further senses the environment surrounding a backscatter tag. Unlike traditional ISAC, the backscatter tag reflects signals from the BS to the NOMA users. These extra signals enhance the communication performance of the two users. During the sensing phase, the BS extracts environmental information from the reflected backscatter signal. Overall, existing studies reveal great potential of FAS for the development of NGMA.

Despite a strong indication that FAMA can handle interference without relying on the CSI at the transmitter side like precoding, NOMA and RSMA do, little is known regarding the capacity achievability of FAMA in general wireless channels. An attempt was made in [189] considering a two-user interference channel with both users equipped with FAS using slow FAMA. The results show that FAMA can achieve a sum-rate comparable to the Han-Kobayashi FAMA scheme in the two-user case, if the channel can be reconfigured to a noise-limited regime. This implies that treating interference as noise can be optimal if FAS can find a port with weak interference. However, in the case of strong interference channels, in which FAS cannot locate any port with weak interference, treating interference as noise becomes suboptimal. In such scenarios, non-unique decoding could prove highly beneficial [190].

Experimental results validating FAMA have recently been reported in [76] using liquid-metal based antennas, [81] using a metamaterial-based design and [82] using RF pixels.

3) Case study for FAS-NGMA: To demonstrate the benefits of FAS in NGMA, we consider a scenario where the BS with $M > 1$ FPAs[12] serves U users over a wireless channel. The received signal of the u-th user is given by

$$y_u = \boldsymbol{b}_u^T \left(\sqrt{\beta_u} \boldsymbol{H}_u \boldsymbol{x} \right) + \eta, \tag{36}$$

where $\boldsymbol{H}_u$ represents the channels from the BS to user u, β_u denotes the path loss from the BS to the u-th user, and $\boldsymbol{x} = \sum_{u=1}^{U} \boldsymbol{w}_u x_u$ represents the linearly precoded transmit signal. Specifically, $\boldsymbol{w}_u$ and x_u are the beamforming vector and the information-bearing signal, respectively, for the u-th user. For brevity, we consider SDMA and power-domain NOMA.

In SDMA, the rate of the u-th user is given as

$$R_u^{\rm SDMA} = \log \left(1 + \frac{\beta_u \left| \boldsymbol{b}_u^T \boldsymbol{H}_u \boldsymbol{w}_u \right|^2}{\sum\limits_{\forall u'} \beta_u \left| \boldsymbol{b}_u^T \boldsymbol{H}_u \boldsymbol{w}_{u'} \right|^2 + N_0} \right). \tag{37}$$

[12] In this paper, the terms 'TAS' and 'FPA' are used interchangeably.

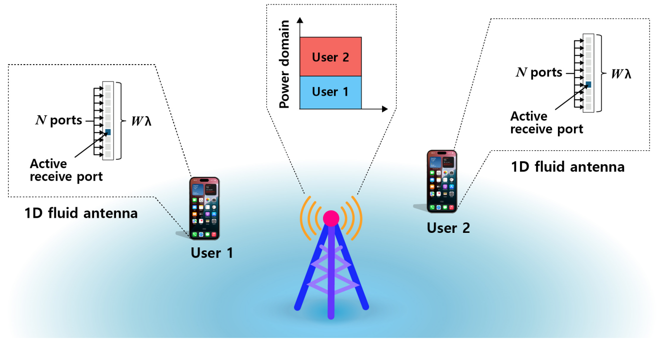

Fig. 12. FAS with NGMA.

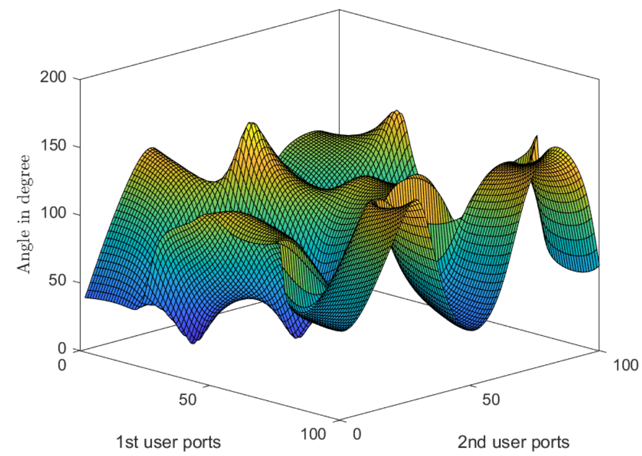

Fig. 13. Channel correlation versus port indices.

In NOMA, we assume that the users are indexed according to the SIC policy ψ so that the u-th user performs SIC for $U-u$ preceding users before decoding its own signal. Consequently, the rate of the u-th user is given as

$$R_u^{\text{NOMA}} = \log\left(1+\frac{\beta_u\left|\boldsymbol{b}_u^T\boldsymbol{H}_u\boldsymbol{w}_u\right|^2}{\sum\limits_{u'<u}\beta_u\left|\boldsymbol{b}_u^T\boldsymbol{H}_u\boldsymbol{w}_{u'}\right|^2+N_0}\right). \tag{38}$$

In this scenario, we minimize the total transmit power of the BS via optimal beamforming and active ports while ensuring that each user satisfies their minimum rate requirements. The optimization problem can be formulated as

$$\min_{\boldsymbol{w}_u,\boldsymbol{a}_u,\forall u} \quad \sum_{\forall u}\left\|\boldsymbol{w}_u\right\|^2 \tag{39a}$$
$$\text{s.t.} \quad R_u^m \geq R_u^{\min}, \forall u, \tag{39b}$$
$$\boldsymbol{b}_u \in \left\{\boldsymbol{e}_1,\ldots,\boldsymbol{e}_N\right\}, \forall u, \tag{39c}$$

where (39a) evaluates the total transmit power of the BS, (39b) ensures that each user satisfies a minimum rate requirement, (39c) makes sure that only one of the ports can be activated, and $m\in\{\text{SDMA},\text{NOMA}\}$. Generally, it is very difficult to solve (39) within polynomial time because it is an NP-hard problem. Nonetheless, the global optimal solution of (39) can be obtained through an exhaustive search over all possible combinations of N^U active user ports and second-order cone programming [191]. Note that given the active ports $\boldsymbol{b}_u,\forall u$, (39) becomes solvable within polynomial time.

To maintain tractability, we consider a scenario where the BS has $M=2$ FPAs serving $U=2$ users, as shown in Fig. 12. Unless stated otherwise, each user is equipped with a 1D fluid antenna featuring $N=100$ ports uniformly distributed along a length of $W\lambda$ with $W=2$. Moreover, the path loss of the u-th user is normalized to $\frac{1}{u}$ for ease of computation, and each user has minimum rate requirement of $R_u^{\min}=1,\forall u$. The channels are generated based on a rich scattering environment model. Given the active ports $\boldsymbol{b}_u,\forall u$, the channel correlation between the u-th user and the u'-th user is measured as

$$\text{corr}_{u,u'} = \arccos\left(\frac{\left\langle\boldsymbol{b}_u^T\boldsymbol{H}_u,\boldsymbol{b}_{u'}^T\boldsymbol{H}_{u'}\right\rangle}{\left\|\boldsymbol{b}_u^T\boldsymbol{H}_u\right\|\left\|\boldsymbol{b}_{u'}^T\boldsymbol{H}_{u'}\right\|}\right). \tag{40}$$

With this, the channels can be referred to as fully correlated at 0° or 180° and completely orthogonal at 90°.

As suggested by the results in Fig. 13, FAS can dynamically reconfigure user channels. This flexibility allows the channels between different users to be either correlated or orthogonalized. Consequently, users can select ports with channels that are either strongly correlated or nearly orthogonal, depending on the multiple access scheme. Nevertheless, it is important to note that the globally optimal ports may not necessarily be those with strong correlation or near-orthogonality. Instead, the global optimal port selection depends on factors such as beamforming, channel gain, and interference.

In Fig. 14, we assess the performance of SDMA and NOMA over different number of ports. Here, we consider a maximum of 5 ports for tractability. As shown, FAS achieves up to 7–10 dB gain over TAS with FPAs as the number of ports increases, thanks to the additional spatial diversity. It is important to recognize that while the performance of FAS-SDMA appears to approach that of FAS-NOMA in this scenario, this simple setup is insufficient to conclude that the performance gain of NOMA over SDMA in FAS is marginal. In fact, a more comprehensive investigation is required to accurately assess the relative advantages of multiple access schemes in FAS. Our objective here is rather to demonstrate that performance of the multiple access can be enhanced through FAS, paving a potential way for more advanced NGMA development.

4) New opportunities and challenges: In general, there are two promising directions to explore multiple access in FAS. One direction is to empower existing coherent transmission strategies with additional DoF using FAS. As shown, position reconfiguration alone can introduce the new capability of adjusting the channels to a certain degree, creating additional spatial diversity to enhance the performance of existing multiple access schemes. However, optimizing the multiple access in conjunction with antenna reconfigurability adds complexity to the optimization process. For instance, while (39) is solvable within polynomial time for TAS, it becomes intractable for FAS. Also, the optimization problem for performing multiple access in TAS becomes even more complex when considering multi-carrier systems, rate splitting techniques, or optimal SIC policies, and this complexity is further amplified in FAS.

Beyond position reconfigurability, additional antenna reconfiguration approaches could offer further performance gains for multiple access schemes with a higher cost of complexity. FAS also facilitates the realization of certain previously overlooked transmission strategies. For example, interference alignment strategy originally designed for time-varying channels in [192] can now be applied in FAS, even under time-invariant conditions. By reconfiguring the antenna position, user channels can be adaptively adjusted, increasing the feasibility of interference alignment. These schemes are known to be more optimal in interference channels and their feasibility could be revisited in FASs. While enhancing existing coherent transmission strategies may be a fruitful direction as it improves the spectral efficiency and energy efficiency, it is important to note that supporting large-scale user deployments remains challenging, as these strategies often require estimating high-dimensional channel coefficients, which directly limits scalability.

This challenge motivates another promising line of research, which is the exploration of new non-coherent transmission strategies. While non-coherent strategies are generally ineffective for TAS, their importance increases with the number of users because relying on CSI at the BS for large-scale user deployments quickly becomes impractical. As a consequence, non-coherent transmission becomes essential, with the objective shifting from achieving high data rates per user to supporting low data rates for massive connectivity. Innovations namely FAMA and CUMA exemplify the unique potential of FAS. Specifically, by opportunistically accessing spatial moments where interference is minimized, FAS can significantly enhance multiuser communication performance. More advanced concepts, such as channel coding [125], [126], can be developed by adapting strategies to specific scenarios or considering other antenna reconfiguration techniques.

Moreover, the concept of blind interference alignment, as introduced in [193], could be leveraged within FAS to optimize performance in device-to-device applications or small-scale networks. Beyond non-coherent strategies, transmission approaches based on statistical CSI also show great promise, as they can efficiently support large user bases while minimizing overhead costs—ideal for scenarios demanding extensive connectivity. It is worth pointing out that while non-coherent strategies hold substantial potential for future wireless communications, developing highly efficient non-coherent transmission strategies has historically been challenging.

C. FAS-NTN Framework

1) Introduction: To achieve ubiquitous connectivity across land, sea, air, and space, satellites and unmanned aerial vehicles (UAVs) have become key components of future wireless systems, driving the development of NTN [194]. An NTN typically consists of a terrestrial terminal, an aerial station, a service link, and a gateway that connects the NTN to the core network through a feeder link [195]. The *aerial station* can be further classified into two types: satellites and UAVs.

Satellites are categorized based on their orbital altitude, which are explained as follows [196]:

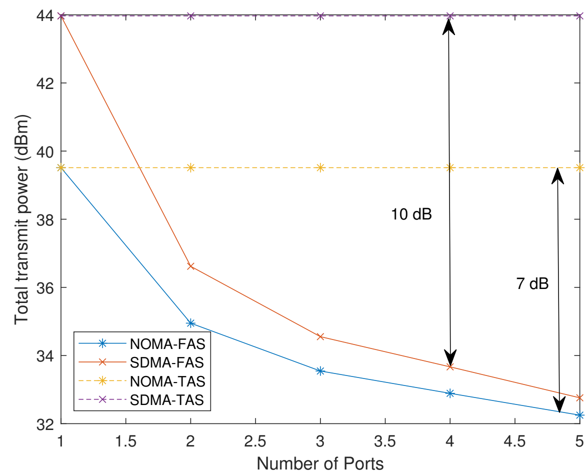

Fig. 14. Total transmit power versus the number of ports.

- **Low-earth orbit (LEO)**: LEO satellites operate at altitudes between 200 km and $2,000$ km, offering lower latency and a better link budget. However, their limited coverage requires deploying a large constellation of satellites to achieve global connectivity.
- **Medium-earth orbit (MEO)**: MEO satellites, positioned at altitudes ranging from $8,000$ km to $20,000$ km, strike a balance between latency and reliable communication links, making them versatile for a range of applications.
- **Geostationary earth orbit (GEO)**: GEO satellites, stationed at an altitude of $35,786$ km above the Earth's equator, provide extensive geographical coverage and are typically visible to terrestrial nodes. However, the significant distance introduces higher delays and attenuation.

UAVs can be classified into two categories [197]:

- **High-altitude platform UAVs (HAP-UAVs)**: They operate in the stratosphere at altitudes of approximately 20 km, and offer rapid deployment capabilities covering wide geographic areas, often spanning hundreds of kilometers. These platforms are a cost-effective and flexible alternative to terrestrial nodes, particularly in rural and remote regions where traditional infrastructure is unavailable. However, HAPs face sustainability challenges, such as maintaining stable positioning and ensuring efficient re-fueling. Examples include balloons and kites.
- **Low-altitude platform UAVs (LAP-UAVs)**: They fly at low altitudes, around a few 100 meters. They are good for their cost-effectiveness, flexibility, and adaptability. LAPs are increasingly utilized to provide broadband wireless connectivity during disasters, temporary events, and as relays for terrestrial nodes. Their on-demand deployment provides significant advantages in energy efficiency and mobility compared to fixed terrestrial infrastructures.

In addition to serving as aerial stations, LAP-UAVs, such as drones, can also function as *aerial users* in diverse applications, including precision agriculture, delivery services, construction monitoring, intelligent transportation systems, and sports analytics [198]. These versatile applications enable operators to generate new revenue streams while positioning drones as valuable tools across numerous industries.

Unlike TAS, FAS allows NTNs to further enhance network performance by dynamically reconfiguring both large-scale and small-scale fading effects. Nonetheless, the high-altitude operation and reconfiguration across different time scales introduce new challenges, necessitating innovative and practical solutions to ensure reliable and efficient performance.

2) Recent advancements: Existing studies have explored the integration of FAS into NTN networks. As discussed in [199], the authors positioned their work as one of the earliest explorations into movable antenna-aided satellite communications. They proposed a joint optimization of antenna positioning and beamforming to enhance satellite beam coverage and mitigate interference, taking into account satellite orbits and coverage requirements within a specific time interval. Also, interestingly, they introduced a low-complexity scheme that utilizes an optimized common antenna position across all time slots. Compared to TAS, the proposed scheme can significantly decrease the interference leakage and increase the average signal-to-leakage ratio of satellite-ground links.

One of the pioneering researches exploring trajectory optimization for multiple flexible antennas is [91]. This study employs AI-driven optimization, leveraging generative diffusion models as the key technology. The results demonstrated that this approach effectively optimizes sum-rate and energy efficiency, offering significant advantages over traditional techniques such as RL. This leads to the idea that FAS in NTN can be used to dynamically reconfigure both large-scale and small-scale fading effects. Consequently, [200] integrated FAS into UAV relay. This study incorporates NOMA and further enhances channel performance by jointly optimizing the active port, power allocation, and UAV altitude to maximize user sum-rate. The findings demonstrated that FAS consistently outperforms TAS. More importantly, the synergy between NOMA and FAS significantly benefits from the joint optimization of both small-scale and large-scale fading, leading to improved performance in UAV communications.

Moreover, the extension to multiple fluid antennas has been investigated in [201]. In particular, the authors maximized the sum-rate by jointly optimizing transmit beamforming, UAV trajectory, and antenna positions. Compared to TAS with fixed configurations, significant performance gains are observed. In addition, [202] examined the integration of RIS mounted on UAVs. While the RIS elements remain fixed in position, the authors considered that this strategy introduces a new DoF by allowing adjustments to the UAV's position and orientation. Their findings highlighted that UAV orientation significantly affects user SNR and that user distribution plays an important role in the effectiveness of the joint optimization. In [203], a low-complexity alternating algorithm was proposed.

Furthermore, position and orientation reconfiguration have also been explored in [204] for UAVs acting as aerial users. The study assumed that the antennas can mechanically move within a defined region, and the orientation of the panel is also mechanically adjustable. These reconfigurations are utilized to mitigate interference from co-channel terrestrial transmissions to the UAV. The results showed that such antenna reconfiguration can significantly enhance the received SINR of the UAV compared to fixed configurations. However, it is important to note that the effects of polarization and depolarization were not considered in [203], [202], [204]. For this reason, we refer to these adjustments as orientation reconfiguration.

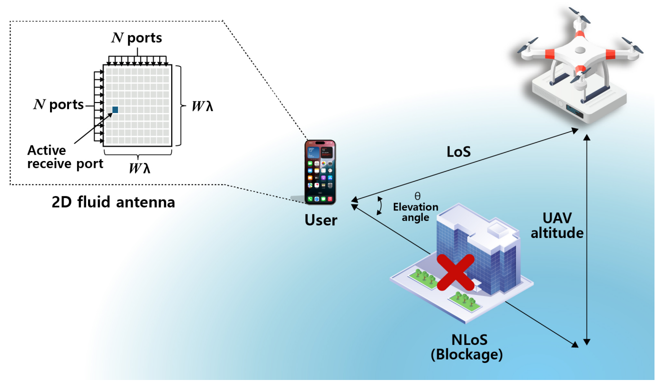

Fig. 15. FAS in NTN.

3) Case study for FAS-NTN: As illustrated in Fig. 15, we analyze a simple scenario involving an aerial BS and a FAS user to illustrate the unique characteristics of FAS in NTN. Before delving into the results, let us briefly review the unique properties of air-to-ground channel modeling [205]. The large-scale fading between the aerial BS and the FAS user can be characterized by a probabilistic LoS and NLoS model [200].

Specifically, the probability of LoS is given by

$$P^{\rm LoS}=\frac{1}{1+\mu e^{\nu(\theta-\mu)}},\tag{41}$$

where μ and ν are constants determined by environmental factors [206]. The elevation angle between the aerial BS and the user is expressed as

$$\theta=\tan^{-1}\left(\frac{|z_0-z_u|}{\hat{d}}\right),\tag{42}$$

where z_0 and z_u represent the heights of the aerial BS and the user, respectively, and $\hat{d}$ is the horizontal distance between them. By contrast, the probability of NLoS is given by

$$P^{\rm NLoS}=1-P^{\rm LoS}.\tag{43}$$

The path loss exponent is modeled as a function of the NLoS probability and is expressed as

$$\alpha=\alpha_{\rm NLoS}P^{\rm NLoS}+\alpha_{\rm LOS},\tag{44}$$

where $\alpha_{\rm LOS}$ is the path loss exponent for the LoS condition, and $\alpha_{\rm NLOS}$ represents the additional attenuation of the path loss exponent in the NLoS condition. Additionally, the Rician K-factor should be modeled as a function of the elevation angle. Specifically, it is expressed as

$$K=k_{\rm min}e^{\left(\frac{2}{\pi}\ln\left(\frac{k_{\rm max}}{k_{\rm min}}\right)\theta\frac{\pi}{180}\right)},\tag{45}$$

in which $k_{\rm max}$ and $k_{\rm min}$ denote the maximum and minimum values of the Rician K-factor, respectively. It can be observed that as the elevation angle θ increases, both the probability

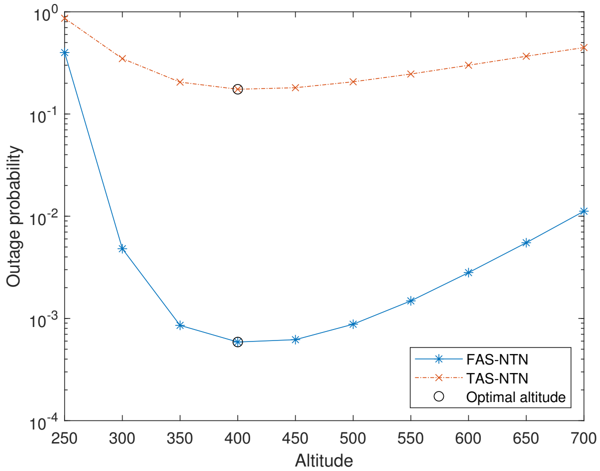

Fig. 16. Outage probability versus the altitude.

of LoS and the Rician K-factor increase. The user's outage probability is characterized as

$$\mathbb{P}\left\{\log\left(1+\frac{P\left|\boldsymbol{b}^{*T}\boldsymbol{h}_{\mathrm{NTN}}\right|^2}{N_0}\right)<R_{\min}\right\}, \tag{46}$$

where $\boldsymbol{b}^*=\boldsymbol{e}_{n^*}$ is the optimal activation vector that provides the highest gain for $\boldsymbol{h}_{\mathrm{NTN}}$. Here, $\boldsymbol{h}_{\mathrm{NTN}}$ captures both the large-scale and small-scale fading effects between the aerial BS and the FAS user. Consequently, both the elevation angle and spatial diversity play significant roles in $\boldsymbol{h}_{\mathrm{NTN}}$, setting it apart from TAS in terrestrial networks.

Fig. 16 shows the outage probability of the FAS user across varying altitudes. In this analysis, the aerial BS is assumed to be positioned at the origin and equipped with a single FPA, while the user is located 300 meters horizontally from the origin. The channel and antenna parameters are configured similarly to those in [200]. As shown, there exists an optimal altitude at which the outage probability for both TAS-NTN and FAS-NTN is minimized. More interestingly, FAS-NTN reveals an additional performance gain over TAS-NTN as it approaches the optimal altitude, while the performance gain is reduced at extremely low or high altitudes. This observation highlights the benefits of FAS in NTN, driven by the joint reconfiguration of both large-scale and small-scale fading.

4) New opportunities and challenges: From the discussions above, particularly in light of recent advancements, a gray area emerges regarding the classification of FAS, as both satellites and UAVs are capable of adjusting their positions and orientations. In this paper, we emphasize that FAS should primarily focus on the reconfigurability of the antenna itself, rather than the position or orientation of the terminal. Otherwise, the random position and orientation of a mobile device could also be classified as FAS, which somewhat diverges from its original motivation. However, the perspective might align with the philosophy of other NGRA systems.

In the context of FAS, we observe that joint reconfiguration at both macroscopic scales (e.g., large-scale fading) and microscopic scales (e.g., small-scale fading) can be effectively leveraged to achieve additional performance gains, making FAS uniquely suited to the development of NTN. While this paper provides an example based on varying the altitude, it is anticipated that similar performance gains can be achieved through trajectory planning when more practical NTN channel models are considered [207]. However, it is important to note that the reconfiguration of large-scale and small-scale fading typically occurs on different timescales. For instance, the position and orientation reconfiguration of an aerial station or aerial user generally takes place over a few seconds, while antenna reconfiguration typically operates on a few milliseconds or less. Therefore, jointly optimizing the additional DoF in FAS-NTN requires both statistical information (e.g., mean or variance) and instantaneous full CSI, making the optimization problem much more complex compared to TAS-NTN.

Furthermore, achieving full coverage in the sky and effectively managing strong interference remain critical challenges in NTN. For example, an aerial node may cause interference to a massive number of terrestrial nodes while simultaneously experiencing significant interference from multiple terrestrial nodes. Additionally, an aerial user could find itself positioned at the null of the associated BS antenna's radiation pattern. Reconfiguring the antenna platform, as well as the position and polarization of the radiating elements at the BS or user, can help improve coverage and overcome strong interference. Other forms of antenna reconfiguration, such as radiation pattern and beamwidth, also hold great promise for advancing NTN. For instance, [208], [209] have shown that antenna reconfiguration can enhance coverage, mitigate interference, and reduce the overhead associated with coordinated interference management schemes (e.g., inter-cell interference coordination or joint transmission). Moreover, concepts from FAS-NGMA could also prove beneficial for NTN development.

D. FAS-ISAC Framework

1) Introduction: In 6G networks, a new paradigm known as ISAC has been introduced, which combines the functionalities of wireless communication and radar sensing into a unified system. By sharing frequency bands and hardware, ISAC significantly enhances spectrum efficiency while reducing costs, positioning it as a cornerstone of next-generation wireless networks [210], [211]. Leveraging advanced technologies such as millimeter-wave, orthogonal frequency division multiplexing (OFDM), and massive MIMO, ISAC systems facilitate real-time, high-resolution data processing and sensing within a single framework. This unified approach is indispensable for a wide range of use-cases, including autonomous vehicles, smart homes, Wi-Fi sensing, and extended reality [212]. This integration makes ISAC a future-ready enabler for the seamless operation of next-generation technologies.

To understand the current developments, the ISAC research can be broadly divided into two streams [210]:

- **Device-free ISAC:** This architecture relies on passive sensing, without the need for the target to actively send or receive signals, and is thus particularly suitable for radar systems in applications such as object detection [213] and tracking in autonomous vehicles [214]. The benefit of this configuration is reduced interference, which is applicable to both monostatic and bistatic radar settings.

- **Device-based ISAC:** This architecture will involve active participation of devices communicating with a BS while self-localizing, facilitating accurate real-time positioning [215]. It can be employed in both cooperative and non-cooperative environments, and is suitable for indoor navigation [216], emergency response, and situations where both communication and positioning are required.

In this context, FAS has emerged as a promising technology to jointly enhance communication and sensing performance of ISAC [217]. FAS leverages position-flexible shape-flexible antenna structures, introducing new DoF for spatial diversity and enabling dynamic adjustments to its RF properties for optimized signal quality. However, despite its benefits, integrating FAS into ISAC systems is not trivial. These include real-time non-convex optimization for port selection, achieving accurate beamforming and channel estimation, and managing resources efficiently in multiuser environments. Here, we shed light on the challenges, strategies, and opportunities for unlocking the full potential of FAS-ISAC in future 6G networks.

2) Recent advancements: ISAC systems have garnered significant attention for their ability to address spectrum congestion while simultaneously supporting communication and sensing functions. Nonetheless, TAS with fixed configurations are inherently limited in spatial DoF and are unable to fully optimize performance. To overcome this limitation, researchers have turned to FAS to enhance ISAC performance. Unlike TAS, FAS can dynamically adjust their shape and positions to reconfigure communication and sensing channels, leading to significant improvements in overall system performance.

Several studies have investigated FAS-ISAC. For instance, [218] proposed a FAS-ISAC framework, where a BS equipped with multiple fluid antennas communicates with users and also detects targets. The optimization of fluid antenna position and dual-functional beamforming under perfect and imperfect CSI was discussed, highlighting the advantages of FAS over fixed-position TAS. Similarly, [219] explored the use of fluid antennas to redefine the ISAC trade-off by introducing an ISAC model that incorporates fluid antenna capabilities. The study optimized transmission beamforming and port selection to minimize power consumption while satisfying both communication and sensing requirements. In addition, [220] studied the joint optimization of antenna position and waveform design, introducing an efficient algorithm to maximize the sum-rate in FAS-ISAC. This approach significantly reduces computational complexity, saving at least 60% of computational resources compared to traditional methods such as particle swarm optimization, while effectively optimizing fluid antenna positions and waveform design to enhance sum-rate performance.

To address the challenges in multiuser ISAC systems, [172] used deep RL (DRL) to optimize fluid antenna port selection and precoding design in multiuser MIMO environments. The study highlighted the potential of DRL for joint optimization of antenna configurations and precoding strategies, even with imperfect CSI. The results showed significant improvements in system performance, demonstrating the effectiveness and applicability of DRL in FAS-ISAC. Extending this concept, [221] examined the position reconfiguration of FAS for communication and sensing functions in both BSs and communication users. Through joint optimization of beamforming and position reconfiguration, the system was shown to outperform TAS-ISAC. Moreover, [222] introduced a FAS with integrated sensing, communication, and computing (ISCC) functionalities for vehicular networks. In this study, an integrated latency optimization problem is formulated to jointly optimize computing resources, receive combining matrices, and antenna positions. The proposed FAS-ISCC revealed notable improvements in resource utilization and reduced latency, demonstrating the versatility of fluid antennas in supporting multifunctional systems beyond sensing and communication.

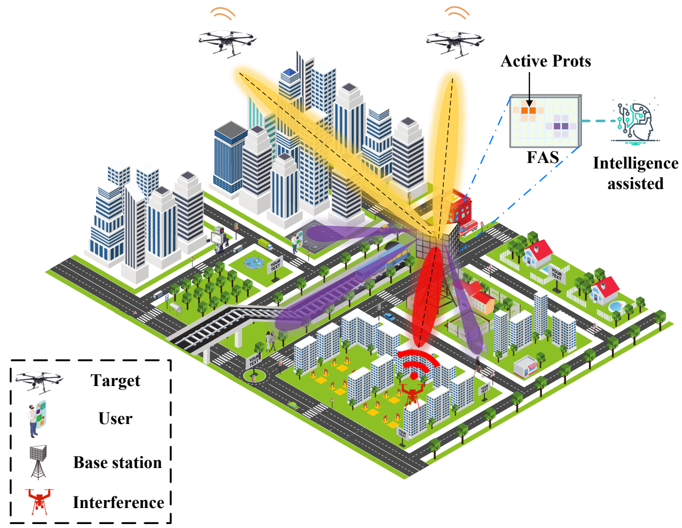

Fig. 17. FAS with ISAC.

As mentioned before, both NOMA and ISAC can be integrated into FAS. In [188], the use of fluid antenna in backscattering scenarios was explored to enhance both sensing and communication. The study showed that combining FAS with NOMA could provide significant performance improvements in both communication rates and sensing accuracy, surpassing fixed-position TAS. Lastly, [223] explored the potential of FAS-ISAC in the near-field by utilizing large-scale transmission and reflection surfaces (XL-STARS) to optimize both sensing and communication performance. The proposed optimization framework effectively balances communication quality while minimizing sensing performance metrics, showcasing the superiority of FAS in advanced ISAC applications.

Overall, research into FAS for ISAC is rapidly advancing, with numerous contributions demonstrating the potential of fluid antenna technology to enhance communication and sensing performance across various scenarios, including multiuser systems, vehicular networks, and near-field communications. These advances pave the way for more efficient and flexible integrated systems, addressing the growing demand for spectrum and resource utilization in modern wireless networks. Besides, it is noteworthy that FAS works well in OFDM settings [224], [225] although further studies are required.

3) Case study for FAS-ISAC: To demonstrate the advantages of FAS, we explore its potential for balancing sensing and communication in ISAC systems here. As illustrated in Fig. 17, let us consider a multicast ISAC scenario where the BS transmits a common signal to U users and utilizes the echo signal to perform sensing on potential targets. The BS is equipped with M fluid antennas (or active radiating elements), where N ports are uniformly distributed along a linear space, and each user is equipped with a FPA. The received signal of the u-th user can be expressed as

$$y_u = \boldsymbol{h}_u^H \boldsymbol{w} x + \eta, \tag{47}$$

where $\boldsymbol{h}_u$ is the channel from the BS to the u-th user, $\boldsymbol{w}$ is the beamforming vector, x is the communication signal, and η is the AWGN with noise level N_0. Since only M ports out of N are activated, the constraint $\|\boldsymbol{w}\|_0 = M$ is required, where $\|\cdot\|_0$ denotes the zero-norm. Accordingly, the communication SNR for the u-th user is given by

$$\gamma_{c,u} = \frac{\left|\boldsymbol{h}_u^H \boldsymbol{w}\right|^2}{N_0}. \tag{48}$$

Also, consider a co-located monostatic MIMO radar with N_r receive antennas uniformly distributed along a linear space. The echo signal received at the radar sensing receiver is

$$\boldsymbol{y} = \boldsymbol{A}\boldsymbol{w}s + \boldsymbol{\eta}, \tag{49}$$

where $\boldsymbol{A} = \boldsymbol{a}_r(\theta)\,\boldsymbol{a}_t^H(\theta)$ represents the sensing channel matrix, $\boldsymbol{a}_r(\theta) = \left[1 \cdots e^{-j2\pi(N_r-1)\triangle_r \sin(\theta)}\right]^T$ is the receive steering vector, and $\boldsymbol{a}_t(\theta_t) = \left[1 \cdots e^{-j2\pi(N-1)\triangle_t \sin(\theta)}\right]^T$ is the transmit steering vector, and $\boldsymbol{\eta}$ is the AWGN of the radar. The average sensing SNR can then be found as

$$\gamma_s = \frac{\|\boldsymbol{A}\boldsymbol{w}\|^2}{N_0}. \tag{50}$$

Let us minimize the total transmit power under the constraints of the minimum sensing SNR requirement, $S_{\min}$, the minimum communication SNR requirement, $R_{\min}$, and the number of activated ports. That is to say, we have [219]

$$\min_{\boldsymbol{w}} \quad \|\boldsymbol{w}\|_2^2 \tag{51a}$$
$$\text{s.t.} \quad \gamma_s \geq S_{\min}, \tag{51b}$$
$$\gamma_{c,u} \geq R_{\min}, u \in \mathcal{U}, \tag{51c}$$
$$\|\boldsymbol{w}\|_0 = M. \tag{51d}$$

In contrast to traditional multicast ISAC systems, the additional constraint in (51d) enforces that only $M < N$ antenna ports can be activated to generate the ISAC signal.

In Fig. 18, the contour curves illustrate the achieved minimum transmit power under various values of $R_{\min}$ and $S_{\min}$. The results demonstrate that FAS-ISAC achieves significantly lower transmit power compared to fixed-position TAS-ISAC for identical sensing and communication constraints, highlighting a superior trade-off. This improvement arises from the optimization of antenna ports, which enhances the spatial directionality of signals used for both sensing and communication, thereby optimizing the overall ISAC system. These findings emphasize the potential of FAS to improve the ISAC trade-off and expand performance boundaries.

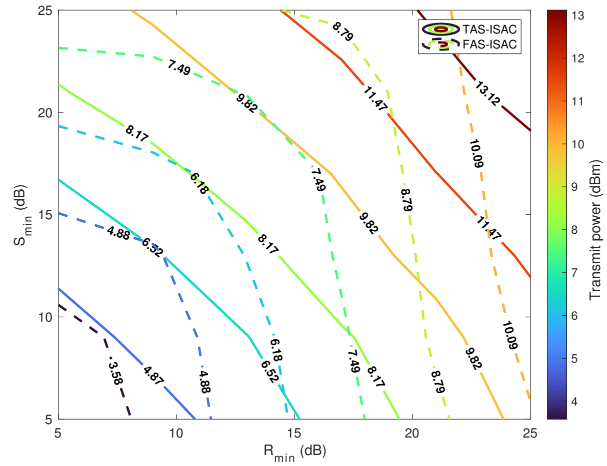

Fig. 18. The trade-off between sensing and communication performance in the considered FAS-ISAC system with $N = 8$, $K = 2$.

4) New opportunities and challenges: The integration of FAS with ISAC presents vast opportunities to enhance system performance and resource efficiency. These technologies complement each other seamlessly as ISAC enables simultaneous communication and environmental sensing, while FAS provides adaptive antenna configurations that dynamically optimize both functions in real-time. As a result, the FAS-ISAC framework can effectively shift the trade-off between sensing and communication performance, offering greater flexibility in balancing these objectives. This synergy is particularly beneficial in dynamic environments, such as autonomous vehicles or 6G networks, where flexibility and precision are essential. In addition, FAS-ISAC can improve sensing accuracy while enhancing privacy, making it an ideal solution for applications in smart cities, industrial IoT, and other advanced scenarios. For example, fluid antennas at the BS can be reconfigured to enhance critical sensing tasks, while fluid antennas at user devices can be adjusted to protect privacy.

However, this integration introduces significant challenges. Designing such a system is highly complex, requiring real-time synchronization and optimization between sensing and communication functions. The simultaneous operation of sensing and communication signals can lead to signal degradation or interference, necessitating advanced techniques such as intelligent beamforming and efficient frequency management. Another challenge is the accurate estimation and modeling of dynamic communication and sensing channels, especially in the presence of various antenna reconfigurations. Furthermore, maintaining energy efficiency in a dynamically reconfigurable antenna system is key, as minimizing the additional power required for antenna adjustments is critical. This is particularly important for mechanical movable antennas or liquid-based antennas, where the energy consumption of motors or pumps can significantly affect overall system performance. Lastly, the integration of sensing functionalities raises potential privacy and security concerns, demanding robust mechanisms to protect user data and ensure system resilience against vulnerabilities.

While FAS offers promising potential to mitigate these issues through its reconfigurability and adaptive capabilities, efficient and practical methods to fully address these challenges remain uncertain and require further exploration.

In short, while the fusion of FAS and ISAC paves the way for advanced, efficient, and flexible systems, addressing the associated challenges in design, interference management, energy efficiency, privacy and security will be vital for unlocking their full potential in future 6G networks.

E. FAS-AI Framework

1) Introduction: The application of AI in wireless communications is rapidly emerging as an inevitable paradigm in 6G networks. Advanced technologies such as deep learning (DL), DRL, and others have demonstrated immense potential in areas such as channel estimation, decoding, coding, signal detection, and beyond. Apparently, AI offers the ability to significantly enhance network performance, optimize resource utilization, and improve network intelligence. As a simple example, AI is expected to enable adaptive resource management by autonomously adjusting network parameters to meet the dynamic demands of large-scale users, thus improving user experiences and ensuring more efficient network operations.

In general, the relevance of AI in wireless communications can be viewed from two complementary perspectives:

- **Wireless communications for AI:** This perspective focuses on tailoring wireless systems to support AI-driven applications. Generally, high-speed and low-latency connections are key for real-time AI inference. To enable seamless interactions between edge devices and the cloud for AI processing, 6G network architectures must be carefully designed. Moreover, IoT serves as a key enabler for collecting vast amounts of data, empowering AI to generate insights beyond human capabilities. Meanwhile, physical layer security adds an extra layer of protection, safeguarding data privacy in federated learning.
- **AI for wireless communications:** This perspective emphasizes the role of AI as a transformative tool to enhance wireless communication systems. More concretely, AI techniques can be employed to predict, optimize, and enhance wireless communication systems across different layers, ranging from the physical layer to the application layer. For instance, AI algorithms can efficiently manage spectrum allocation, power distribution, and user associations in dynamic and complex environments. On the other hand, AI-based models can provide accurate CSI or traffic pattern predictions across different domains, allowing preemptive adjustments to network configurations to improve quality-of-service (QoS).

Presumably, the integration of FAS with AI should elevate these perspectives to the next level. FAS offers significant advantages over TAS by enabling position-flexible and shape-flexible antenna structures that improve network performance and adaptability. However, the implementation of FAS also introduces high complexities to the wireless communication systems. To fully leverage AI-driven applications in FAS, it is essential to first address these complexities. Below we provide examples how AI techniques can be utilized in FAS.

- **AI-enabled prediction:** The efficiency of FAS depends on activating the most suitable ports to ensure optimal channel conditions for communication. However, the high resolution of FAS introduces significant overheads in channel estimation and signal reception. To address this challenge, AI technologies can be leveraged to optimize the channel estimation process using machine learning techniques, thereby reducing the required estimation overhead. For channel extrapolation, acquiring complete and accurate CSI within the coherence time period is a significant challenge for FAS. To overcome this, encoder and attention mechanisms can be utilized to construct basis vectors from the CSI of observable ports. A decoder can then use these vectors along with the local correlations between ports to estimate the CSI of unknown ports. This approach facilitates effective extrapolation from limited observations to complete channel information. Since channel mapping relationships often exhibit nonlinear characteristics, DL is particularly well-suited [226].
- **AI-enabled optimization:** To optimize FAS for a specific performance metric, joint optimization of port selection and beamforming strategies is essential. To this end, DRL can be used to derive optimal strategies for both. A reward function can be defined to quantify the impact of the selected port on overall system performance. For instance, a port that maximizes the strength of the received signal or minimizes the required transmission power could be assigned a positive reward. After each port selection, feedback from the environment is captured in the form of the reward function value. Through iterative updates, the process converges to the optimal port selection strategy based on the DRL principle. The bandit learning framework can also be utilized to address the port selection issue without the instantaneous full CSI in time-varying channel conditions [227]. On the other hand, DL can be adopted to rapidly design optimal beamforming vectors for various services, such as wireless data transmission, wireless energy transmission, and sensing [228], [229].

Regardless of the two complementary perspectives, the exploration of FAS and AI is always beneficial. On one hand, AI acts as a transformative tool to address complex optimization challenges in FAS. On the other hand, the improved network performance achieved through FAS enhances the efficiency of AI applications. However, to fully harness this synergy in 6G networks, it is essential to cultivate a comprehensive understanding of both interdisciplinary fields.

2) Recent advancements: Existing studies have explored the combination of FAS and AI, with some emphasizing on optimizing port selection and channel estimation, while others delving into leveraging FAS to enhance AI applications. For instance, [230] proposed combining AI with fluid antennas to facilitate the system management. Leveraging the strong spatial correlation between ports within a given space, several machine learning-based FAS algorithms have been discussed. These algorithms potentially improve the network rates and channel estimation, even when observations are limited, and greatly outperform the best antenna selection algorithms in multi-antenna systems occupying the same space. This provides compelling practical evidence supporting FAS as an innovative approach to enhancing spatial diversity.

Building upon this work, it has been observed that FAS is also highly effective in multiuser communications. In particular, when the user is equipped with a fluid antenna, FAMA can be employed. The integration of AI with FAMA has been investigated, with [231] highlighting several AI technologies, particularly DL techniques, as promising tools for enhancing FAMA performance. For example, long short-term memory (LSTM) networks can be used to infer the SINR of unobserved ports by treating SINR information as a time (or space) series. This approach, combined with the 'predict, optimize, and plan', referred to as SPO+LSTM, has been proposed in [232] to improve the performance of FAS. Similarly, this technique has been applied in slow FAMA [233]. Specifically, [233] developed a DL-based low-complexity port selection scheme, and it was illustrated that this method can achieve significant reductions in outage probability and improvements in multiplexing gain from relatively few port observations.

Beyond port selection, the integration of FAS and AI can significantly improve the accuracy of channel estimation, reconstruction, interpolation, and extrapolation. This is particularly critical in FAS as the substantial overhead associated with channel acquistion for infinitely many ports could severely impact system performance. To address this, several studies have explored machine learning-based solutions. For instance, [100] examined the challenges of high-resolution channel estimation and discussed how machine learning techniques can efficiently reduce overhead. In [234], machine learning technique was proposed to recover the complete channel from measurements at a limited number of predefined ports, even under varying correlation conditions. In addition, [235] and [236] introduced a successive Bayesian reconstructor that employs kernel-based sampling and regression techniques for channel estimation while [237] presented a model-driven channel extrapolation algorithm based on the theoretical analysis of existing channel models, enabling accurate extrapolation for all ports based on observations from only a small number of ports.

As discussed earlier, AI techniques can be applied in FAS to solve optimal beamforming problems. For example, [172] proposed an end-to-end learning framework utilizing DL for joint optimization problems. By using DL and DRL, real-time decision-making and optimization are achieved in dynamic environments, improving the performance of the FAS-ISAC. Most recently in [238], a DL framework was developed to address the non-convex and multi-fold challenges inherent in optimizing receive beamforming and antenna element positioning. The study formulates the beamforming problem as a Rayleigh quotient, while employing a multi-layer perceptron (MLP) to determine optimal antenna positioning. This DL-based approach offers an effective anti-jamming strategy in communication scenarios with interference sources, enhancing communication efficiency by maximizing the SINR.

Focusing on using FAS for AI, [239] demonstrated how FAS can significantly enhance learning performance by leveraging

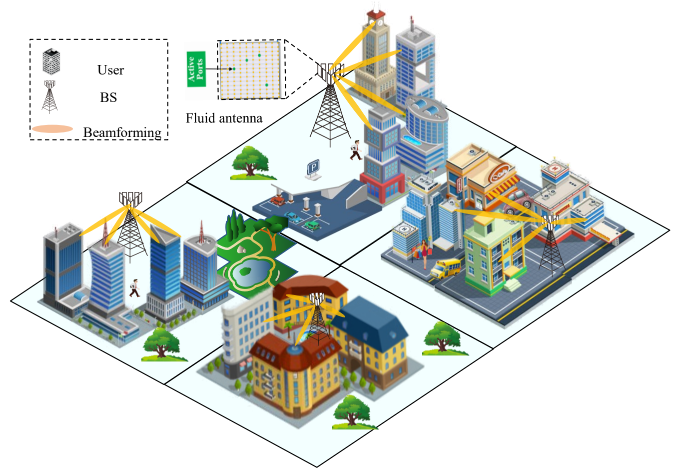

Fig. 19. FAS with AI.

the additional DoF provided by position reconfiguration. The study investigated the convergence of an over-the-air federated learning (OTA-FL) system and analyzed the optimality gap to understand the impact of FAS on learning performance. To minimize the gap in dynamic radio environments, a Markov decision process was utilized and a recurrent deep deterministic policy gradient algorithm was proposed. This approach enhances the reliability of model aggregation and enables real-time decision-making and optimization in dynamic user environments. Moreover, FAS can also facilitate over-the-air computations, facilitating distributed AI and machine learning processing in the wave domain. Specifically, [240] investigated a fluid antenna-enhanced over-the-air computation (AirComp) system, where the transceiver design and the antenna position vector are jointly optimized. The study showed that FAS can greatly reduce the mean squared error (MSE) between the target and estimated function values, outperforming TAS.

Evidently, the combination of FAS and AI has demonstrated its potential across various scenarios. Through the application of AI, FAS can enhance communication efficiency, reduce overhead, and achieve real-time decision-making and optimization in dynamic environments. Conversely, the application of FAS can enhance the learning performance for AI-driven applications, a great potential over the TAS counterpart.

3) Case study for FAS-AI: To showcase the benefits of AI in FAS, we consider a complex optimization problem in multi-cell networks over an extended period of time. The received signal of the u-th user in the c-th cell at time slot t can be expressed as

$$y_{(c,u)}^{[t]}=\sum_{b=1}^{4}\left(\boldsymbol{h}_{b,(c,u)}^{[t]}\right)^{H}\boldsymbol{B}_b^{[t]}\boldsymbol{W}_b^{[t]}\boldsymbol{x}_b^{[t]}+\eta_{(c,u)}^{[t]},\tag{52}$$

where $\boldsymbol{h}_{b,(c,u)}^{[t]}\in\mathbb{C}^{N\times 1}$ represents the complex channel vector from the b-th BS to the u-th user in the c-th cell, $\boldsymbol{W}_b^{[t]}=\left[\boldsymbol{w}_{b,1}^{[t]},\dots,\boldsymbol{w}_{b,U}^{[t]}\right]\in\mathbb{C}^{M\times U}$ denotes the precoding matrix at the b-th BS, $\boldsymbol{x}_b^{[t]}\in\mathbb{C}^{U\times 1}$ represents the transmitted signal of the b-th BS to its U associated users, and $\eta_{(c,u)}^{[t]}$ is the AWGN with a noise level of N_0. When fluid antennas are deployed at

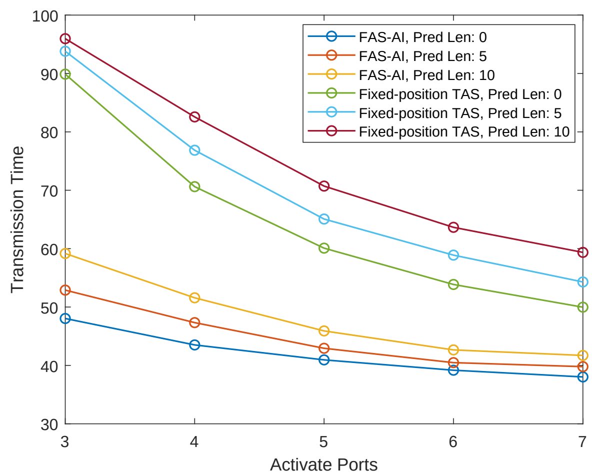

Fig. 20. Transmission time versus the number of active ports.

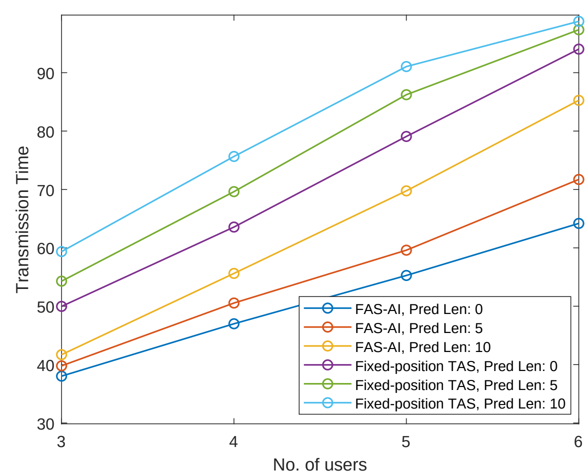

Fig. 21. Transmission time versus the number of users.

the BSs, we have the activation port matrix, $\boldsymbol{B}_b^{[t]} \in \mathbb{R}^{N\times M}$, which defines the subset of active ports at the b-th BS. Without loss of generality, we assume that the u-th user in the c-th cell is associated to the b-th BS if and only if $c = b$. Also, in (52), four cells are assumed. Consequently, the SINR of the u-th user in the b-th cell can be formulated as

$$\gamma_{b,u}^{[t]} = \frac{\left|\left(\boldsymbol{h}_{b,(b,u)}^{[t]}\right)^H \boldsymbol{B}_b^{[t]} \boldsymbol{w}_{b,u}^{[t]}\right|^2}{I_{b,u} + \sum\limits_{b'\neq b} I_{b',u} + N_0}, \tag{53}$$

where

$$I_{b,u} = \sum_{u'\neq u} \left|\left(\boldsymbol{h}_{b,(b,u')}^{[t]}\right)^H \boldsymbol{B}_b^{[t]} \boldsymbol{w}_{b,u'}^{[t]}\right|^2, \tag{54}$$

and

$$I_{b',u} = \left\|\left(\mathbf{h}_{b',(b,u)}^{t}\right)^H \boldsymbol{B}_{b'}^{[t]} \mathbf{W}_{b'}^{t}\right\|_2^2, \tag{55}$$

represent the inter-user interference within the b-th cell and the inter-cell interference from the b'-th cell, respectively. The rate of the u-th user in the b-th cell is given by

$$R_{(b,u)}^{[t]} = \delta B_w \log\left(1 + \gamma_{b,u}^{[t]}\right), \tag{56}$$

where B_w is the system bandwidth and δ is the transmission interval. Overall, this rate represents the maximum transmission rate that can be transmitted to the u-th user in the b-th cell given the transmission interval δ.

As depicted in Fig. 19, this case study considers a multi-cell communication scenario. The scenario involves four square regions, each with a side length of 100 meters. At the center of each cell is a BS with a transmit power of 20 dBm, equipped with a fluid antenna measuring 20 cm $\times$ 20 cm, featuring a 10×10 port distribution. The BS operates at a frequency of 3.4 GHz with a bandwidth of 20 MHz, while users are randomly distributed within each square region. Each user is required to transmit 3 MB of data. The goal is to minimize the total time required for all users in a cell to complete their transmissions by optimizing the selection of ports, power allocation, and precoding across different time slots.

Fig. 20 illustrates the transmission time required to serve a fixed number of users with different numbers of activated ports. In this analysis, 'Pred Len:0' refers to a scenario where no prediction is employed (or a prediction step of 0), meaning that the BS makes decisions based solely on current information. By contrast, 'Pred Len:5' means that the BS incorporates predictions for the next 5 steps into its current decision-making process, with 'Pred Len:10' following a similar logic. As observed, our results demonstrate that transmission time generally decreases as the number of activated ports increases, with the curves converging as the number of activated ports becomes larger. This highlights the additional DoF introduced by position reconfiguration in FAS. On the other hand, Fig. 21 illustrates the transmission time required to serve different number of users with a fixed number of activated ports, set to 7 in this case. The results clearly show that FAS-AI outperforms fixed-position TAS across different user counts, demonstrating the effectiveness of FAS in enhancing system performance and ensuring scalability in dynamic scenarios.

4) New opportunities and challenges: Two compelling directions arise from the integration of FAS and AI. The first direction focuses on leveraging AI to enhance FAS performance. This direction focuses on optimizing the systems where both the BS and users may be equipped with shape-flexible, position-flexible antennas. Promising strategies include using DL for optimization across various reconfigurations and adopting DL models such as masked autoencoders to accurately extrapolate the full CSI. Specifically, advanced AI techniques, such as DL, DRL, and others, can effectively address complex optimization challenges, including combinatorial and large-scale optimization problems. Besides, DL excels at uncovering hidden nonlinear relationships in CSI, enabling accurate reconstruction of full CSI from limited observations. Furthermore, AI's ability to tackle problems without relying on predefined assumptions makes it a general, transformative tool for enhancing system performance in practical environments.

The second direction explores performance enhancements in AI-driven applications compared to TAS. The reconfigurability of fluid antennas can effectively address stringent communication requirements, such as minimizing transmission delays, achieving specific sensing accuracy, and meeting high learning precision in highly complex environments. In addition, emerging concepts such as mobile edge computing, and caching, or directly facilitating computations in the wave domain by leveraging the various reconfigurability in FAS, could further advance AI's capabilities, paving the way for the development of more robust and efficient AI applications.

F. Other Emerging Technologies

There are undoubtedly many other technologies that could benefit from the integration of FAS and other NGRA systems, which are not covered in this article. These include, but are not limited to, full-duplex communications [241], [242], physical layer security [243], [244], [245], wireless power transfer [246], [247], light fidelity (Li-Fi), and quantum technologies. Although we cannot explore all of them in this paper, the main takeaway here is that FAS holds significant untapped potential for enhancing 6G services. For an overview, readers are referred to [69], [92], which outlines the advantages, disadvantages, and open research challenges associated with these technologies. It is important to note that while FAS and other NGRA systems may not substantially improve every performance metric, they can deliver meaningful benefits in specific scenarios. By leveraging new flexibility of antenna reconfigurations, it is possible to achieve considerable performance enhancements without compromising overall system efficiency. As Bruce Lee famously said, "*Water can flow, or it can crash. Be water, my friend.*" In the same spirit, we say, "*Be water, my antenna.*" since FAS can either match or outperform fixed-position TAS, thanks to its supreme flexibility.

IV. Conclusion

This paper introduced FAS with multi-dimensional reconfigurations, an NGRA system that allows dynamic reconfiguration of the antenna platform, position, polarization, and size of the radiating elements to enhance wireless communication performance, representing the original concept of FAS. While this system provides additional DoF and flexibility, acquiring full CSI and optimizing such a system pose significant challenges. Therefore, it is essential to investigate low-complexity yet efficient approaches to enhance network performance. Furthermore, scenarios and applications can be identified where certain antenna reconfigurations can be omitted if their impact is negligible, allowing the focus to remain on reconfigurations that deliver substantial benefits. This system holds significant potential for advancing non-coherent multiple access strategies. Nonetheless, further exploration of materials and antenna design is necessary to develop practical hardware. In addition, we reviewed the integration of FAS and other NGRA systems with emerging technologies. This included a brief introduction to these technologies, an overview of recent advances in their integration with FAS, a case-by-case analysis of the benefits, and a discussion of the new opportunities and challenges they present. Overall, we showed that FAS not only complements other applications and scenarios but also revealed that limited reconfiguration can still achieve significant gains or foster new innovations in communications. Nevertheless, the potential of FAS remains vast, with many possibilities for exploration.

Acknowledgement

We would like to express our heartfelt gratitude to the FAS and NGRA system experts from various domains, including Kin-Fai Tong, Steve Hang Wong, Boyang Liu, Hao Xu, Jiaqi Zou, Hanjiang Hong, Farshad Rostami Ghadi, Noor Waqar, Boyi Tang, Halvin Yang, and Salah Boubkar Salah Abdou, for their invaluable insights, engaging discussions, and thoughtful feedback on various aspects of this paper.

References

[1] J. Mitola, "Cognitive radio for flexible mobile multimedia communications," in *Proc. IEEE Int. Workshop Mobile Multimedia Commun. (MoMuC'99)*, pp. 3–10, 15-17 Nov. 1999, San Diego, CA, USA.

[2] E. Bastug, M. Bennis, M. Medard and M. Debbah, "Toward interconnected virtual reality: Opportunities, challenges, and enablers," *IEEE Commun. Mag.*, vol. 55, no. 6, pp. 110–117, Jun. 2017.

[3] D. Gündüz *et al.*, "Beyond transmitting bits: Context, semantics and task-oriented Communications," *IEEE J. Select. Areas Commun.*, vol. 41, no. 1, pp. 5–41, Jan. 2023.

[4] N. González-Prelcic *et al.*, "The integrated sensing and communication revolution for 6G: Vision, techniques, and applications," *Proc. IEEE*, vol. 112, no. 7, pp. 676–723, Jul. 2024.

[5] V.-P. Bui, S. R. Pandey, A. Casparsen, F. Chiariotti, and P. Popovski, "The role of game networking in the fusion of physical and digital worlds through 6G wireless networks," *IEEE Commun. Mag.*, vol. 63, no. 3, pp. 204–211, Mar. 2025.

[6] International Telecommunication Union - Radiocommunication Sector, "Recommendation ITU-R M.2160-0 M series: Mobile, radiodetermination, amateur and related satellite services - framework and overall objectives of the future development of IMT for 2030 and beyond," *ITU Publications – Recommendations*, Nov. 2023.

[7] C.-X. Wang *et al.*, "On the road to 6G: Visions, requirements, key technologies, and testbeds," *IEEE Commun. Surv. & Tut.*, vol. 25, no. 2, pp. 905–974, Secondquarter 2023.

[8] W. Saad, M. Bennis, and M. Chen, "A vision of 6G wireless systems: Applications, trends, technologies, and open research problems," *IEEE Netw.*, vol. 34, no. 3, pp. 134–142, May/Jun. 2020.

[9] F. Tariq *et al.*, "A speculative study on 6G," *IEEE Wireless Commun.*, vol. 27, no. 4, pp. 118–125, Aug. 2020.

[10] Z. Zhang *et al.*, "6G wireless networks: Vision, requirements, architecture, and key technologies," *IEEE Veh. Technol. Mag.*, vol. 14, no. 3, pp. 28–41, Sept. 2019.

[11] J. G. Andrews, T. E. Humphreys, and T. Ji, "6G takes shape," *IEEE BITS Inf. Theory Mag.*, vol. 4, no. 1, pp. 2–24, Mar. 2024.

[12] E. Basar *et al.*, "Reconfigurable intelligent surfaces for 6G: Emerging hardware architectures, applications, and open challenges," *IEEE Veh. Technol. Mag.*, vol. 19, no. 3, pp. 27–47, Sept. 2024.

[13] L. Dai *et al.*, "Reconfigurable intelligent surface-based wireless communications: Antenna design, prototyping, and experimental results," *IEEE Access*, vol. 8, pp. 45913–45923, 2020.

[14] C. Pan *et al.*, "Reconfigurable intelligent surfaces for 6G systems: Principles, applications, and research directions," *IEEE Commun. Mag.*, vol. 59, no. 6, pp. 14–20, Jun. 2021.

[15] Y. Liu, C. Ouyang, Z. Ding, and R. Schober, "The road to next-generation multiple access: A 50-year tutorial review," *arXiv preprint*, arXiv:2403.00189, 2024.

[16] Y. Xiao *et al.*, "Space-air-ground integrated wireless networks for 6G: Basics, key technologies, and future trends," *IEEE J. Select. Areas Commun.*, vol. 42, no. 12, pp. 3327–3354, Dec. 2024.

[17] F. Liu *et al.*, "Integrated sensing and communications: Toward dual-functional wireless networks for 6G and beyond," *IEEE J. Select. Areas Commun.*, vol. 40, no. 6, pp. 1728–1767, Jun. 2022.

[18] K. B. Letaief, W. Chen, Y. Shi, J. Zhang and Y.-J. A. Zhang, "The roadmap to 6G: AI empowered wireless networks," *IEEE Commun. Mag.*, vol. 57, no. 8, pp. 84–90, Aug. 2019.

[19] J. Zhang, H. Miao, P. Tang, L. Tian, and G. Liu, "New mid-band for 6G: Several considerations from the channel propagation characteristics perspective," *IEEE Commun. Mag.*, vol. 63, no. 1, pp. 175–180, Jan. 2025.

[20] W. Jiang *et al.*, "Terahertz communications and sensing for 6G and beyond: A comprehensive review," *IEEE Commun. Surv. & Tut.*, vol. 26, no. 4, pp. 2326–2381, Fourthquarter 2024.

[21] Z. Wang *et al.*, "Extremely large-scale MIMO: Fundamentals, challenges, solutions, and future directions," *IEEE Wireless Commun.*, vol. 31, no. 3, pp. 117–124, Jun. 2024.

[22] C. Huang *et al.*, "Holographic MIMO surfaces for 6G wireless networks: Opportunities, challenges, and trends," *IEEE Wireless Commun.*, vol. 27, no. 5, pp. 118–125, Oct. 2020.

[23] Z. Wan, J. Zhu, and L. Dai, "Can continuous aperture MIMO obtain more mutual information than discrete MIMO?," *IEEE Commun. Lett.*, vol. 27, no. 12, pp. 3185–3189, Dec. 2023.

[24] Y. Liu *et al.*, "CAPA: Continuous-aperture arrays for revolutionizing 6G wireless communications," *arXiv preprint*, arXiv:2412.00894, 2024.

[25] E. Björnson *et al.*, "Enabling 6G performance in the upper mid-band by transitioning from massive to gigantic MIMO," *arXiv preprint*, arXiv:2407.05630, 2024.

[26] S. Thomas, J. S. Virdi, A. Babakhani, and I. P. Roberts, "A survey on advancements in THz technology for 6G: Systems, circuits, antennas, and experiments," *arXiv preprint*, arXiv:2407.01957, 2024.

[27] Z. Wang *et al.*, "A tutorial on extremely large-scale MIMO for 6G: Fundamentals, signal processing, and applications," *IEEE Commun. Surv. & Tut.*, vol. 26, no. 3, pp. 1560–1605, Thirdquarter 2024.

[28] W. Rotman and A. Maestri, "An electromechanically scannable trough waveguide array," *1958 IRE Int. Convention Record*, 1960, pp. 67–83, York, NY, USA.

[29] D. Di Fonzo, P. Karmel and A. Atia, "A multiple shaped beam reconfigurable satellite antenna," in *Proc. Antennas & Propag. Soc. Int. Symp.*, pp. 457–460, 1979, Seattle, WA, USA.

[30] A. Alper and J. Arnbak, "Capacity allocation and reservation in common-user satellite communications systems with a reconfigurable multiple-beam antenna and a nonlinear repeater," *IEEE Trans. Commun.*, vol. 28, no. 9, pp. 1681–1692, Sept. 1980.

[31] G. H. Huff and J. T. Bernhard, *Reconfigurable antennas*, C.A. Balanis (ed.), Modern Antenna Handbook, John Wiley & Sons, 2008.

[32] O. Christogeorgos, E. Okon and Y. Hao, "An ultrawideband (35:1) shared-aperture antenna array with multihyperuniform disorder," *IEEE Trans. Antennas & Propag.*, vol. 72, no. 7, pp. 5794–5809, Jul. 2024.

[33] J. R. Henderson, T. G. Saunders, H. Yuan, J. Briscoe and Y. Hao, "Joule-heated vanadium dioxide switch design for reconfigurable millimeter-wave antenna arrays," *IEEE Antennas & Wireless Propag. Lett.*, vol. 23, no. 11, pp. 3729–3733, Nov. 2024.

[34] S. D. Campbell, G. Mackertich-Sengerdy, D. H. Werner and Y. Hao, "Guest editorial: Special cluster on advances in reconfigurable electromagnetic devices," *IEEE Antennas & Wireless Propag. Lett.*, vol. 23, no. 11, pp. 3689–3693, Nov. 2024.

[35] E. R. Brown, "RF-MEMS switches for reconfigurable integrated circuits," *IEEE Trans. Microwave Theory and Tech.*, vol. 46, no. 11, pp. 1868–1880, Nov. 1998.

[36] L. Jofre, B. A. Cetiner and F. De Flaviis, "Miniature multi-element antenna for wireless communications," *IEEE Trans. on Antennas and Propag.*, vol. 50, no. 5, pp. 658–669, May 2002.

[37] J. T. Aberle, S.-H. Oh, D. T. Auckland and S. D. Rogers, "Reconfigurable antennas for wireless devices," *IEEE Antennas and Prop. Mag.*, vol. 45, no. 6, pp. 148–154, Dec. 2003.

[38] B. A. Cetiner *et al.*, "Multifunctional reconfigurable MEMS integrated antennas for adaptive MIMO systems," *IEEE Commun. Mag.*, vol. 42, no. 12, pp. 62–70, Dec. 2004.

[39] B. A. Cetiner and H. Jafarkhani, "Method and apparatus for an adaptive multiple-input multiple-output (MIMO) wireless communications systems," U.S. Patent 7469152, 2008.

[40] B. A. Cetiner and H. Jafarkhani, "Method and apparatus for an adaptive multiple-input multiple-output (MIMO) wireless communications systems," U.S. Patent 7620424, 2009.

[41] J. Mitola and G. Q. Maguire, "Cognitive radio: Making software radios more personal," *IEEE Pers. Commun.*, vol. 6, no. 4, pp. 13–18, Aug. 1999.

[42] S. Haykin, "Cognitive radio: Brain-empowered wireless communications," *IEEE J. Select. Areas Commun.*, vol. 23, no. 2, pp. 201–220, Feb. 2005.

[43] T. Yucek and H. Arslan, "A survey of spectrum sensing algorithms for cognitive radio applications," *IEEE Commun. Surv. & Tut.*, vol. 11, no. 1, pp. 116–130, Firstquarter 2009.

[44] J. D. Boerman and J. T. Bernhard, "Performance study of pattern reconfigurable antennas in MIMO communication systems," *IEEE Trans. Antennas & Propag.*, vol. 56, no. 1, pp. 231–236, Jan. 2008.

[45] Y. Cai, Y. J. Guo and T. S. Bird, "A frequency reconfigurable printed Yagi-Uda dipole antenna for cognitive radio applications," *IEEE Trans. Antennas & Propag.*, vol. 60, no. 6, pp. 2905–2912, Jun. 2012.

[46] C. G. Christodoulou, Y. Tawk, S. A. Lane and S. R. Erwin, "Reconfigurable antennas for wireless and space applications," *Proc. IEEE*, vol. 100, no. 7, pp. 2250–2261, Jul. 2012.

[47] S. V. Hum and J. Perruisseau-Carrier, "Reconfigurable reflectarrays and array lenses for dynamic antenna beam control: A review," *IEEE Trans. Antennas & Propag.*, vol. 62, no. 1, pp. 183–198, Jan. 2014.

[48] H. A. Majid, M. K. A. Rahim, M. R. Hamid and M. F. Ismail, "Frequency and pattern reconfigurable slot antenna," *IEEE Trans. Antennas & Propag.*, vol. 62, no. 10, pp. 5339–5343, Oct. 2014.

[49] L. Ge and K.-M. Luk, "Frequency-reconfigurable low-profile circular monopolar patch antenna," *IEEE Trans. Antennas & Propag.*, vol. 62, no. 7, pp. 3443–3449, Jul. 2014.

[50] Z. Li, E. Ahmed, A. M. Eltawil and B. A. Cetiner, "A beam-steering reconfigurable antenna for WLAN applications," *IEEE Trans. Antennas & Propag.*, vol. 63, no. 1, pp. 24–32, Jan. 2015.

[51] W. Lin and H. Wong, "Wideband circular-polarization reconfigurable antenna with L-shaped feeding probes," *IEEE Antennas & Wireless Propag. Lett.*, vol. 16, pp. 2114–2117, Apr. 2017.

[52] A. J. Paulraj and T. Kailath, "Increasing capacity in wireless broadcast systems using distributed transmission/directional reception (DTDR)," U.S. Patent US5345599A, granted 1994, expired 2012.

[53] G. J. Foschini, "Layered space-time architecture for wireless communication in a fading environment when using multi-element antennas," *Bell Labs Tech. J.*, vol. 1, no. 2, pp. 41–59, Autumn 1996.

[54] G. J. Foschini, and M. Gans, "On limits of wireless communications in a fading environment when using multiple antennas," *Wireless Pers. Commun.*, vol. 6, pp. 311–335, 1998.

[55] V. Tarokh, N. Seshadri and A. R. Calderbank, "Space-time codes for high data rate wireless communication: Performance criterion and code construction," *IEEE Trans. Inf. Theory*, vol. 44, no. 2, pp. 744–765, Mar. 1998.

[56] V. Tarokh, H. Jafarkhani and A. R. Calderbank, "Space-time block codes from orthogonal designs," *IEEE Trans. Inf. Theory*, vol. 45, no. 5, pp. 1456–1467, Jul. 1999.

[57] H. Jafarkhani, *Space-time coding: theory and practice*, Cambridge University Press, 2005.

[58] G. G. Raleigh and J. M. Cioffi, "Spatio-temporal coding for wireless communication," *IEEE Trans. Commun.*, vol. 46, no. 3, pp. 357–366, Mar. 1998.

[59] K.-K. Wong, R. D. Murch, R.-K. Cheng, and K. B. Letaief, "Optimizing the spectral efficiency of multiuser MIMO smart antenna systems," in *Proc. IEEE Wireless Commun. Netw. Conf.*, vol. 1, pp. 426–430, 23-28 Sept. 2000, Chicago, IL, USA.

[60] K.-K. Wong, R. D. Murch and K. B. Letaief, "Performance enhancement of multiuser MIMO wireless communication systems," *IEEE Trans. Commun.*, vol. 50, no. 12, pp. 1960–1970, Dec. 2002.

[61] S. Vishwanath, N. Jindal and A. Goldsmith, "Duality, achievable rates, and sum-rate capacity of Gaussian MIMO broadcast channels," *IEEE Trans. Inf. Theory*, vol. 49, no. 10, pp. 2658–2668, Oct. 2003.

[62] L.-U. Choi and R. D. Murch, "A transmit preprocessing technique for multiuser MIMO systems using a decomposition approach," *IEEE Trans. Wireless Commun.*, vol. 3, no. 1, pp. 20–24, Jan. 2004.

[63] Q. H. Spencer, A. L. Swindlehurst and M. Haardt, "Zero-forcing methods for downlink spatial multiplexing in multiuser MIMO channels," *IEEE Trans. Sig. Process.*, vol. 52, no. 2, pp. 461–471, Feb. 2004.

[64] D. Gesbert, M. Koutouris, R. W. Heath, Jr., C.-B. Chae, and T. Salzer, "Shifting the MIMO Paradigm," *IEEE Sig. Proc. Mag.*, vol. 24, no. 5, pp. 36-46, Sept. 2007

[65] T. L. Marzetta, "Noncooperative cellular wireless with unlimited numbers of base station antennas," *IEEE Trans. on Wireless Commun.*, vol. 9, no. 11, pp. 3590–3600, Nov. 2010.

[66] D. A. Urquiza Villalonga, H. OdetAlla, M. J. Fernández-Getino Garcia, and A. Flizikowski, "Spectral efficiency of precoded 5G-NR in single and multi-user scenarios under imperfect channel knowledge: A comprehensive guide for implementation," *Electronics*, vol. 11, no. 24 (article number: 4237), Dec. 2022.

[67] F. Fazel, A. Grau, H. Jafarkhani, and F. D. Flaviis, "Space-time-state block coded MIMO communication systems using reconfigurable antennas," *IEEE Trans. on Wireless Commun.*, vol. 8, no. 12, pp. 6019–6029, Dec. 2009.
[68] A. Shojaeifard *et al.*, "MIMO evolution beyond 5G through reconfigurable intelligent surfaces and fluid antenna systems," *Proc. IEEE*, vol. 110, no. 9, pp. 1244–1265, Sept. 2022.
[69] W. K. New *et al.*, "A tutorial on fluid antenna system for 6G networks: Encompassing communication theory, optimization methods and hardware designs," *IEEE Commun. Surv. & Tut.*, vol. 24, no. 4, pp. 2325–2377, Aug. 2025.
[70] T. Wu *et al.*, "Fluid antenna systems enabling 6G: Principles, applications, and research directions," to appear in *IEEE Wireless Commun.*, arXiv:2412.03839, 2024.
[71] K.-K. Wong, K.-F. Tong, Y. Zhang, and Z. Zheng, "Fluid antenna system for 6G: When Bruce Lee inspires wireless communications," *Elect. Lett.*, vol. 56, no. 24, pp. 1288–1290, Nov. 2020.
[72] K.-K. Wong, K.-F. Tong, Y. Shen, Y. Chen, and Y. Zhang, "Bruce Lee-inspired fluid antenna system: Six research topics and the potentials for 6G," *Front. Commun. Netw. Sec. Wireless Commun.*, vol. 3, Mar. 2022.
[73] S. Lee, *Be water, my friend: The teachings of Bruce Lee*. Flatiron Books, 2020.
[74] Y. Huang, L. Xing, C. Song, S. Wang, and F. Elhouni, "Liquid antennas: Past, present and future," *IEEE Open J. Antennas & Propag.*, vol. 2, pp. 473–487, Mar. 2021.
[75] J. O. Martinez *et al.*, "Toward liquid reconfigurable antenna arrays for wireless communications," *IEEE Commun. Mag.*, vol. 60, no. 12, pp. 145–151, Dec. 2022.
[76] Y. Shen *et al.*, "Design and implementation of mmWave surface wave enabled fluid antennas and experimental results for fluid antenna multiple access," *arXiv preprint*, arXiv:2405.09663, May 2024.
[77] R. Wang *et al.*, "Electromagnetically reconfigurable fluid antenna system for wireless communications: Design, modeling, algorithm, fabrication, and experiment," *arXiv preprint*, arXiv:2502.19643v2, 2025.
[78] S. Basbug, "Design and synthesis of antenna array with movable elements along semicircular paths," *IEEE Antennas Wireless Propag. Lett.*, vol. 16, pp. 3059–3062, Oct. 2017.
[79] L. Zhu and K. K. Wong, "Historical review of fluid antenna and movable antenna," *arXiv preprint*, arXiv:2401.02362v2, 2024.
[80] M. C. Johnson, S. L. Brunton, N. B. Kundtz, and J. N. Kutz, "Sidelobe canceling for reconfigurable holographic metamaterial antenna," *IEEE Trans. Antennas & Propag.*, vol. 63, no. 4, pp. 1881–1886, Apr. 2015.
[81] B. Liu, K.-F. Tong, K. K. Wong, C.-B. Chae, and H. Wong, "Programmable meta-fluid antenna for spatial multiplexing in fast fluctuating radio channels," *Optics Express*, vol. 33, no. 13, pp. 28898–28915, 2025.
[82] J. Zhang *et al.*, "A novel pixel-based reconfigurable antenna applied in fluid antenna systems with high switching speed," *IEEE Open J. Antennas & Propag.*, vol. 6, no. 1, pp. 212–228, Feb. 2025.
[83] S. Shen, K. K. Wong, and R. Murch, "Antenna coding empowered by pixel antennas," to appear in *IEEE Trans. Commun.*, doi:10.1109/TCOMM.2025.3621089, 2025.
[84] M. Gal-Katziri, A. Fikes, and A. Hajimiri, "Flexible active antenna arrays," *npj Flexible Elect.*, vol. 6, no. 1, p. 85, Oct. 2022.
[85] S. Zhu and R. Langley, "Dual-band wearable textile antenna on an EBG substrate," *IEEE Trans. Antennas & Propag.*, vol. 57, no. 4, pp. 926–935, Apr. 2009.
[86] Y.-L. Zheng *et al.*, "Unobtrusive sensing and wearable devices for health informatics," *IEEE Trans. Biomedical Eng.*, vol. 61, no. 5, pp. 1538–1554, May 2014.
[87] W.-J. Lu *et al.*, "Fluid antennas: Reshaping intrinsic properties for flexible radiation characteristics in intelligent wireless networks," accepted in *IEEE Commun. Mag.*, vol. 63, no. 5, pp. 40–45, May 2025.
[88] K. K. Wong, A. Shojaeifard, K.-F. Tong, and Y. Zhang, "Performance limits of fluid antenna systems," *IEEE Commun. Lett.*, vol. 24, no. 11, pp. 2469–2472, Nov. 2020.
[89] K.-K. Wong, A. Shojaeifard, K.-F. Tong, and Y. Zhang, "Fluid antenna systems," *IEEE Trans. Wireless Commun.*, vol. 20, no. 3, pp. 1950–1962, Mar. 2021.
[90] L. Zhu, W. Ma, and R. Zhang, "Movable antennas for wireless communication: Opportunities and challenges," *IEEE Commun. Mag.*, vol. 62, no. 6, pp. 114–120, Jun. 2024.
[91] J. Zheng *et al.*, "Flexible-position MIMO for wireless communications: Fundamentals, challenges, and future directions," *IEEE Wireless Commun.*, vol. 31, no. 5, pp. 18–26, Oct. 2024.
[92] I. Krikidis, C. Psomas, A. K. Singh, and K. Jamieson, "Optimizing configuration selection in reconfigurable-antenna MIMO systems: Physics-inspired heuristic solvers," *IEEE Trans. Commun.*, vol. 72, no. 12, pp. 8010–8023, Dec. 2024.
[93] S. Yang *et al.*, "Flexible antenna arrays for wireless communications: Modeling and performance evaluation," *arXiv preprint*, arXiv:2407.04944, 2024.
[94] N. Shlezinger, G. C. Alexandropoulos, M. F. Imani, Y. C. Eldar and D. R. Smith, "Dynamic metasurface antennas for 6G extreme massive MIMO communications," *IEEE Wireless Commun.*, vol. 28, no. 2, pp. 106–113, Apr. 2021.
[95] L. You *et al.*, "Energy efficiency maximization of massive MIMO communications with dynamic metasurface antennas," *IEEE Trans. Wireless Commun.*, vol. 22, no. 1, pp. 393–407, Jan. 2023.
[96] J. Carlson, M. R. Castellanos, and R. W. Heath, "Hierarchical codebook design with dynamic metasurface antennas for energy-efficient arrays," *IEEE Trans. Wireless Commun.*, vol. 23, no. 10, pp. 14790–14804, Oct. 2024.
[97] Y. Ghasempour, R. Shrestha, A. Charous, E. Knightly, and D. M. Mittleman, "Single-shot link discovery for terahertz wireless networks," *Nature Commun.*, vol. 11, no. 1, p. 2017, Apr. 2020.
[98] Y. Gabay *et al.*, "Leaky waveguide antennas for downlink wideband THz communications," in *Proc. IEEE Int. Conf. Acoustics, Speech Sig. Process. (ICASSP)*, pp. 9111–9115, 14-19 Apr. 2024, Seoul, South Korea.
[99] K.-K. Wong, W. K. New, X. Hao, K.-F. Tong, and C.-B. Chae, "Fluid antenna system–Part I: Preliminaries," *IEEE Commun. Lett.*, vol. 27, no. 8, pp. 1919–1923, Aug. 2023.
[100] K.-K. Wong, K.-F. Tong, and C.-B. Chae, "Fluid antenna system–Part II: Research opportunities," *IEEE Commun. Lett.*, vol. 27, no. 8, pp. 1924–1928, Aug. 2023.
[101] K.-K. Wong, K.-F. Tong, and C.-B. Chae, "Fluid antenna system–Part III: A new paradigm of distributed artificial scattering surfaces for massive connectivity," *IEEE Commun. Lett.*, vol. 27, no. 8, pp. 1929–1933, Aug. 2023.
[102] R. Bhagavatula, C. Oestges, and R. W. Heath, "A new double-directional channel model including antenna patterns, array orientation, and depolarization," *IEEE Trans. Veh. Technol.*, vol. 59, no. 5, pp. 2219–2231, Jun. 2010.
[103] M. Mizmizi *et al.*, "Conformal metasurfaces: A novel solution for vehicular communications," *IEEE Trans. Wireless Commun.*, vol. 22, no. 4, pp. 2804–2817, Apr. 2023.
[104] H. Xu *et al.*, "Capacity maximization for FAS-assisted multiple access channels," *IEEE Trans. Commun.*, vol. 73, no. 7, pp. 4713–4731, Jul. 2025.
[105] Y. Xu *et al.*, "Energy efficiency maximization under delay-outage probability constraints using fluid antenna systems," in *Proc. IEEE Statistical Sig. Process. Workshop (SSP)*, pp. 105–109, 2-5 Jul. 2023, Hanoi, Vietnam.
[106] F. R. Ghadi, K. K. Wong, F. Javier López-Martinez, and K. F. Tong, "Copula-based performance analysis for fluid antenna systems under arbitrary fading channels," *IEEE Commun. Lett.*, vol. 27, no. 11, pp. 3068–3072, Nov. 2023.
[107] W. K. New, K.-K. Wong, H. Xu, K.-F. Tong, and C.-B. Chae, "Fluid antenna system: New insights on outage probability and diversity gain," *IEEE Trans. Wireless Commun.*, vol. 23, no. 1, pp. 128–140, Jan. 2024.
[108] J. D. Vega-Sánchez, L. Urquiza-Aguiar, M. C. P. Paredes, and D. P. M. Osorio, "A simple method for the performance analysis of fluid antenna systems under correlated Nakagami-m fading," *IEEE Wireless Commun. Lett.*, vol. 13, no. 2, pp. 377–381, Feb. 2024.
[109] P. D. Alvim *et al.*, "On the performance of fluid antennas systems under α-μ fading channels," *IEEE Wireless Commun. Lett.*, vol. 13, no. 1, pp. 108–112, Jan. 2024.
[110] F. R. Ghadi *et al.*, "A Gaussian copula approach to the performance analysis of fluid antenna systems," *IEEE Trans. Wireless Commun.*, vol. 23, no. 11, pp. 17573–17585, Nov. 2024.
[111] W. K. New, K.-K. Wong, H. Xu, K.-F. Tong, and C.-B. Chae, "An information-theoretic characterization of MIMO-FAS: Optimization, diversity-multiplexing tradeoff and q-outage capacity," *IEEE Trans. Wireless Commun.*, vol. 23, no. 6, pp. 5541–5556, Jun. 2024.
[112] C. Guo, F. Liu, S. Chen, C. Feng, and Z. Zeng, "Advances on exploiting polarization in wireless communications: Channels, technologies, and applications," *IEEE Commun. Surv. & Tutorials*, vol. 19, no. 1, pp. 125–166, Firstquarter 2017.
[113] A. Ludwig, "The definition of cross polarization," *IEEE Trans. Antennas & Propag.*, vol. 21, no. 1, pp. 116–119, Jan. 1973.
[114] R. Zhang, Y. Shao, and Y. C. Eldar, "Polarization aware movable antenna," *arXiv preprint*, arXiv:2411.06690, 2024.

[115] M. R. Castellanos and R. W. Heath, "Linear polarization optimization for wideband MIMO systems with reconfigurable arrays," *IEEE Trans. Wireless Commun.*, vol. 23, no. 3, pp. 2282–2295, Mar. 2024.

[116] G. Mu *et al.*, "Outage performance analysis of dual-polarized fluid antenna systems," in *Proc. IEEE Int. Conf. Commun. Workshops (ICC Workshops)*, pp. 1720–1725, 9-13 Jun. 2024, Denver, CO, USA.

[117] C. Oestges, M. Guillaud, and M. Debbah, "Multi-polarized MIMO communications: Channel model, mutual information and array optimization," in *Proc. IEEE Wireless Commun. Netw. Conf. (WCNC)*, pp. 1057–1061,11-15 Mar. 2007, Hong Kong, China.

[118] J. M. Jornet *et al.*, "The evolution of applications, hardware design, and channel modeling for terahertz (THz) band communications and sensing: Ready for 6G?," *Proc. IEEE*, doi:10.1109/JPROC.2024.3412828, 2024.

[119] D. Moltchanov *et al.*, "A tutorial on mathematical modeling of 5G/6G millimeter wave and terahertz cellular systems," *IEEE Commun. Surv. & Tut.*, vol. 24, no. 2, pp. 1072–1116, Secondquarter 2022.

[120] Y. Ghasempour, C.-Y. Yeh, R. Shrestha, D. Mittleman, and E. Knightly, "Single shot single antenna path discovery in THz networks," in *Proc. Annual Int. Conf. Mobile Comput. Netw.*, vol. 18, pp. 1–18, Apr. 2020.

[121] A. Sutinjo, M. Okoniewski, and R. H. Johnston, "Radiation from fast and slow traveling waves," *IEEE Antennas & Propag. Mag.*, vol. 50, no. 4, pp. 175–181, Aug. 2008.

[122] K.-K. Wong and K.-F. Tong, "Fluid antenna multiple access," *IEEE Trans. Wireless Commun.*, vol. 21, no. 7, pp. 4801–4815, Jul. 2022.

[123] K.-K. Wong, D. Morales-Jimenez, K.-F. Tong, and C.-B. Chae, "Slow fluid antenna multiple access," *IEEE Trans. Commun.*, vol. 71, no. 5, pp. 2831–2846, May 2023.

[124] K.-K. Wong, C.-B. Chae, and K.-F. Tong, "Compact ultra massive antenna array: A simple open-loop massive connectivity scheme," *IEEE Trans. Wireless Commun.*, vol. 23, no. 6, pp. 6279–6294, Jun. 2024.

[125] H. Hong, K. K. Wong, K. F. Tong, H. Shin, and Y. Zhang, "Coded fluid antenna multiple access over fast fading channels," *IEEE Wireless Commun. Lett.*, vol. 14, no. 4, pp. 1249–1253, Apr. 2025.

[126] H. Hong, K. K. Wong, K. F. Tong, H. Xu, and H. Li, "5G-coded fluid antenna multiple access over block fading channels," *IET Elect. Lett.*, vol. 61, no. 1, Jan./Dec. 2025.

[127] E. Basar *et al.*, "Wireless communications through reconfigurable intelligent surfaces," *IEEE Access*, vol. 7, pp. 116753–116773, Aug. 2019.

[128] M. Di Renzo *et al.*, "Smart radio environments empowered by reconfigurable intelligent surfaces: How it works, state of research, and the road ahead," *IEEE J. Select. Areas Commun.*, vol. 38, no. 11, pp. 2450–2525, Nov. 2020.

[129] Y. Han, W. Tang, S. Jin, C.-K. Wen and X. Ma, "Large intelligent surface-assisted wireless communication exploiting statistical CSI," *IEEE Trans. Veh. Technol.*, vol. 68, no. 8, pp. 8238–8242, Aug. 2019.

[130] C. Huang, A. Zappone, G. C. Alexandropoulos, M. Debbah, and C. Yuen, "Reconfigurable intelligent surfaces for energy efficiency in wireless communication," *IEEE Trans. Wireless Commun.*, vol. 18, no. 8, pp. 4157–4170, Aug. 2019.

[131] Q. Wu and R. Zhang, "Intelligent reflecting surface enhanced wireless network via joint active and passive beamforming," *IEEE Trans. Wireless Commun.*, vol. 18, no. 11, pp. 5394–5409, Nov. 2019.

[132] L. Dai *et al.*, "Reconfigurable intelligent surface-based wireless communications: Antenna design, prototyping, and experimental results," *IEEE Access*, vol. 8, pp. 45913–45923, Mar. 2020.

[133] R. Liu *et al.*, "Sustainable wireless networks via reconfigurable intelligent surfaces (RISs): Overview of the ETSI ISG RIS," *arXiv preprint*, arXiv:2406.05647v1, Jun. 2024.

[134] P. Wang, J. Fang, X. Yuan, Z. Chen, and H. Li, "Intelligent reflecting surface-assisted millimeter wave communications: Joint active and passive precoding design," *IEEE Trans. Veh. Technol.*, vol. 69, no. 12, pp. 14960–14973, Dec. 2020.

[135] C. Huang, R. Mo, and C. Yuen, "Reconfigurable intelligent surface assisted multiuser MISO systems exploiting deep reinforcement learning," *IEEE J. Select. Areas Commun.*, vol. 38, no. 8, pp. 1839–1850, Aug. 2020.

[136] W. K. New *et al.*, "Coordinated reconfigurable intelligent surface for cellular-connected UAV," in *Proc. IEEE Int. Symp. Telecomm. Technol. (ISTT)*, pp. 42–47, 21-22 Oct. 2024, Langkawi Island, Malaysia.

[137] Z. Zhang *et al.*, "Active RIS vs. passive RIS: Which will prevail in 6G?," *IEEE Trans. Commun.*, vol. 71, no. 3, pp. 1707–1725, Mar. 2023.

[138] K. Zhi, C. Pan, H. Ren, K. K. Chai, and M. Elkashlan, "Active RIS versus passive RIS: Which is superior with the same power budget?," *IEEE Commun. Lett.*, vol. 26, no. 5, pp. 1150–1154, May 2022.

[139] C. Y. Goh *et al.*, "Energy efficient relay for unmanned aerial vehicle with onboard hybrid reconfigurable intelligent surfaces," in *Proc. IEEE Int. Conf. Commun. (ICC)*, pp. 3452–3457, 9-13 Jun. 2024, Denver, CO, USA.

[140] A. Taha, M. Alrabeiah, and A. Alkhateeb, "Deep learning for large intelligent surfaces in millimeter wave and massive MIMO systems," in *Proc. IEEE Global Commun. Conf. (GLOBECOM)*, pp. 1–6, 9-13 Dec. 2019, Waikoloa, HI, USA.

[141] H. Liu, X. Yuan and Y.-J. A. Zhang, "Matrix-calibration-based cascaded channel estimation for reconfigurable intelligent surface assisted multiuser MIMO," *IEEE J. Select. Areas Commun.*, vol. 38, no. 11, pp. 2621–2636, Nov. 2020.

[142] L. Wei *et al.*, "Channel estimation for RIS-empowered multi-user MISO wireless communications," *IEEE Trans. Commun.*, vol. 69, no. 6, pp. 4144–4157, Jun. 2021.

[143] J. He, H. Wymeersch and M. Juntti, "Channel estimation for RIS-aided mmWave MIMO systems via atomic norm minimization," *IEEE Trans. Wireless Commun.*, vol. 20, no. 9, pp. 5786–5797, Sept. 2021.

[144] F. Rostami Ghadi *et al.*, "On performance of RIS-aided fluid antenna systems," *IEEE Wireless Commun. Lett.*, vol. 13, no. 8, pp. 2175–2179, Aug. 2024.

[145] J. Yao *et al.*, "A framework of FAS-RIS systems: Performance analysis and throughput optimization," *IEEE Trans. Wireless Commun.*, doi:10.1109/TWC.2025.3590458, 2024.

[146] J. Yao *et al.*, "FAS-RIS communication: Model, analysis, and optimization," *IEEE Trans. Veh. Technol.*, vol. 74, no. 6, pp. 9938–9943, Jun. 2025.

[147] X. Lai *et al.*, "FAS-RIS: A block-correlation model analysis," *IEEE Trans. Veh. Technol.*, vol. 74, no. 2, pp. 3412–3417, Feb. 2025.

[148] X. Wei, W. Mei, Q. Wu, B. Ning, and Z. Chen, "Movable antennas meet intelligent reflecting surface: When do we need movable antennas?," *arXiv preprint*, arXiv:2408.15668, 2024.

[149] J. Yao *et al.*, "FAS vs. ARIS: Which is more important for FAS-ARIS communication systems?," *IEEE Trans. Wireless Commun.*, doi:10.1109/TWC.2025.3594617, 2025.

[150] J. Chen *et al.*, "Low-complexity beamforming design for RIS-assisted fluid antenna systems," in *Proc. IEEE Int. Conf. Commun. Workshops (ICC Workshops)*, pp. 1377–1382, 9-13 Jun. 2024, Denver, CO, USA.

[151] A. S. Alwakeel, A. M. El-Rifaie, G. Moustafa, and A. M. Shaheen, "Newton Raphson based optimizer for optimal integration of FAS and RIS in wireless systems," *Results in Engineering*, vol. 25, Mar. 2025.

[152] J. Zhu *et al.*, "Fluid antenna empowered index modulation for RIS-aided mmWave transmissions," *IEEE Trans. Wireless Commun.*, vol. 24, no. 2, pp. 1635–1647, Feb. 2025.

[153] F. R. Ghadi *et al.*, "Secrecy performance analysis of RIS-aided fluid antenna systems," *arXiv preprint*, arXiv:2408.14969, 2024.

[154] J. Zheng *et al.*, "Unlocking FAS-RIS security analysis with block-correlation model," *IEEE Wireless Commun. Lett.*, vol. 14, no. 7, pp. 2029–2033, Jul. 2025.

[155] J. Ye, P. Zhang, X.-P. Li, L. Huang, and Y. Liu, "Joint beamforming and position optimization for fluid RIS-aided ISAC systems," *arXiv preprint*, arXiv:2501.13339v2, 2025.

[156] A. Salem, K. K. Wong, G. Alexandropoulos, C.-B. Chae, and R. Murch, "A first look at the performance enhancement potential of fluid reconfigurable intelligent surface," *arXiv preprint*, arXiv:2502.17116v1, 2025.

[157] K. K. Wong, K. F. Tong, Z. Chu, and Y. Zhang, "A vision to smart radio environment: Surface wave communication superhighways," *IEEE Wireless Commun.*, vol. 28, no. 1, pp. 112–119, Feb. 2021.

[158] H. Liu *et al.*, "Path loss and surface impedance models for surface wave-assisted wireless communication system," *IEEE Access*, vol. 12, pp. 125786–125799, Aug. 2024.

[159] Z. Chu *et al.*, "On propagation loss for reconfigurable surface wave communications," *IEEE Trans. Commun.*, vol. 73, no. 3, pp. 1547–1559, Mar. 2025.

[160] W. K. New *et al.*, "Channel estimation and reconstruction in fluid antenna system: Oversampling is essential," *IEEE Trans. Wireless Commun.*, vol. 24, no. 1, pp. 309–322, Jan. 2025.

[161] W. Ma, L. Zhu, and R. Zhang, "Multi-beam forming with movable-antenna array," *IEEE Commun. Lett.*, vol. 28, no. 3, pp. 697–701, Mar. 2024.

[162] Y. Liu *et al.*, "Reconfigurable intelligent surfaces: Principles and opportunities," *IEEE Commun. Surv. & Tut.*, vol. 23, no. 3, pp. 1546–1577, Mar. 2021.

[163] H. Xu *et al.*, "Channel estimation for FAS-assisted multiuser mmwave systems," *IEEE Commun. Lett.*, vol. 28, no. 3, pp. 632–636, Mar. 2024.

[164] J. An, M. Debbah, T. J. Cui, Z. N. Chen, and C. Yuen, "Emerging technologies in intelligent metasurfaces: Shaping the future of wireless communications," *arXiv preprint*, arXiv:2411.19754, 2024.

[165] P. Mursia *et al.*, "T3DRIS: Advancing conformal RIS design through in-depth analysis of mutual coupling effects," *arXiv preprint*, arXiv: 2404.05261, 2024.

[166] K.-K. Wong, "Transmitter CSI-free RIS-randomized CUMA for extreme massive connectivity," *IEEE Open J. Commun. Soc.*, vol. 5, pp. 6890–6902, 2024.

[167] J. Wittman, "Categorization of multiple-access/random-access modulation techniques," *IEEE Trans. Commun. Technol.*, vol. 15, no. 5, pp. 724–725, 1967.

[168] D. Falconer, F. Adachi, and B. Gudmundson, "Time division multiple access methods for wireless personal communications," *IEEE Commun. Mag.*, vol. 33, no. 1, pp. 50–57, Jan. 1995.

[169] Z. Ding *et al.*, "A survey on non-orthogonal multiple access for 5G networks: Research challenges and future trends," *IEEE J. Select. Areas Commun.*, vol. 35, no. 10, pp. 2181–2195, Oct. 2017.

[170] Y. Mao *et al.*, "Rate-splitting multiple access: Fundamentals, survey, and future research trends," *IEEE Commun. Surv. & Tut.*, vol. 24, no. 4, pp. 2073–2126, Apr. 2022.

[171] Z. Wu and L. Dai, "Multiple access for near-field communications: SDMA or LDMA?," *IEEE J. Select. Areas Commun.*, vol. 41, no. 6, pp. 1918–1935, Jun. 2023.

[172] C. Wang *et al.*, "Fluid antenna system liberating multiuser MIMO for ISAC via deep reinforcement learning," *IEEE Trans. Wireless Commun.*, vol. 23, no. 9, pp. 10879–10894, Sept. 2024.

[173] K.-K. Wong, K.-F. Tong, Y. Chen, and Y. Zhang, "Fast fluid antenna multiple access enabling massive connectivity," *IEEE Commun. Lett.*, vol. 27, no. 2, pp. 711–715, Feb. 2023.

[174] K. Wong, K. Tong, Y. Chen, and Y. Zhang, "Closed-form expressions for spatial correlation parameters for performance analysis of fluid antenna systems," *Elect. Lett.*, vol. 58, no. 11, pp. 454–457, Apr. 2022.

[175] K.-K. Wong, K.-F. Tong, Y. Chen, and Y. Zhang, "Maximizing the network outage rate for fast fluid antenna multiple access systems," *IET Commun.*, vol. 17, no. 8, pp. 928–939, May 2023.

[176] K.-K. Wong, K.-F. Tong, Y. Chen, and Y. Zhang, "Extra-large MIMO enabling slow fluid antenna massive access for millimeter-wave bands," *Elect. Lett.*, vol. 58, no. 25, pp. 1016–1018, Dec. 2022.

[177] H. Xu *et al.*, "Revisiting outage probability analysis for two-user fluid antenna multiple access system," *IEEE Trans. Wireless Commun.*, vol. 23, no. 8, pp. 9534–9548, Aug. 2024.

[178] K.-K. Wong, "Compact ultra massive array (CUMA) with 4 RF chains for massive connectivity," in *Proc. IEEE Int. Workshop Sig. Process. Adv. Wireless Commun. (SPAWC)*, pp. 286–290, 10-13 Sept. 2024, Lucca, Italy.

[179] K.-K. Wong, K.-F. Tong, Y. Chen, Y. Zhang, and C.-B. Chae, "Opportunistic fluid antenna multiple access," *IEEE Trans. Wireless Commun.*, vol. 22, no. 11, pp. 7819–7833, Nov. 2023.

[180] N. Waqar *et al.*, "Opportunistic fluid antenna multiple access via team-inspired reinforcement learning," *IEEE Trans. Wireless Commun.*, vol. 23, no. 9, pp. 12068–12083, Sept. 2024.

[181] W. K. New *et al.*, "Fluid antenna system enhancing orthogonal and non-orthogonal multiple access," *IEEE Commun. Lett.*, vol. 28, no. 1, pp. 218–222, Jan. 2024.

[182] N. Li, P. Wu, B. Ning, and L. Zhu, "Sum rate maximization for movable antenna enabled uplink NOMA," *IEEE Wireless Commun. Lett.*, vol. 13, no. 8, pp. 2140–2144, Aug. 2024.

[183] Y. Zhou, W. Chen, Q. Wu, X. Zhu, and N. Cheng, "Movable antenna empowered downlink NOMA systems: Power allocation and antenna position optimization," *IEEE Wireless Commun. Lett.*, vol. 13, no. 10, pp. 2772–2776, Oct. 2024.

[184] F. R. Ghadi, K.-K. Wong, F. J. López-Martínez, L. Hanzo, and C.-B. Chae, "Fluid antenna-aided rate-splitting multiple access," *IEEE Trans. Veh. Technol.*, doi:10.1109/TVT.2025.3599709, 2025.

[185] C. Zhang *et al.*, "Sum rate maximization for movable antenna-aided downlink RSMA systems," *arXiv preprint*, arXiv:2411.08509, 2024.

[186] J. Zheng *et al.*, "FAS-assisted NOMA short-packet communication systems," *IEEE Trans. Veh. Technol.*, vol. 73, no. 7, pp. 10732–10737, Jul. 2024.

[187] L. Tlebaldiyeva, S. Arzykulov, T. A. Tsiftsis, and G. Nauryzbayev, "Exploiting FAS for cooperative NOMA-based full-duplex mmwave networks with imperfections," *Ad Hoc Netw.*, vol. 155, p. 103400, 2024.

[188] F. R. Ghadi, K.-K. Wong, F. J. López-Martínez, H. Shin, and L. Hanzo, "Performance analysis of FAS-aided NOMA-ISAC: A backscattering scenario," *IEEE Internet Things J.*, doi:10.1109/JIOT.2025.3612478, 2025.

[189] W. K. New, K.-K. Wong, H. Xu, K.-F. Tong, and C.-B. Chae, "Achievability of fluid antenna multiple access: A Han-Kobayashi's comparison," in *Proc. IEEE Global Commun. Conf. (GLOBECOM) Workshops*, pp. 1201–1206, 4-8 Dec. 2023, Kuala Lumpur, Malaysia.

[190] F. R. Ghadi *et al.*, "Fluid antenna multiple access with simultaneous non-unique decoding in strong interference channel," *IEEE Trans. Wireless Commun.*, doi:10.1109/TWC.2025.3578280, 2025.

[191] Z.-Q. Luo and W. Yu, "An introduction to convex optimization for communications and signal processing," *IEEE J. Select. Areas Commun.*, vol. 24, no. 8, pp. 1426–1438, Aug. 2006.

[192] V. R. Cadambe and S. A. Jafar, "Interference alignment and degrees of freedom of the k-user interference channel," *IEEE Trans. Inf. Theory*, vol. 54, no. 8, pp. 3425–3441, Aug. 2008.

[193] H. Yang, W. Shin, and J. Lee, "Hierarchical blind interference alignment over interference networks with finite coherence time," *IEEE Trans. Sig. Process.*, vol. 64, no. 5, pp. 1289–1304, May 2016.

[194] M. M. Azari *et al.*, "Evolution of non-terrestrial networks from 5G to 6G: A survey," *IEEE Commun. Surv. & Tut.*, vol. 24, no. 4, pp. 2633–2672, Apr. 2022.

[195] 3GPP-TR 38.811, "Study on new radio (NR) to support non-terrestrial networks (release 15)," *Technical Report*, May 2020.

[196] M. Giordani and M. Zorzi, "Non-terrestrial networks in the 6G era: Challenges and opportunities," *IEEE Netw.*, vol. 35, no. 2, pp. 244–251, Feb. 2021.

[197] W. K. New and C. Y. Leow, "Unmanned aerial vehicle (UAV) in future communication system," in *Proc. IEEE Asia-Pacific Conf. Commun. (APCC)*, pp. 217–222, 11-13 Oct. 2021, Kuala Lumpur, Malaysia.

[198] W. K. New, C. Y. Leow, K. Navaie, Y. Sun, and Z. Ding, "Application of NOMA for cellular-connected UAVs: Opportunities and challenges," *Science China Inf.n Sciences*, vol. 64, pp. 1–14, Mar. 2021.

[199] L. Zhu, X. Pi, W. Ma, Z. Xiao, and R. Zhang, "Dynamic beam coverage for satellite communications aided by movable-antenna array," *IEEE Trans. Wireless Commun.*, vol. 24, no. 3, pp. 1916–1933, Mar. 2025.

[200] S. B. S. Abdou *et al.*, "Sum-rate maximization for UAV relay-aided fluid antenna system with NOMA," in *Proc. IEEE Int. Symp. Telecommun. Technol. (ISTT)*, pp. 53–58, 21-22 Oct. 2024, Langkawi Island, Malaysia.

[201] W. Liu *et al.*, "UAV-enabled wireless networks with movable-antenna array: Flexible beamforming and trajectory design," *IEEE Wireless Commun. Lett.*, vol. 14, no. 3, pp. 566–570, Mar. 2025.

[202] C. Liu *et al.*, "UAV-enabled passive 6D movable antennas: Joint deployment and beamforming optimization," *arXiv preprint*, arXiv:2412.11150, 2024.

[203] X.-W. Tang, Y. Shi, Y. Huang, and Q. Wu, "UAV-mounted movable antenna: Joint optimization of UAV placement and antenna configuration," *arXiv preprint*, arXiv:2409.02469, 2024.

[204] T. Ren *et al.*, "6D movable antenna enhanced interference mitigation for cellular-connected UAV communications," *arXiv preprint*, arXiv:2409.13278, 2024.

[205] W. K. New, C. Y. Leow, K. Navaie, and Z. Ding, "Robust non-orthogonal multiple access for aerial and ground users," *IEEE Trans. Wireless Commun.*, vol. 19, no. 7, pp. 4793–4805, Jul. 2020.

[206] A. Al-Hourani, S. Kandeepan, and A. Jamalipour, "Modeling air-to-ground path loss for low altitude platforms in urban environments," in *Proc. IEEE Global Commun. Conf. (GLOBECOM)*, pp. 2898–2904, 8-12 Dec. 2014, Austin, TX, USA.

[207] S. Jie Seah *et al.*, "Empirical channel models for UAV communication: A comparative study," *IEEE Access*, vol. 12, pp. 96740–96756, Jul. 2024.

[208] W. K. New, C. Y. Leow, K. Navaie, Y. Sun, and Z. Ding, "Interference-aware NOMA for cellular-connected UAVs: Stochastic geometry analysis," *IEEE J. Select. Areas Commun.*, vol. 39, no. 10, pp. 3067–3080, Oct. 2021.

[209] W. K. New, C. Y. Leow, K. Navaie, and Z. Ding, "Aerial-terrestrial network NOMA for cellular-connected UAVs," *IEEE Trans. Veh. Technol.*, vol. 71, no. 6, pp. 6559–6573, Jun. 2022.

[210] A. Liu *et al.*, "A survey on fundamental limits of integrated sensing and communication," *IEEE Commun. Surv. & Tut.*, vol. 24, no. 2, pp. 994–1034, Feb. 2022.

[211] F. Liu *et al.*, "Integrated sensing and communications: Toward dual-functional wireless networks for 6G and beyond," *IEEE J. Select. Areas Commun.*, vol. 40, no. 6, pp. 1728–1767, Jun. 2022.

[212] S. Lu *et al.*, "Integrated sensing and communications: Recent advances and ten open challenges," *IEEE Internet of Things J.*, vol. 11, no. 11, pp. 19094–19120, Jun. 2024.

[213] Q. Shi, L. Liu, S. Zhang, and S. Cui, "Device-free sensing in OFDM cellular network," *IEEE J. Select. Areas Commun.*, vol. 40, no. 6, pp. 1838–1853, Jun. 2022.

[214] X. Cheng, D. Duan, S. Gao, and L. Yang, "Integrated sensing and communications (ISAC) for vehicular communication networks (VCN)," *IEEE Internet of Things J.*, vol. 9, no. 23, pp. 23441–23451, Dec. 2022.

[215] Z. Zhang *et al.*, "Target localization in cooperative ISAC systems: A scheme based on 5G NR OFDM signals," *IEEE Trans. Commun.*, vol. 73, no. 5, pp. 3562–3578, May 2025.

[216] C. Liu *et al.*, "Learning-based predictive beamforming for integrated sensing and communication in vehicular networks," *IEEE J. Select. Areas Commun.*, vol. 40, no. 8, pp. 2317–2334, Aug. 2022.

[217] K. Meng, C. Masouros, K. K. Wong, A. P. Petropulu, and L. Hanzo, "Integrated sensing and communication meets smart propagation engineering: Opportunities and challenges," *IEEE Netw.*, vol. 39, no. 2, pp. 278–285, Mar. 2025.

[218] T. Hao *et al.*, "Fluid-antenna enhanced ISAC: Joint antenna positioning and dual-functional beamforming design under perfect and imperfect CSI," *IEEE Trans. Veh. Technol.*, doi:10.1109/TVT.2025.3574072, 2025.

[219] J. Zou *et al.*, "Shifting the ISAC trade-off with fluid antenna systems," *IEEE Wireless Commun. Lett.*, vol. 13, no. 12, pp. 3479–3483, Dec. 2024.

[220] Q. Zhang *et al.*, "An efficient sum-rate maximization algorithm for fluid antenna-assisted ISAC system," *IEEE Commun. Lett.*, vol. 29, no. 1, pp. 200–204, Jan. 2025.

[221] L. Zhou, J. Yao, M. Jin, T. Wu, and K.-K. Wong, "Fluid antenna-assisted ISAC systems," *IEEE Wireless Commun. Lett.*, vol. 13, no. 12, pp. 3533–3537, Dec. 2024.

[222] Y. Zuo *et al.*, "Fluid antenna-enabled integrated sensing, communication, and computing systems," *arXiv preprint*, arXiv:2409.11622, 2024.

[223] J. Zhou, Y. Yang, Z. Yang, and M. Shikh-Bahaei, "Fluid antenna-assisted near-field system," *arXiv preprint*, arXiv:2409.20472, 2024.

[224] H. Hong *et al.*, "FAS meets OFDM: Enabling wideband 5G NR," *IEEE Trans. Commun.*, doi:10.1109/TCOMM.2025.3591751, 2025.

[225] H. Hong, K. K. Wong, H. Xu, *et al.*, "Downlink OFDM-FAMA in 5G-NR systems," *IEEE Trans. Wireless Commun.*, doi:10.1109/TWC.2025.3577771, 2025.

[226] H. Zhang *et al.*, "Learning-induced channel extrapolation for fluid antenna systems using asymmetric graph masked autoencoder," *IEEE Wireless Commun. Lett.*, vol. 13, no. 6, pp. 1665–1669, Jun. 2024.

[227] J. Zou, S. Sun, and C. Wang, "Online learning-induced port selection for fluid antenna in dynamic channel environment," *IEEE Wireless Commun. Lett.*, vol. 13, no. 2, pp. 313–317, Feb. 2024.

[228] L. Zhang, H. Yang, Y. Zhao, and J. Hu, "Joint port selection and beamforming design for fluid antenna assisted integrated data and energy transfer," *IEEE Wireless Commun. Lett.*, vol. 13, no. 7, pp. 1833–1837, Jul. 2024.

[229] T. Hao, C. Shi, Y. Guo, B. Xia, and F. Yang, "Fluid-antenna enhanced integrated sensing and communication: Joint antenna positioning and beamforming design," in *Proc. IEEE/CIC Int. Conf. Commun. China (ICCC)*, pp. 956–961, 7-9 Aug. 2024, Hangzhou, China.

[230] C. Wang *et al.*, "AI-empowered fluid antenna systems: Opportunities, challenges, and future directions," *IEEE Wireless Commun.*, vol. 31, no. 5, pp. 34–41, Oct. 2024.

[231] A. F. M. S. Shah, M. Ali Karabulut, E. Cinar, and K. M. Rabie, "A survey on fluid antenna multiple access for 6G: A new multiple access technology that provides great diversity in a small space," *IEEE Access*, vol. 12, pp. 88410–88425, Jun. 2024.

[232] Z. Chai, K.-K. Wong, K.-F. Tong, Y. Chen, and Y. Zhang, "Port selection for fluid antenna systems," *IEEE Commun. Lett.*, vol. 26, no. 5, pp. 1180–1184, May 2022.

[233] N. Waqar, K.-K. Wong, K.-F. Tong, A. Sharples, and Y. Zhang, "Deep learning enabled slow fluid antenna multiple access," *IEEE Commun. Lett.*, vol. 27, no. 3, pp. 861–865, Mar. 2023.

[234] S. Ji, C. Psomas, and J. Thompson, "Correlation-based machine learning techniques for channel estimation with fluid antennas," in *Proc. IEEE Int. Conf. Acoustics, Speech & Sig. Process. (ICASSP)*, pp. 8891–8895, 14-19 Apr. 2024, Seoul, South Korea.

[235] Z. Zhang, J. Zhu, L. Dai, and R. W. Heath, "Successive Bayesian reconstructor for FAS channel estimation," in *Proc. IEEE Wireless Commun. Netw. Conf. (WCNC)*, 21-24 Apr. 2024, Dubai, United Arab Emirates.

[236] Z. Zhang, J. Zhu, L. Dai, and R. W. Heath Jr, "Successive Bayesian reconstructor for channel estimation in fluid antenna systems," *IEEE Trans. Wireless Commun.*, vol. 24, no. 3, pp. 1992–2006, Mar. 2025.

[237] G. Li, H. Zhang, C. Wang, and B. Wang, "Model-driven channel extrapolation for massive fluid antenna," in *Proc. IEEE Int. Conf. Commun. Workshops (ICC Workshops)*, pp. 1146–1151, 9-13 Jun. 2024, Denver, CO, USA.

[238] X. Tang *et al.*, "Deep learning-assisted jamming mitigation with movable antenna array," *IEEE Trans. Veh. Technol.*, vol. 74, no. 9, pp. 14865–14870, Sept. 2025.

[239] M. Ahmadzadeh, S. Pakravan, G. A. Hodtani, M. Zeng, and J.-Y. Chouinard, "Enhancement of over-the-air federated learning by using AI-based fluid antenna system," *arXiv preprint*, arXiv:2407.03481, 2024.

[240] D. Zhang *et al.*, "Fluid antenna array enhanced over-the-air computation," *IEEE Wireless Commun. Lett.*, vol. 13, no. 6, pp. 1541–1545, Jun. 2024.

[241] C. Skouroumounis and I. Krikidis, "Fluid antenna-aided full duplex communications: A macroscopic point-of-view," *IEEE J. Select. Areas Commun.*, vol. 41, no. 9, pp. 2879–2892, Sept. 2023.

[242] L. Tlebaldiyeva, S. Arzykulov, T. A. Tsiftsis, and G. Nauryzbayev, "Full-duplex cooperative NOMA-based mmWave networks with fluid antenna system (FAS) receivers," in *Proc. Int. Balkan Conf. Commun. Netw. (BalkanCom)*, 5-8 Jun. 2023, Istanbul, Turkey.

[243] B. Tang *et al.*, "Fluid antenna enabling secret communications," *IEEE Commun. Lett.*, vol. 27, no. 6, pp. 1491–1495, Jun. 2023.

[244] H. Xu *et al.*, "Coding-enhanced cooperative jamming for secret communication in fluid antenna systems," *IEEE Commun. Lett.*, vol. 28, no. 9, pp. 1991–1995, Sept. 2024.

[245] F. Rostami Ghadi *et al.*, "Physical layer security over fluid antenna systems: Secrecy performance analysis," *IEEE Trans. Wireless Commun.*, vol. 23, no. 12, pp. 18201–18213, Dec. 2024.

[246] X. Lin, H. Yang, Y. Zhao, J. Hu, and K.-K. Wong, "Performance analysis of integrated data and energy transfer assisted by fluid antenna systems," in *Proc. IEEE Int. Conf. Commun. (ICC)*, pp. 2761–2766, 9-13 Jun. 2024, Denver, CO, USA.

[247] L. Zhou *et al.*, "Fluid antenna-assisted simultaneous wireless information and power transfer systems," *IEEE Trans. Veh. Technol.*, vol. 74, no. 5, pp. 8285–8290, May 2025.

[248] H. Xiao *et al.*, "From fixed to fluid: Unlocking the new potential with fluid RIS (FRIS)," *arXiv preprint*, arXiv:2509.18899, 2025.

[249] H. Hong *et al.*, "A contemporary survey on fluid antenna systems: Fundamentals and networking perspectives," *IEEE Trans. Netw. Sci. & Eng.*, doi:10.1109/TNSE.2025.3613225, 2025.

BIOGRAPHY

(Aven) Wee Kiat New (Member, IEEE) received the B.I.T. degree in Data Communications and Networking from Multimedia University, the M.Eng.Sc. degree in Electrical Engineering from the University of Malaya, and the Ph.D. degree in Electrical Engineering from Universiti Teknologi Malaysia. He was a Visiting Researcher with Lancaster University, U.K., and the University of Cyprus. He served as a Research Fellow with the Department of Electronic and Electrical Engineering, University College London (UCL), U.K., and is currently a Visiting Research Fellow in the same department. He is now a Short-Range Wireless Researcher with Huawei, Singapore, focusing on short-range wireless standards and emerging wireless technologies.

His research interests include information theory, optimization, stochastic processes, machine learning, and their applications in emerging areas of communications. He serves as an Associate Editor for the IEEE Transactions on Vehicular Technology and the IEEE Transactions on Communications, and as a Guest Editor for the IEEE Journal on Selected Areas in Communications and the IEEE Journal on Selected Topics in Signal Processing. He also serves as Vice-Chair of the IEEE ComSoc WTC SIG on Fluid Antenna Systems, is a founding member of the IEEE ComSoc TCCN SIG on Fluid Antenna Systems, and acts as General Co-Chair for the Globecom 2025 Workshop on Fluid Antenna Systems and the VTC 2025-Spring Workshop on Fluid Antenna Systems for 6G. He was a tutorial speaker at ICC 2025 and MICC 2023, and previously served as TPC Co-Chair for the ICC 2024 Workshop on Fluid Antenna Systems for 6G. His research has received several recognitions, including the the 2025 IEEE SPS Malaysia Best Journal Paper Award, the 2024 IEEE ISTT Best Paper Award, the 2024 IEEE MAPE Best Student

Paper Award, the 2023 IEEE SPS Malaysia Best Ph.D. Thesis Award, the 2021 IEEE Malaysia ComSoc/VTS Best Paper Award, and the IEEE Malaysia AP/MTT/EMC Best Paper Awards in 2022, 2021, and 2020.

Kai-Kit Wong (M'01-SM'08-F'16) received the BEng, the MPhil, and the PhD degrees, all in Electrical and Electronic Engineering, from the Hong Kong University of Science and Technology, Hong Kong, in 1996, 1998, and 2001, respectively. He moved to the United Kingdom in 2004 and is presently Chair in Wireless Communications at the Department of Electronic and Electrical Engineering, University College London, UK. He was the first researcher proposing multiuser MIMO back in 2000. He is Fellow of IEEE and IET and is also on the editorial board of several international journals. He served as the Editor-in-Chief for IEEE Wireless Communications Letters between 2020 and 2023.

Chao Wang (M'20) received the B.S., M. S. and Ph.D. degrees, in information and communication engineering from Xi'an Jiaotong University, Xi'an, China, in 2008, 2013, and 2016, respectively. He is currently an Associate Professor with the State Key Laboratory of Integrated Services Networks, School of Telecommunications Engineering, Xidian University. His current research interests include 5G & 6G wireless networks and key technologies, physical-layer security, covert communications, and deep learning and its application in the optimization of wireless communications . He was a recipient of the Excellent Doctoral Dissertation Award of Shaanxi Province in 2018 and China Institute of Communications in 2016, the Best Paper Awards at the IEEE ICCC 2014 and IEEE SAGC 2020, respectively.

Chan-Byoung Chae (Fellow, IEEE) received the Ph.D. degree in electrical and computer engineering from The University of Texas at Austin (UT), USA in 2008, where he was a member of wireless networking and communications group (WNCG).

Prior to joining UT, he was a Research Engineer at the Telecommunications R&D Center, Samsung Electronics, Suwon, South Korea, from 2001 to 2005. He is currently an Underwood Distinguished Professor with the School of Integrated Technology, Yonsei University, South Korea. Before joining Yonsei University, he was with Bell Labs, Alcatel-Lucent, Murray Hill, NJ, USA, from 2009 to 2011, as a Member of Technical Staff, and Harvard University, Cambridge, MA, USA, from 2008 to 2009, as a Post-Doc. Research Fellow.

Dr. Chae was a recipient/co-recipient of the Ministry of Education Award in 2024, the KICS Haedong Scholar Award in 2023, the CES Innovation Award in 2023, the IEEE ICC Best Demo Award in 2022, the IEEE WCNC Best Demo Award in 2020, the Best Young Engineer Award from the National Academy of Engineering of Korea (NAEK) in 2019, the IEEE DySPAN Best Demo Award in 2018, the IEEE/KICS Journal of Communications and Networks Best Paper Award in 2018, the IEEE INFOCOM Best Demo Award in 2015, the IEIE/IEEE Joint Award for Young IT Engineer of the Year in 2014, the KICS Haedong Young Scholar Award in 2013, the IEEE Signal Processing Magazine Best Paper Award in 2013, the IEEE ComSoc AP Outstanding Young Researcher Award in 2012, and the IEEE VTS Dan. E. Noble Fellowship Award in 2008.

Dr. Chae has held several editorial positions, including Editor-in-Chief of the IEEE Transactions on Molecular, Biological, and Multi-Scale Communications, Senior Editor of the IEEE Wireless Communications Letters, and Editor for the IEEE Communications Magazine, IEEE Transactions on Wireless Communications, and IEEE Wireless Communications Letters. He was an IEEE ComSoc Distinguished Lecturer from 2020 to 2023 and is an IEEE VTS Distinguished Lecturer from 2024 to 2025. He is an IEEE Fellow and elected member of the National Academy of Engineering of Korea.

Ross Murch (S'84-M'90-SM'98-F'09) received the bachelor's and Ph.D. degrees in Electrical and Electronic Engineering from the University of Canterbury, New Zealand. He is currently a Chair Professor in the Department of Electronic and Computer Engineering (ECE) at the Hong Kong University of Science and Technology (HKUST). He is also the founding Editor-in-Chief of the IEEE Journal of Selected Topics in Electromagnetics, Antennas and Propagation which was launched in January 2025. Prof. Murch's research focus is creating new RF wave technology for making a better world. His unique expertise lies in his combination of knowledge from both electromagnetics and wireless communication systems and he has published widely in both areas with over 200 journal publications. He has also supervised over 50 research graduate students in these areas and is the inventor of 20+ patents. He became a Fellow of IEEE for his "Contributions to Multiple Antenna Systems for Wireless Communication" in 2010. He is also a Fellow of IET, HKAE, INAE, NASI, HKIE and in 2023 won the IEEE Communications Society Wireless Technical Committee Recognition Award. Prof. Murch was also an Area Editor for IEEE Transactions on Wireless Communications and Editor for IEEE Journal of Selected Areas in Communication: Wireless series (the precursor to IEEE Transactions on Wireless Communications). He has also been a guest editor for IEEE Proceedings and IEEE Journal of Selected Areas in communication. Prof. Murch also enjoys teaching and has won several teaching awards. He has served IEEE in several roles and was Department Head of ECE@HKUST from 2009-2015.

Hamid Jafarkhani (Fellow, IEEE) is a Distinguished Professor at the Department of Electrical Engineering and Computer Science, University of California, Irvine. He was a Visiting Scholar at Harvard University in 2015, a Visiting Professor at the California Institute of Technology in 2018, and a Visiting Research Scholar at Duke University in 2023. He was the 2020-2022 elected Faculty Chair of the UCI School of Engineering.

Dr. Jafarkhani was an IEEE ComSoc Distinguished lecturer. Among his awards are the NSF Career Award, the UCI Distinguished Mid-Career Faculty Award for Research, the School of Engineering Excellence in Research Senior Career Award, the IEEE Marconi Prize Paper Award in Wireless Communications, the IEEE Communications Society Award for Advances in Communication, the IEEE Wireless Communications Technical Committee Recognition Award, the IEEE Signal Processing and Computing for Communications Technical Recognition Award, and the IEEE Eric E. Sumner Award. He is the 2017 Innovation Hall of Fame Inductee at the University of Maryland's School of Engineering.

Dr. Jafarkhani is listed as an ISI highly cited researcher. According to Thomson Scientific, he is one of the top 10 most-cited researchers in the field of "computer science" during 1997-2007. He is a Fellow of AAAS, an IEEE Fellow, a Fellow of NAI, and the author of the book "Space-Time Coding: Theory and Practice."

Yang Hao (Fellow, IEEE) received the Ph.D. degree in computational electromagnetics from the Centre for Communications Research, University of Bristol, Bristol, U.K., in 1998.

He was a Post-Doctoral Research Fellow with the School of Electronic, Electrical and Computer Engineering, University of Birmingham, Birmingham, U.K. He is currently a Professor of antennas and electromagnetics with the Antenna Engineering Group, Queen Mary University of London, London, U.K. He is also a holder of QinetiQ/Royal Academy of Engineering Research Chair.

Over the past 25 years, Dr. Yang Hao has led a number of major interdisciplinary research projects as Principal Investigator. These include his Directorship of the L4.6 million EPSRC QUEST Programme Grant and his role as Co-Investigator and Management Board Member of the L23 million Cambridge Graphene Centre. His research has been internationally recognized through his seminal books Antennas and Radio Propagation for Body-Centric Wireless Communications and FDTD Modeling of Metamaterials: Theory and Applications (Artech House, USA), as well as highly cited papers published in leading journals such as Nature Communications, Advanced Science, Physical Review Letters, Applied Physics Letters, IEEE Proceedings, and IEEE Transactions. Dr. Hao's research has significantly advanced the international standing of U.K. antenna and electromagnetic research, generating over 25,000 citations and resulting in several patents in collaboration with industry. His work has been translated into practical applications, particularly in transformation optics and metamaterials, leading to novel lens antenna technologies for satellite communications. He has been instrumental in establishing a complete supply chain—from electromagnetic modelling, materials design and fabrication, to lens manufacturing and antenna system integration. This work directly enabled the creation of Isotropic Systems Ltd. (now All.Space), a deep-tech startup based in Berkshire, U.K., now valued at over $100 million. He has supervised more than 80 Ph.D. students and postdoctoral researchers, many of whom have gone on to leadership positions in academia and industry, including four who have founded their own spin-out companies.

Dr. Hao is a Fellow of the Royal Academy of Engineering (RAEng), the Institution of Engineering and Technology (IET), and the Institute of Electrical and Electronics Engineers (IEEE). His pioneering research has been recognized through numerous international honours, including the AF Harvey Research Prize (IET, 2013), the Royal Society Wolfson Research Merit Award (2013-2017), and the BAE Systems Chairman?s Silver Award (2014). More recently, he received the John Kraus Antenna Award and the Fred W. Ellersick Prize from the IEEE in 2024, as well as the EurAAP Antenna Award from the European Association of Antennas and Propagation. He has served on the EPSRC Strategic Advisory Board, where he helped shape the U.K.?s national research strategy in RF/microwave engineering and advanced manufacturing. In addition, he has contributed to several high-impact policy and foresight reports, including the Royal Society?s Machine Learning Roadmap (2016) and the IET?s Future Industry Strategy White Paper (2017). Internationally, Dr. Hao has demonstrated outstanding leadership within the IEEE community. He served as Editor-in-Chief of the IEEE Antennas and Wireless Propagation Letters (2013-2017), founded the open-access journal EPJ Applied Metamaterials in 2015, and is currently Chair of the IEEE Antennas and Propagation Society Publications Committee. He has also served as a member of the IEEE AP-S Administrative Committee and chaired the Royal Society Theo Murphy International Scientific Meeting.